AD_____

Award Number: DAMD17-96-1-6189

TITLE: Biology of Somatostatin and Somatostatin Receptors in Breast Cancer

PRINCIPAL INVESTIGATOR: Dr. Yogesh C. Patel

CONTRACTING ORGANIZATION: McGill University,
Montreal, Quebec, Canada H3A 1A1

REPORT DATE: September 2000

TYPE OF REPORT: FINAL

PREPARED FOR: U.S. Army Medical Research and Materiel Command
Fort Detrick, Maryland 21702-5012

REPORT DOCUMENTATION PAGE

Form Approved
OMB No. 074-0188

1. AGENCY USE ONLY (Leave blank)	2. REPORT DATE	3. REPORT TYPE AND DATES COVERED
	September 2000	Final (12 Aug 96 – 11 Aug 00)

4. TITLE AND SUBTITLE
Biology of Somatostatin and Somatostatin Receptors in Breast Cancer

5. FUNDING NUMBERS
DAMD17-96-1-6189

6. AUTHOR(S)
Dr. Yogesh C. Patel

7. PERFORMING ORGANIZATION NAME(S) AND ADDRESS(ES)
McGill University
Montreal, Quebec, Canada H3A 1A1
E-Mail: yogesh.patel@muhc.mcgill.ca

8. PERFORMING ORGANIZATION REPORT NUMBER

9. SPONSORING / MONITORING AGENCY NAME(S) AND ADDRESS(ES)
U.S. Army Medical Research and Materiel Command
Fort Detrick, Maryland 21702-5012

10. SPONSORING / MONITORING AGENCY REPORT NUMBER

11. SUPPLEMENTARY NOTES
This report contains colored photos

12a. DISTRIBUTION / AVAILABILITY STATEMENT
Approved for Public Release; Distribution Unlimited

12b. DISTRIBUTION CODE

13. ABSTRACT *(Maximum 200 Words)*

Breast tumors show rich expression of multiple SSTR subtypes and may be amenable to treatment with selective SST compounds. All five SSTRs variably inhibit cell growth. When studied as individual subtypes expressed in host cells, SSTR3 is the only isoform that induces apoptosis whereas SSTR1,2,4 and 5 promote cell growth arrest with SSTR5 exerting the most potent effect. Both apoptotic and cytostatic signalling are dependent on receptor-mediated activation of SHP-1. Cytostasis then proceeds through activation of Rb and p21 whereas apoptosis is associated with caspase-8-mediated intracellular acidification and decrease in mitochondrial membrane potential. Apoptotic signalling by SSTR3 requires molecular signals in the receptor C-tail. Likewise, the C-tail of hSSTR5, and specifically its phosphorylation state is crucial for the ability of this receptor to initiate cytostatic signalling. Endogenous SSTRs that are coexpressed as multiple subtypes in the same cell are capable of associating as functional heterodimeric receptors whose properties differ from those of the separate monomer components. Although SSTR3 is the only subtype that undergoes apoptosis when studied as a monotransfectant, SSTR1,2, and 5 are also capable of inducing apoptosis when coexpressed with SSTR3. This means that SSTR3 is an obligatory receptor for SST-induced apoptosis but that other SSTR subtypes can also induce apoptosis through heterodimerization with SSTR3.

14. SUBJECT TERMS
Breast cancer

15. NUMBER OF PAGES 97

16. PRICE CODE

17. SECURITY CLASSIFICATION OF REPORT	18. SECURITY CLASSIFICATION OF THIS PAGE	19. SECURITY CLASSIFICATION OF ABSTRACT	20. LIMITATION OF ABSTRACT
Unclassified	Unclassified	Unclassified	Unlimited

TABLE OF CONTENTS

INTRODUCTION

Somatostatin (SST) a naturally occurring regulatory peptide is produced in neural, endocrine, and immune cells, and exerts potent effects on many different tissue targets (1). The cellular actions of SST include the inhibition of secretion of hormones and growth factors as well as modulation of neurotransmission and cell proliferation and are mediated by a family of 7 transmembrane domain G protein coupled receptors with five distinct subtypes (SSTR1-5) that are encoded by separate genes located on five different chromosomes (1,2). The five receptor subtypes bind the natural SST peptides SST-14 and SST-28 with high affinity. Short synthetic octapeptide analogs such as octreotide which is used clinically, bind well to only three of the subtypes SSTR2,3,5 (1,2). Nonpeptide agonists that bind selectively to single subtypes have recently been identified (3). In contrast to the antisecretory properties of SST, its antiproliferative effects were relatively late in being recognized and came about largely through use of the longacting analog octreotide in the early 1980's for the treatment of hormone hypersecretion from pancreatic, intestinal, and pituitary tumors (4,5). It was noted that SST not only blocked hormone hypersecretion from these tumors but also caused variable tumor shrinkage through an additional antiproliferative effect. The antiproliferative effects of SST have since been demonstrated in normal dividing cells, e.g. intestinal mucosal cells, activated lymphocytes, and inflammatory cells as well as *in vivo* in solid tumors, e.g. DMBA-induced or transplanted rat mammary carcinomas, and cultured cells derived from both endocrine and epithelial tumors (pituitary, thyroid, breast, prostate, colon, pancreas, lung, and brain) (1). These effects involve cytostatic (growth arrest) and cytotoxic (apoptotic) actions and are mediated (i) directly by SSTRs present on tumor cells, and (ii) indirectly via SSTRs present on nontumor cell targets to inhibit the secretion of hormones and growth factors that promote tumor growth and to inhibit angiogenesis, promote vasoconstriction, and modulate immune cell function (1, 6-8). All five SSTR subtypes acting via several different signal transduction pathways have been implicated. Most interest is focused on protein phosphatases (PTP) that dephosphorylate receptor tyrosine kinases or that modulate the MAPK signalling cascade, thereby attenuating mitogenic signal transduction (1). A SST-sensitive PTP was first described in 1985 in human pancreatic cancer cells and has since been demonstrated in normal pancreatic acinar cells, human coronary smooth muscle cells, human breast and prostate cancer cells, and rat pancreatic and thyroid tumor cells (1, 9). All five SSTR subtypes have been shown to stimulate PTP activity in various transfected cells (1). SSTR-induced activation of PTP is sensitive to pertussis toxin and orthovanadate (10). The PTP activity associated with SST action has been attributed to the SH2 domain containing cytosolic PTPs whose members include SHP-1 (SHPTP1/PTP1C) and SHP-2 (SHPTP2/PTP1D/syp) (11). SHP-1 is known to dephosphorylate and inactivate both receptor tyrosine kinases and nonreceptor tyrosine kinases, e.g. jak-2. Direct evidence has shown an important role of SHP1 in SSTR-mediated PTP activation and antiproliferative signalling (1,12). Like PTP, all of the SSTRs have been shown to modulate the MAPK pathway, either positively or negatively, in a PTP-dependent manner to effect cell growth inhibition (1). The precise steps linking the ligand activated receptor to PTP stimulation and mitogenic signalling remain to be determined. Four of the receptors (SSTR1,2,4,5) induce cell cycle arrest via PTP-dependent modulation of MAPK, associated with induction of the retinoblastoma tumor suppressor protein (Rb) and p21 (1, 7). The maximal effect is exerted by SSTR5 followed by SSTR2, 4, and 1. In contrast, SSTR3 uniquely triggers PTP-dependent apoptosis accompanied

by activation of p53 and the pro-apoptotic protein Bax (6, 13). SSTR3 induced apoptotic signalling requires molecular signals in the receptor cytoplasmic tail (C-tail), and involves the activation of a cation insensitive acidic endonuclease and caspase-8-mediated intracellular acidification (14-16). Likewise, C-tail truncation mutants of hSSTR5 display progressive loss of antiproliferation indicating that the molecular signals for cytostatic signalling also reside in the receptor C-tail (Task 14, this report).

Major strides have been made over the last four years in our laboratory and elsewhere towards understanding the subtype-selectivity and signalling mechanisms underlying the antiproliferative actions of SST. Despite this experimental success, SST analogs such as octreotide (which bind SSTR2,3,5 but not SSTR1 and 4) have so far produced variable clinical effects on tumor growth due to a number of reasons such as patient selection (e.g. early vs end stage disease), the absence of appropriate SSTRs in the tumors being treated (e.g. tumors expressing SSTR1 and SSTR4 will not respond to octreotide; SSTR3 expression is required for inducing apoptosis), the presence of mutated p53 gene which abbrogates the apoptotic effect of SST, and the dose and duration of treatment. Future work will need to address these issues to optimize the oncological utility of SST compounds.

LONGTERM OBJECTIVES

The longterm goal of this four-year proposal was **to elicit the pattern of expression of the five individual SSTR subtypes in breast tumor, to determine whether their pattern of expression can provide an independent prognostic marker, and whether the SSTRs are modulated by estrogens and anti-estrogens.** In addition, we set out **to determine the subtype selectivity for the antiproliferative effects of SST as well as the role of PTP, p53, and other downstream effectors in mediating the cytostatic and cytotoxic effects of SST.**

Whilst our broad objectives remained unchanged from those proposed in the original application, we made a number of directional changes as a result of new leads from our own work or from other laboratories in the field. These were discussed in detail on page 7 of the year 3 Annual Report and resulted in three new tasks that were included for the final year. A list of the 12 originally proposed tasks and the three new tasks is shown below. Specific tasks (new and ongoing) for year 4 are marked by an asterisk and described in detail. Progress on the remaining tasks has been described fully in previous reports and only the main findings are recapitulated here for completion.

DETAILS OF PROGRESS

LIST OF SPECIFIC TASKS PROPOSED IN THE ORIGINAL APPLICATION

1) RT-PCR analysis of SSTR1-5 mRNA expression in human breast tumors.
2) *In situ* hybridization analysis of SSTR1-5 mRNA in human breast tumors.
* 3) Immunocytochemical analysis of SSTR1-5 in human breast tumors.
4) Analysis of SSTR expression in breast tumor cell lines.
* 5) Antireceptor blockade experiments with SSTR1-5 antisera.
* 6) Antisense knockout of SSTR1-5.
7) Regulation of SSTR1-5 by estrogens/tamoxifen.
8) Correlation between SSTR subtype selective binding, PTP activation and growth inhibition.
* 9) SSR subtype selectivity for PTP association.
* 10) Subtype selectivity for SSTR induced apoptosis.
* 11) Involvement of PTP in apoptosis.
* 12) Overexpression and antisense blockade of SSTRs for effects on apoptosis.

NEW TASKS PROPOSED FOR YEAR 4 IN REVISED SOW

* 13) Mutational analysis of the C-tail of hSSTR3.
* 14) Mutational analysis of the C-tail of hSSTR5.
* 15) Completion of studies of cAMP effects on SSTR mediated apoptosis.

TASK 1. <u>Expression of SSTR1-5 mRNA in Human Breast Tumor Tissue</u>

The expression of SSTR1-5 mRNA was analysed by semiquantitative RT-PCR in frozen slices of primary human breast tumor tissue. 90 samples were analysed in year 1, 50 in year 2, and 50 in year 30. The level of SSTR subtype expression was correlated with tumor histology and estrogen (ER) and progesterone (PR) receptor levels. All tumors expressed at least one SSTR subtype and frequently featured more than one SSTR isoform. The prevalence of the five SSTRs was 91% (SSTR1), 96% (SSTR2), 98% (SSTR3), 76% (SSTR4), and 54% (SSTR5) (Fig. 1). Statistical analysis showed a strong positive correlation between SSTR3 expression and tumor grade. Induction of SSTR3 in high grade tumors occurred differentially at the expense of the other subtypes (SSTR1, 2, 4) and may represent a response to increasing malignancy, perhaps as a compensatory mechanism to regulate proliferative activity through apoptosis. Expression of SSTR1, 2, and 4 correlated strongly with ER levels and SSTR2 expression additionally correlated positively with PR levels.

This task is now completed and has been described in detail in the Annual Reports of years 1, 2, and 3.

TASK 2. ***In Situ* Hybridization Analysis**

This task was cancelled as explained in the year 2 Annual Report and substituted with the more specific receptor immunocytochemistry technique due to the successful development of a panel of polyclonal antireceptor antibodies against each of the five human receptor subtypes.

***TASK 3. Immunocytochemical Analysis of SSTR1-5 in Tumor Samples**

Our objective with this task is to (i) correlate SSTR1-5 mRNA expression as determined by RT-PCR with receptor protein expression by immunocytochemistry in a subset of human breast tumor samples, and (ii) to determine the cellular pattern of expression of SSTR1-5 in tumor cells and peritumoral structures. The results of 16 tumors analysed in a blinded fashion for SSTR1-5 expression by immunocytochemistry by a breast tumor pathologist (Dr. P. Watson, University of Manitoba) were described in last year's report. We found the histological preservation in these Tumor Bank cryosections less than optimal compared to regular fixed breast tumor sections cut from paraffin blocks. Nonetheless, there was good concordance between mRNA and protein expression of 69% (SSTR1), 69% (SSTR2), 50% (SSTR3), 56% (SSTR4), and 50% (SSTR5) in this first batch. We have now analysed a further 19 samples by immunocytochemistry with the help of in-house pathologists to optimize the reading and interpretation of the histology. These results are presented in Tables 1 and 2 and show very good correlation between the presence of mRNA and receptor protein with a % match of 84% for SSTR1, 79% for SSTR2, 89% for SSTR3, 68% for SSTR4, 68% for SSTR5, and 78% for all five receptors. We found receptor immunoreactivity variably localized both in tumor cells as well as in surrounding peritumoral structures especially blood vessels (endothelial and smooth muscle cells), immune cells, and to a lesser extent stromal cells. This task is now completed with the important outcome that SSTR immunocytochemistry using a panel of antipeptide receptor antibodies such as that developed by us can be applied for routine analysis of SSTR subtype expression in surgical samples of breast tumor tissue.

TASK 4. Analysis of SSTR1-5 Expression in Breast Tumor Cell Lines

This task was completed and described in detail in the year 2 Annual Report (1998). In summary, RT-PCR analysis was employed for characterizing SSTR1-5 mRNA expression in ER^+ (MCF-7, T47D, ZR75-1) and ER^- (MB231) human breast cancer cell lines. Like solid tumors, the cell lines expressed multiple SSTR subtypes but with no obvious distinction between ER^+ and ER^- cell lines. There were, however, interesting differences in that the overall level of SSTR expression in cell lines was less than that in the solid tumors. For instance SSTR3 was well expressed in the solid tumors but relatively poorly expressed in cell lines. SSTR5, a weak subtype in solid tumors, was relatively better expressed in the cell lines. A likely explanation for the difference is the probable induction of SSTR expression in solid tumors by circulating hormones or locally by growth factors, cytokines, and other mediators produced from peritumoral structures, e.g. stroma, blood vessels, and immune cells. These results confirm the well known differences between tumor cells *in vivo* and *in vitro* and indicate that in the case of SSTRs, the various breast cancer cell lines, although useful for studying SSTR biology, do not necessarily reflect endogenous tumor SSTR

expression and function.

***TASKS 5 & 6. Antireceptor Blockade of SSTR1-5 and Antisense Knockout of SSTR1-5**

These two tasks share a common objective and are discussed together. The experimental protocols and results obtained so far with the antisense experiments have been described in detail in the year 3 Annual Report. We originally proposed these experiments to identify SSTR subtype(s) mediating the antiproliferative effect of SST. Early in our studies, however, (year 1) we were able to establish that all five SSTRs negatively regulated cell growth when studied as monotransfectants in CHO-K1 cells (6). SSTR3 uniquely induced apoptosis whereas the other four subtypes produced variable degrees of cell cycle arrest (SSTR5 > 2 > 4 > 1). As a result of this finding, we focused on signalling mechanisms and concentrated our work on subtype-specific antiproliferative responses mediated by the two key subtypes, SSTR3 and SSTR5. The antisense experiments helped to confirm and extend the results obtained with recombinant SSTRs individually expressed in CHO-K1 cells, to endogenous SSTRs in breast cancer cell lines expressing multiple receptor isoforms. These experiments were technically demanding and were optimized for MCF-7 cells which had a sturdy growth pattern, and expressed four of the SSTR subtypes, SSTR1 (+++), SSTR2 (+), SSTR3 (+/-), and SSTR5 (+++) whose relative abundance was determined by semiquantitative RT-PCR analysis of mRNA and of receptor protein by immunocytochemistry. SSTR4 (a weak antiproliferative subtype in CHO-K1 cells) was not expressed in MCF-7 cells and was, therefore, not studied by antisense targetting. Cells were grown in coverslips and treated for 4 days with phosphorothioate modified antisense oligonucleotides (ODNs) or control sense ODNs. The experimental conditions have been described fully in the year 3 Annual Report. Based on published *in vitro* antisense experiments to knockout the SST gene in cultured lymphocytes, we started with ODN concentrations of 25 μg/ml which were extremely toxic to MCF-7 cells (17). An optimal ODN concentration of 2-3.5 μg/ml was determined. Four days of treatment with antisense ODN to SSTR1,2,3,5 resulted in a marked decrease in expression of the corresponding SSTR protein as determined by immunocytochemistry (Fig. 2). The decrease was specific and was not seen in sense ODN exposed cells. The total number of cells in each coverslip was analysed by cell count. The results of the first set of experiments were presented in Fig. 1 of last year's (1999) Annual Report. We have repeated and extended these results which show a significant increase in the proliferative activity of cells treated with antisense ODNs to SSTR3 and SSTR5 compared to sense ODNs. Blockade of SSTR1 and SSTR2 produced small 21% and 13% increases in cell growth compared to control but these differences failed to reach statistical significance. Following 4 days of incubation with antisense ODNs to SSTR1 and SSTR2, treatment with 1 μm SST-14 produced 25-37% decrease in cell numbers comparable to the results obtained with sense ODN treatment. On the other hand, four days of antisense treatment with SSTR3 and SSTR5 ODNs markedly attenuated the ability of SST (1 μm) to inhibit cell growth (12-15% reduction in cell numbers compared to 35-43% in sense ODN treated controls). These results in MCF-7 cells confirm the relatively high potency of SSTR3 and SSTR5 in inducing antiproliferation that we also found in transfected CHO-K1 cells. The pronounced SSTR3 effect in these cells is interesting given the relatively low level expression of this receptor mRNA in these cells. There is little doubt, however, that these cells express functional SSTR3 receptors as shown in recent studies (described in task 10) with the SSTR3-selective nonpeptide

agonist L-796778 which induces apoptosis in MCF-7 cells. With the availability of subtype-selective agonists like L-796778 for each of the five receptors, we decided not to duplicate the antisense experiments with immunoblockade studies of each receptor for subtype-selective antiproliferative effects and instead substituted these experiments with studies of the effects of these analogs on cell proliferation and apoptosis in MCF-7 cells (described in task 10). This decision was also influenced by two other developments (i) the realization that our panel of SSTR antibodies were of variable quality and were not all equally effective in blocking individual receptor function, and (ii) a major observation from our laboratory showing that members of the SSTR family interact on the membrane to form novel heterodimeric receptor complexes with binding and signalling properties distinct from those of the individual receptor monomers. This discovery prompted a new set of experiments to check whether receptors other than the SSTR3 subtype could induce apoptosis by forming heterodimers with SSTR3 (described in task 10).

TASK 7. Regulation of SSTR1-5 by Estrogens/Tamoxifen

The effect of estradiol and tamoxifen on SSTR1-5 mRNA expression was characterized in MCF-7 cells and described in detail in our last annual (1999) report. The essential findings consisted of the demonstration of a dose-dependent stimulation by estradiol of SSTR1 mRNA from 10^{-12}-10^{-8} M with inhibition at higher (10^{-7} M) concentration. Estrogen also stimulated SSTR5 mRNA at 10^{-12}-10^{-7} M with a biphasic dose response curve but was without effect on SSTR3 and SSTR2. SSTR4 was not detectable in this cell line either in the basal state or following estrogen treatment. The effects of tamoxifen revealed dose-dependent biphasic response with SSTR1 and SSTR5 mRNA, low doses (10^{-12} M) being inhibitory and higher doses (10^{-10}-10^{-7} M) being stimulatory. SSTR3 and SSTR2 mRNA also showed small but distinct increases in mRNA levels at high tamoxifen concentrations. These are mainly descriptive and time consuming studies showing complex subtype-selective effects of both estrogens and tamoxifen on SSTR mRNA expression. Because of this, we have decided not to pursue these effects in other tumor cell lines as originally proposed.

TASK 8. Correlation Between SSTR Subtype Selective Binding, PTP Activation, and Growth Inhibition

This task was almost completed as described in the year 3 Annual Report. In summary, we have reported in two successive Molecular Endocrinology papers (6, 7) that negative growth regulation by SST is SSTR subtype specific and triggers cell cycle arrest predominantly via SSTR5 (and to a lesser extent SSTR2, SSTR4, and SSTR1) or apoptosis uniquely through the SSTR3 subtype. We showed that SSTR3 mediated apoptosis is associated with induction of p53 and Bax whereas cytostatic signalling is accompanied by induction of Rb and p21. We also established that both cytostatic and cytotoxic effects are mediated via PTP and that the divergence of subtype selective cytostatic and cytotoxic signalling occurs distal to the regulation of PTP. As offshoots of these observations, we proposed two new tasks to characterize by mutagenesis the role of the cytoplasmic C-tail domain of hSSTR5 and hSSTR3 in cytostatic and cytotoxic signalling respectively. In the case of hSSTR5 we have already reported that C-tail truncation mutants display progressive loss of antiproliferative signalling proportional to the length of deletion as reflected by

the marked decrease in the effects of SST on membrane translocation of cytosolic PTP and induction of Rb and Gi arrest (7). The mutational analysis was extended to point mutations and are described in Task 14. In the case of hSSTR3, C-tail deletion mutants and chimeric receptors were created and characterized for antiproliferative effects and are described under Task 13. The remaining new lead from this task that we mentioned in the last Annual Report was to look at the effects of the nonpeptide receptor monoselective analogs of SST for subtype-selective antiproliferative signalling in MCF-7 cells which we have completed as described in Task 10.

***TASKS 9 & 11. <u>SSTR Subtype Selectivity For PTP Association and Involvement of PTP in Apoptosis and Cell Growth Arrest</u>**

Based on our finding that SHP-1 is the PTP involved in mediating the antiproliferative action of SST in tumor cells, we embarked on studies to characterize the effect of ectopic expression of SHP-1 or its catalytically inactive mutant (SHP-1C455S) in CHO-K1 cells expressing hSSTR3 or hSSTR5.

(A) ***Elucidation of the Role of SHP-1 in hSSTR3 Signaled Apoptosis***

We showed that stable ectopic expression of wild type SHP-1 and hSSTR3 in CHO-K1 cells amplified the apoptotic effect of SST (Fig. 3). Conversely, hSSTR3-mediated cytotoxic signalling was totally abolished by ectopically expressed catalytically inactive SHP-1 (Fig. 3). These effects were established by the SHP-1 dependency of SST-induced apoptosis (Fig. 3), intracellular acidification (Fig. 4), and decrease in mitochondrial membrane potential (Fig. 5). Additionally, we have delineated the temporal sequence of events linking caspase activation, acidification, and mitochondrial dysfunction during hSSTR3 initiated cytotoxic signalling. SHP-1-mediated activation of caspase-8 is required for SST-induced decrease in pH_i whereas caspase-3 is induced only when there is acidification (Fig. 6). Treatment of hSSTR3 expressing CHO-K1 cells with SST results in a decrease in pH_i which is also necessary for the reduction in mitochondrial membrane potential (Fig. 7). These data from SSTR3 transfected CHO-K1 cells extend our published findings in MCF-7 cells (16) that SHP-1 and caspase-8-mediated acidification occurs at a site other than the mitochondrion and that disruption of mitochondrial function leading to release of cytochrome C and activation of caspase-9 merely plays an amplifying role in SST-induced apoptosis.

(B) ***Elucidation of the Role of SHP-1 in hSSTR5 Mediated Cell Growth Arrest***

We have previously reported that the cytostatic action of SST mediated via hSSTR5 is prevented by inhibition of PTP activity (7). In ongoing studies, we have demonstrated that such signalling is SHP-1-dependent in that it is amplified by ectopic expression of this enzyme and abrogated by SHP-1C455S (Fig. 8). Specifically, we observed that the induction of Rb increased 3.5 fold in SHP-1 transfected CHO-K1-hSSTR5 cells following exposure of the cells to 100 nM D-Trp^8 SST for 4 h compared to a 2.2 fold increase in mock transfected cells. Although the maximal response was similar in both cells, as expected it occurred faster in SHP-1 overexpressing cells (12 h vs 24 h in control cells) presumably reflecting the finite nature of this response. Inactivation of SHP-1 with the catalytically inactive mutant, abolished

SST mediated induction of Rb.

The observation that hSSTR3-signalled apoptosis as well as hSSTR5-mediated inhibition of cell cycle progression are both SHP-1-dependent suggests that subtype-selective diversity of antiproliferative signalling occurs distal to SHP-1 and underscores the importance of the need to elucidate the subtype-selective signalling mechanisms that are differentially coupled to SHP-1.

***TASK 10. Subtype Selectivity For SSTR-Induced Apoptosis**

This task was completed with our report in Molecular Endocrinology that SSTR3 is the sole subtype which induces apoptosis (6). Nonetheless, we went beyond this observation to dissect out the sequence of molecular events involved in SSTR apoptotic signalling and demonstrated that SHP-1-/caspase-8-mediated acidification occurs at a site other than the mitochondrion and that SST-induced apoptosis is not dependent on disruption of mitochondrial function and caspase-9 activation (reported in J. Biol. Chem.) (16). With our finding that SSTRs form functional heterodimers with members of the receptor family, we have now expanded the model of hSSTR3 induced apoptosis to include other receptor subtypes (18,19). Although SSTR3 is the only subtype that induces apoptosis when studied as a monotransfectant, this situation is very different to breast cancer cells which typically coexpress SSTR3 with several other subtypes (reviewed in Task 1 and Fig. 1). This is not a property of tumor cells since normal cells such as islet, pituitary, immune cells, and brain neurons also express multiple SSTR subtypes (1). All of the SSTRs, however, bind the natural SST ligands, SST-14 and SST-28, with comparable low nanomolar affinity, and all five receptors also share common signalling pathways such as the ability to inhibit adenylyl cyclase and to activate PTP, raising the question of whether multiple SSTRs in the same cell are redundant, or whether they interact for greater functional diversity (1, 18). We addressed this question using hSSTR5 and hSSTR1 as models and showed that SSTRs assemble as functional homo- and heterodimers (experimental details in J. Biol. Chem., ref. 18). Homodimerization was shown in the case of hSSTR5 by functional complementation of two partially active mutants, a binding-deficient mutant of the second extracellular loop, and a binding-competent signalling-deficient C-tail deletion mutant (Δ C-tail hSSTR5). Coexpression of the two receptors rescued the loss of adenylyl cyclase coupling by Δ C-tail hSSTR5, suggesting that the binding-competent mutant associates with and signals through the C-tail of the binding-deficient mutant. Similar rescue of the loss of adenylyl cyclase coupling of Δ C-tail hSSTR5 by cotransfection with wild type hSSTR1 provided evidence of hSSTR5/hSSTR1 heterodimerization. Dimeric association altered SSTR functions such as ligand binding affinity and agonist-dependent receptor internalization and upregulation. Direct physical evidence for the association of SSTRs in intact cells was obtained by photobleaching fluorescence resonance energy transfer (pbFRET) microscopy. pbFRET analysis was applied to hSSTR5 expressed in CHO-K1 cells and showed that this receptor exists as a monomer in the basal state but undergoes dose-dependent increase in dimerization when treated with SST-14 (10^{-10}-10^{-6} M) suggesting that dimerization is induced by agonist binding. Having demonstrated that SSTRs form functional heterodimers with other family members, we wondered whether SSTRs other than SSTR3 could induce apoptosis through heterodimerization with SSTR3. This hypothesis was tested in

MCF-7 cells. Cells were treated for 48 h with 10^{-9}-10^{-7} M concentrations of subtype-selective nonpeptide agonists of SSTR1-5 described by Rohrer et al (3) and obtained through courtesy of Merck Laboratories, Rahway, New Jersey. These are organic compounds with the following characteristics: L-797591, L-779976, and L-803087 display low nanomolar affinity (expressed as Ki) for hSSTR1 (Ki 1.4 nM), hSSTR2 (Ki 0.05 nM), and hSSTR4 (Ki 0.7 nM) representing 120, 6200, and 285-fold selectivity respectively for these subtypes. L-796778 binds to hSSTR3 with Ki 24 nM representing 50-fold selectivity and L-817818 displays selectivity for two of the subtypes hSSTR5 and hSSTR1 (Ki 0.4 and 3.3 nM respectively). The compounds were dissolved in DMSO, diluted in culture medium and were well tolerated by the cells. Control experiments were carried out using our panel of stable CHO-K1 cells individually transfected with hSSTR1-5. Cells undergoing apoptosis were identified morphologically by staining with the dye HOECHST 33342 and TUNEL assays which detect chromatin condensation and nuclear shrinkage (HOECHST) and *in situ* DNA fragmentation (TUNEL) (20, 21). Fig. 9 shows the effect of the subtype selective SSTR agonists on induction of apoptosis as assessed by TUNEL Assay in CHO-K1 cells separately expressing SSTR1-5. Apoptosis occurred only in the SSTR3 monotransfectants confirming the unique cytotoxic property of this subtype. In contrast to the CHO-K1 cell monotransfectants, when MCF-7 cells were treated with the same subtype-selective SSTR agonists, apoptosis occurred through activation of multiple subtypes (Fig. 10). Thus, in addition to the SSTR3 agonist, agonists for SSTR1,2, and 5 also induced apoptosis (Fig. 10). TUNEL assays showed 23%, 22%, 19%, and 18% of apoptotic cells at 48 h following treatment with 100 nM agonist, comparable to the number obtained with SST-14 or to the SSTR1 selective peptide agonist SCH-275. As expected, the SSTR4-selective agonist was without effect, consistent with the known absence of this subtype in MCF-7 cells (Fig. 10). In summary, therefore, when SSTR1-5 are studied individually as monotransfectants, only SSTR3 induces apoptosis. In MCF-7 cells which coexpress SSTR1,2,3,5, however, treatment with selective agonists induces apoptosis via all four SSTRs. In light of our finding that SSTRs can interact through heterodimerization, the differential ability of SSTR1,2,5 to induce apoptosis when coexpressed with SSTR3 but not when expressed alone, suggests that SSTR3 is an obligatory subtype for SST-induced apoptosis, but that other SSTR subtypes can also induce apoptosis when coexpressed with SSTR3, likely through formation of SSTR3 heterodimers. These are exciting results which we will develop further with renewed funding.

***TASK 12. <u>Overexpression and Antisense Blockade of SSTRs For Effects on Apoptosis</u>**

This task became somewhat simplistic with our finding that SSTR3 is the sole receptor that signals SST-dependent apoptosis. It was essentially completed as described in our last Annual Report (1999) and led to a major new task to analyse by mutagenesis the role of the C-tail of hSSTR3 in apoptotic signalling, a study that we have now completed as described under task 13. Additionally, we have carried out new studies describing the induction of apoptosis by several SSTR subtypes through the formation of putative heterodimers with SSTR3 described under Task 10. Antisense experiments to further establish the primacy of SSTR3 in mediating SST-induced apoptosis were carried out as an extension of the antisense knockout experiments in Task 6 using MCF-7 cells as a model. Cells were treated with antisense or sense ODNs for 4 days followed by treatment with SST (1 μm) for 24 and 48 h. Cells were fixed, permeabilized, and analysed for

apoptotic cells by HOECHST and TUNEL assays. Following treatment of MCF-7 cells with ODNs to SSTR1 and SSTR2 to inactivate these two receptor subtypes, the subsequent exposure to SST resulted in 25% and 40% apoptotic cells at 24 h and 48 h respectively comparable to the apoptotic index in control sense ODN treated cells, as well as cells maintained in normal culture medium. Treatment with SST after antisense blockade of SSTR5 produced a small but not significant 5-10% decrease in the number of apoptotic cells. Treatment with SST following antisense blockade of SSTR3, however, reduced the percentage of apoptotic cells from 23% to 10% at 24 h and from 40% to 15% at 48 h providing further evidence for a selective effect of SSTR3 in mediating SST-induced apoptosis. Complementary evidence based on the effects of overexpressing SSTR3 was obtained in HEK cells transfected with hSSTR3 to give receptor expression of 1200 fmol/mg protein. Compared to control nontransfected HEK cells which showed a 2.6 fold increase in viable cells at 6 days of culture (assessed by the MTT assay) (22), cells overexpressing hSSTR3 displayed 20% decrease in proliferative activity over the same time interval. TUNEL assays confirmed apoptosis as the mechanism for the reduced proliferative activity of these cells in the absence of SST ligand. Apoptotic cells were detected early during culture and occurred at a steady 10-15% level during the 6 days of culture. This means that constitutive activation of SSTR3 induced by receptor overexpression triggers apoptosis. Our attempts to study the antiproliferative effect of hSSTR5 through overexpression were unsuccessful because despite several transfections, we failed to produce a stable HEK cell line overexpressing this subtype.

***TASK 13. <u>Mutational Analysis of The C-Tail of hSSTR3</u>**

To characterize the structural determinants of SSTR3-dependent apoptosis, we conducted mutational analysis of the role of the cytoplasmic C-tail of hSSTR3 in inducing apoptosis, with the following mutants (Fig. 11): (i) deletion of the C-tail of hSSTR3; (ii) introduction of a cysteine residue 12 amino acids downstream from the 7th transmembrane domain to create a putative palmitoylation anchor. hSSTR3 is the only SSTR whose C-tail does not possess a palmitoylation site for anchoring the proximal C-tail to the membrane, shown in other receptor subtypes to be important in receptor function (1, 23). (iii) chimeric hSSTR3/hSSTR5 receptors substituting the C-tail of hSSTR3 with that of hSSTR5 and the C-tail of hSSTR5 with that of hSSTR3. Mutant and chimeric receptors were constructed by the PCR overlap extension technique and purified by sequencing (24). Wild type, mutant, and chimeric receptors were stably expressed in HEK293 cells to achieve comparable levels of expression (Fig. 12). The binding affinity (K_D) and capacity (Bmax) of the mutant receptors was similar to that of wild type receptors, and like wild type receptors the mutant receptors were all functionally coupled to inhibition of adenylyl cyclase measured as dose-dependent inhibition of forskolin-stimulated cAMP by SST-14 (Fig. 12). The number of viable cells were analysed by MTT assay, and cells undergoing apoptosis were monitored by TUNEL and HOECHST assays. Compared to nontransfected HEK cells, wild type hSSTR3 cells treated with SST-14 (100 nM) showed 59% inhibition of cell growth at day 4 (Fig. 13). The palmitoylation mutant showed reduced ability to inhibit SST-14 induced cell growth, down to 48% whereas the C-tail deletion mutant displayed virtually complete loss of antiproliferation. The two chimeric receptors retained full ability to inhibit cell growth. To determine the contribution of apoptosis to the antiproliferative effect of SST-14, cells were analysed by HOECHST and TUNEL assays at day

2. Quantitative data for TUNEL assays are presented in Fig. 14. Compared to 28% apoptosis shown by wild type hSSTR3, the palmitoylation mutant displayed reduced 16% apoptosis. Deletion of the hSSTR3 C-tail abolished apoptosis and likewise substitution of the hSSTR3 C-tail with that of hSSTR5 markedly attenuated apoptosis. On the other hand, substitution of the C-tail of hSSTR5, **a nonapoptotic subtype** with that of hSSTR3 resulted in gain of apoptotic function by hSSTR5, with a potent response comparable to that of wild type hSSTR3. Representative HOECHST and TUNEL stained cells from this experiment are depicted in Fig. 15 and show nuclear shrinkage and *in situ* DNA fragmentation which was more pronounced in the case of wild type hSSTR3 and the hSSTR3 C-tail/SSTR5 chimera. Although both chimeric receptors exerted comparable cell growth inhibition, the underlying mechanisms are different involving apoptosis only in the case of the SSTR3 C-tail substituting chimera, and presumably cytostasis in the case of the reverse chimera. Finally, the dissociated effect of some of the mutants on G protein coupled adenylyl cyclase inhibition (Fig. 12) and induction of apoptosis (Fig. 14) indicates a specific functional role of the hSSTR3 C-tail in triggering cytotoxic signalling through direct protein-protein interaction. The finding that deletion of the C-tail of SSTR3 abrogates SSTR3-induced apoptosis whereas substitution of the C-tail of SSTR5 with that of SSTR3 confers apoptosis in the chimeric receptor clearly suggests that apoptotic signalling by SSTR3 is dependent on molecular signals in the receptor C-tail. Identification of these regulatory sequences and the intracellular proteins that interact with them to initiate the apoptotic signalling cascade will be pursued through renewed funding.

***TASK 14. <u>Mutational Analysis of the C-Tail of hSSTR5</u>**

In this set of experiments, we aimed to identify the structural determinants within the C-tail of hSSTR5 that regulate subtype-selective antiproliferative signalling. Following our initial documentation that cell growth inhibition leading to apoptosis occurs uniquely via hSSTR3 (6), we reported subsequently that negative regulation of cell growth by hSSTR5 leads to cell cycle arrest but not apoptosis (7). hSSTR5 mediated antiproliferative signalling leads to the induction of Rb and the cyclin-dependent kinase inhibitor p21 followed by Gi cell cycle arrest. Western blot analysis of hSSTR5 expressing CHO-K1 cells treated with octreotide revealed an increase in the hypophosphorylated form of Rb (7). Since phosphorylation of Rb is required for cell cycle exit from Gi to S, these findings suggest that SST regulates Rb phosphorylation under conditions that induce cell growth arrest. C-tail truncation mutants of hSSTR5 displayed progressive loss of antiproliferative signalling suggesting a crucial role of the C-tail domain of hSSTR5 in cytostatic signalling. Since phosphorylation on serine and threonine residues plays an important role in G protein coupled receptor regulatory functions such as effector coupling, agonist-dependent desensitization and internalization, we have extended our study of the requirement of the C-tail of hSSTR5 in cytostatic signalling to an investigation of the role of phosphorylation sites within the C-tail. We have constructed 7 mutant hSSTR5 receptors by PCR mutagenesis in which putative phosphorylation sites on Threonine (T) and Serine (S) residues were replaced by Alanine (A) residues as follows: S314A, S325A, T333A, T347A, T351A, T360A, and S361A (schematically depicted in Fig. 16). To date the four Threonine mutants T333A, T347A, T351A, and T360A, have been stably transfected in CHO-K1 cells, characterized pharmacologically for binding (K_D and Bmax), coupling to adenylyl cyclase (determined as percent inhibition of forskolin-stimulated

cAMP) and coupling to cytostatic signalling (assessed as change in Gi/S ratio and induction of Rb). The four mutants displayed comparable K_D and Bmax compared to wild type hSSTR5 (Table 3). Likewise the four mutant receptors retained the ability to inhibit forskolin-stimulated cAMP levels with dose-dependent maximum inhibition comparable to wild type hSSTR5. Interestingly, all four mutations significantly affected the coupling of hSSTR5 to antiproliferative signalling. Three of the mutants T333A, T347A, and T360A displayed near total loss of the ability to induce Rb; the T351A mutant showed a 4-fold reduction in the efficacy of the receptor to signal Rb induction (Fig. 17). These changes were correlated with the inability of the four mutants to signal cell cycle arrest as indicated by the effect of SST treatment on Gi/S ratio in these cells (Fig. 18). This work is still in progress and will test the remaining three mutants to complete the analysis of all putative C-tail phosphorylation sites. The results that we have obtained already are dramatic and show a critical role of phosphorylation in cytostatic signalling by the C-tail of hSSTR5. Furthermore, the dissociated effect between adenylyl cyclase coupling and antiproliferative signalling indicates that phosphorylation of C-tail residues is not required for receptor coupling to adenylyl cyclase and that the cAMP signalling pathway does not influence cytostatic signalling by hSSTR5.

*TASK 15. Studies of cAMP Effects on SSTR-Mediated Apoptosis

In the last Annual Report we had begun an investigation of the interaction between SST-induced apoptosis and the cAMP signalling pathway and shown that apoptosis is inhibited by cAMP-mediated prevention of acidification. Increasing intracellular cAMP with dbcAMP or forskolin before and during SST treatment attenuated SST-induced acidification and prevented apoptosis in MCF-7 cells. Addition of dbcAMP to cells during SST treatment, however, showed that once acidification sets in, cAMP is ineffective in preventing apoptosis. It was our plan to conduct futher experiments to investigate the underlying mechanisms. Since cAMP is known to phosphorylate and inactivate the Na^+/H^+ exchanger (NHE), our findings suggest the involvement of NHE in SST-induced acidification. We tried to embark on studies of SSTR3-induced modulation of NHE but were simply overwhelmed by the scope of this undertaking given that there are six NHE isoforms and that we would have to characterize at least three of the principal ones in SSTR3/NHE cell cotransfectants. Such studies will also have to be coupled with our ongoing work on the mutational analysis of the hSSTR3 C-tail. Accordingly, although mainly descriptive, we are preparing a manuscript of our existing results of the interaction between SST-induced apoptosis and the cAMP signalling pathway (presented in Fig. 4 of last year's report) and will pursue the mechanisms involving NHE and intracellular acidification through separate funding.

KEY RESEARCH ACCOMPLISHMENTS

- Showing that the incidence of SSTR1-5 mRNA expression by RT-PCR displays overall 78% correlation with SSTR1-5 protein expression by immunocytochemistry. Receptor immunoreactivity is localized both in tumor cells as well as in surrounding peritumoral structures especially blood vessels, immune cells, and stromal cells. SSTR immunocytochemistry can thus be applied for routine analysis of SSTR subtype expression in surgical samples of breast tumor tissue.

- Showing that overexpression of hSSTR3 in HEK-293 cells leads to constitutive induction of apoptosis.

- Showing that antisense blockade of hSSTR3 in MCF-7 cells blocks SST-induced apoptosis in these cells.

- Demonstrating that overexpression of SHP-1 amplifies the apoptotic effect of SST and that inactivation of SHP by dominant negative expression of catalytically inactive SHP-1 abolishes hSSTR3-mediated cytotoxic signalling. SHP-1-dependent, SST-induced apoptosis is associated with activation of caspase-8 and decrease in mitochondrial membrane potential.

- Showing that hSSTR5 exists in the basal state as inactive monomer. Activation by SST induces dose-dependent formation of functional homodimers. hSSTR5 also forms heterodimers with hSSTR1. Heterodimerization results in novel receptors with pharmacological properties distinct from those of the separate monomer components.

- Showing that SSTR3 is the only subtype that undergoes apoptosis when studied as a monotransfectant, but that in MCF-7 cells which coexpress SSTR1,2,3,5, treatment with nonpeptide agonists selective for each subtype induces apoptosis via all four SSTRs likely through formation of heterodimers with SSTR3.

- Showing that deletion of the C-tail of hSSTR3 abrogates SSTR3-induced apoptosis whereas substitution of the C-tail of SSTR5 with that of SSTR3 confers apoptosis in the chimeric receptor.

- Showing that cytostatic signalling by hSSTR5 associated with induction of Rb is SHP-1-dependent, is amplified by overexpression of this enzyme and abrogated by blockade of the enzyme with catalytically inactive SHP-1.

- Showing that point mutations of putative phosphorylation sites in the C-tail of hSSTR5 block the ability of the receptor to undergo SST promoted Rb induction and cell cycle arrest.

REPORTABLE OUTCOMES

1) Rocheville, M., D. Lange, U. Kumar, R. Sasi, R.C. Patel, and Y.C. Patel. Subtypes of the somatostatin receptor assemble as functional homo- and heterodimers. J. Biol. Chem. 275:7862-7869, 2000.

2) Liu, D., G. Martino, M. Thangaraju, M. Sharma, F. Halwani, S-H Shen, Y.C. Patel, and C.B. Srikant. Caspase-8-mediated intracellular acidification preceeds mitochondrial dysfunction in somatostatin-induced apoptosis. J. Biol. Chem. 275:9244-9250, 2000.

3) Patel, Y.C. Somatostatin. In Principles & Practice of Endocrinology and Metabolism, Becker, K. (Ed), Third Edition, J.B. Lippincott Co., 2000 (in press).

4) Papotti, M., Kumar, U., Volante, M., Pecchioni, C., and Patel, Y.C. Immunohistochemical detection of somatostatin receptor types 1-5 in medullary carcinoma of the thyroid. Clinical Endocrinology 2000 (in press).

5) Patel, Y.C. et al. Immunohistochemical and mRNA expression of SSTR types 1-5 in primary human breast cancer. Correlation with tumor pathology, estrogen, and progesterone receptor status. Cancer Research (in preparation).

6) Rocheville, M., Kumar, U., Srikant, C.B., Chan, M. and Patel, Y.C. Apoptotic signalling by somatostatin receptor type 3 (SSTR3) requires molecular signals in the receptor C-tail. J. Biol. Chem. (in preparation).

7) Rocheville, M., Kumar, U., Patel, R.C., and Patel, Y.C. Induction of apoptosis by multiple SSTR subtypes through formation of hetero-oligomers with SSTR3. (Manuscript in preparation).

8) Rocheville, M., Srikant, C.B., and Patel, Y.C. Putative phosphorylation sites in carboxyl-terminus of human somatostatin receptor type 5 mediate agonist-dependent regulation and cytostatic signalling. J. Biol. Chem. (In preparation).

9) Liu, D., Patel, Y.C., and Srikant, C.B. Somatostatin-induced apoptosis is inhibited by cAMP-mediated prevention of acidification. (Manuscript in preparation).

10) Liu, D., Martino, G., Thangaraju, M., Sharma, M., Halwani, F., Shen, S-H, and Patel, Y.C. SHP-1-dependent, caspase-8-mediated, acidification and apoptosis are not dependent on mitochondrial dysfunction. Program Annual Meeting American Association For Cancer Research, San Francisco, CA., April 1-5, 2000 (Abstr. #987).

11) Patel, Y.C., Rocheville, M., Semaan, L., Sasi, R., Srikant, C.B., Khare, S., Chan, M., and Patel, Y.C. Apoptotic signalling by somatostatin receptor type 3 (SSTR3) requires molecular signals in the receptor C-tail. Department of Defense Breast Cancer Research Program Meeting: Era of Hope, Atlanta, Georgia, June 8-12, 2000.

12) Srikant, C.B., Sharma, K., Thangaraju, M., Liu, D., Patel, Y.C., and Shen, S-H. hSSTR subtype-selectivity for cytotoxic and cytostatic antiproliferative signalling. Department of Defense Breast Cancer Research Program Meeting: Era of Hope, Atlanta, Georgia, June 8-12, 2000.

13) Rocheville, M., Kumar, U., Semaan, L., Sasi, R., Srikant, C.B., Khare, S., Chan, M., and Patel,

Y.C. Apoptotic signalling by somatostatin receptor type 3 (SSTR3) requires molecular signals in the receptor C-tail. Program Annual Meeting U.S. Endocrine Society, Toronto, Canada, June 21-24, 2000.

14) Rocheville, M., Kumar, U., and Patel, Y.C. Multiple somatostatin receptor subtypes (SSTRs) can induce apoptosis through formation of hetero-oligomers with SSTR3. Program 11th International Congress of Endocrinology, Sydney, Australia, October 29-November 2, 2000.

15) Srikant, C.B., Sharma, K., Thangaraju, M., Liu, D., Martino, G., Patel, Y.C., and Shen, S-H. Cytotoxic and cytostatic antiproliferative actions of somatostatin. Program 11th International Congress of Endocrinology, Sydney, Australia, October 29-November 2, 2000.

CONCLUSIONS

Breast tumors show rich expression of multiple SSTR subtypes and may be amenable to treatment with selective SST compounds. All five SSTRs variably inhibit cell growth. When studied as individual subtypes expressed in host cells, SSTR3 is the only isoform that induces apoptosis whereas SSTR1,2,4 and 5 promote cell growth arrest with SSTR5 exerting the most potent effect. Both apoptotic and cytostatic signalling are dependent on receptor-mediated activation of SHP-1. Cytostasis then proceeds through activation of Rb and p21 whereas apoptosis is associated with caspase-8-mediated intracellular acidification and decrease in mitochondrial membrane potential. Apoptotic signalling by SSTR3 requires molecular signals in the receptor C-tail. Likewise, the C-tail of hSSTR5, and specifically its phosphorylation state is crucial for the ability of this receptor to initiate cytostatic signalling. Endogenous SSTRs that are coexpressed as multiple subtypes in the same cell are capable of associating as functional heterodimeric receptors whose properties differ from those of the separate monomer components. Although SSTR3 is the only subtype that undergoes apoptosis when studied as a monotransfectant, SSTR1,2, and 5 are also capable of inducing apoptosis when coexpressed with SSTR3. This means that SSTR3 is an obligatory receptor for SST-induced apoptosis but that other SSTR subtypes can also induce apoptosis through heterodimerization with SSTR3.

REFERENCES

1) Patel, Y.C. Somatostatin and its receptor family. Frontiers in Neuroendocrinology 20:157-198, 1999.
2) Reisine, T. and Bell, G.I. Molecular biology of somatostatin receptors. Endocre. Rev. 16:427-442, 1995.
3) Rohrer, S.P., Birzin, E.T., Mosley, R. T. Rapid identification of subtype-selective agonists of the somatostatin receptor through combinatorial chemistry. Science 282:737-740, 1998.
4) Lamberts, S.W.J., Van Der Lely, A-J, Deherder, W.W. et al. Drug therapy: Octreotide. New Eng. J. Med. 334:246-254, 1996.
5) Patel, Y.C. Somatostatin. In Principles & Practice of Endocrinology and Metabolism, Becker

K. (Ed), Third Edition, J.B. Lippincott Co., pp. ----, 2000 (in press).

6) Sharma, K., Patel, Y.C., Srikant, C.B. Subtype-selective induction of p53-dependent apoptosis but not cell cycle arrest by human somatostatin receptor 3. Mol. Endocrinol. 10:1688-1696, 1996.
7) Sharma, K., Patel, Y.C., Srikant, C.B. C-terminal region of human somatostatin receptor 5 is required for induction of Rb and Gi cell cycle arrest. Mol. Endocrinol. 13:82-90, 1999.
8) Patel, Y.C., M.T. Greenwood, R. Panetta, N. Hukovic, S. Grigorakis, L-A Robertson and C.B. Srikant. Metabolism 45 (8):31-38, 1996.
9) Hierowski, M.T., Liebow, C., Dusapin, K., Schally, A.V. Stimulation by somatostatin of dephosphorylation of membrane proteins in pancreatic cancer Mia PaCA-2 cell line. FEBS Lett 179:252-256, 1985.
10) Pan, M.G., Florio, T., Stork, P.J.S. G protein activation of a hormone-stimulated phosphatase in human tumor cells. Science 256:1215-1217, 1992.
11) Neel, B. Structure and function of SH2-domain containing tyrosine phosphatase. Semin Cell Biol. 4:419-432, 1993.
12) Srikant, C.B. and Shen, S-H. Octapeptide somatostatin analog SMS201-995 induces translocation of intracellular PTP-1C to membranes in MCF-7 human breast cancer adenocarcinoma cells. Endocrinology 137:3461-3468, 1996.
13) Sharma, K., Srikant, C.B. Induction of wild type p53 Bax and acidic endonuclease during somatostatin signalled apoptosis in MCF-7 human breast cancer cells. Int. J. Cancer 76:259-266, 1998.
14) Rocheville, M., Kumar, U., Semaan, L., Sasi, R., Srikant, C.B., Khare, S., Chan, M., and Patel, Y.C. Apoptotic signalling by somatostatin receptor type 3 (SSTR3) requires molecular signals in the receptor C-tail. Program 82nd Annual Meeting of the US Endocrine Society, Toronto, Canada, June 2000, p. 175 (Abstr. #706).
15) Sharma, K., C.B. Srikant. G protein coupled receptor signalled apoptosis is associated with activation of a cation insensitive acidic endonuclease and intracellular acidification. Biochem. Biophys. Res. Commun. 242:134-140, 1998.
16) Liu, D., Martino, G., Thangaraju, M., Sharma, M., Halwani, F., Shen, S-H, Patel, Y.C., and Srikant, C.B. Caspase-8-mediated intracellular acidification preceeds mitochondrial dysfunction in somatostatin-induced apoptosis. J. Biol. Chem. 275:9244-9250, 2000.
17) Aguila, M.C., Rodriguez, A.M., Aguila-Mansilla, H.N., and Lee, W.T. Somatostatin antisense oligodeoxynucleotide-mediated stimulation of lymphocyte proliferation in culture. Endocrinology 137:1585-1590, 1996.
18) Rocheville, M., Lange, D., Kumar, U., Sasi, R., Patel, R.C., and Patel, Y.C. Subtypes of the somatostatin receptor assemble as functional homo- and heterodimers. J. Biol. Chem. 275:7862-7869, 2000.
19) Rocheville, M., Lange, D., Kumar, U., Patel, S.C., Patel, R.C., and Patel, Y.C. Receptors for dopamine and somatostatin form heterodimers with enhanced functional activity. Science 288:154-157, 2000.
20) Forloni, G., Lucca, E., Angeretti, N., Chiesa, R., and Vezzani, A. Neuroprotective effect of somatostatin on NO, apoptotic NMDA-induced neuronal death. Role of Cyclic GMP. J. Neuro. Chem. 68:319-327, 1996.

21) Simonian, N.A., Getz, R.L., Leveque, J.C., Konradi, C., and Coyle, J.T. Kainate induces apoptosis in neurons. Neuroscience 74:675-683, 1996.
22) Liu, Y., Peterson, D.A., Kimura, H. and Schubert, D. Mechanism of cellular 3-(4,5-dimethylthiazole2-YL)-2,5 diphenyltetrazolium bromide MTT reduction. J. Neurochem. 69:581-593, 1997.
23) Hukovic, N., Panneta, R., Kumar, U., Rocheville, M., and Patel, Y.C. The cytoplasmic tail of the human somatostatin receptor type 5 is crucial for interaction with adenylyl cyclase and in mediating desensitization and internalization. J. Biol. Chem. 273:21416-21422, 1998.
24) Hukovic, N., Rocheville, M., Kumar, U., Sasi, R., Khare, S. and Patel, Y.C. Agonist-dependent upregulation of human somatostatin receptor type 1 (hSSTR1) requires molecular signals in the cytoplasmic C-tail. J. Biol. Chem. 274:24550-24558, 1999.

KEY PERSONNEL SUPPORTED BY THIS AWARD

Chan, M.
Khare, S.
Sasi, R.
Kumar, U.
Glinka, Y.
Geci, C.
Allard, B.

TABLE 1

COMPARISON OF SSTR1-5 mRNA EXPRESSION WITH SSTR1-5 IMMUNOCYTOCHEMISTRY IN HUMAN BREAST TUMOR SAMPLES (Study 2) (n=19)

CASE #	SSTR1	SSTR2	SSTR3	SSTR4	SSTR5
10817	++++ 0	++ 1	+ 1	++ 1	- 1
11238	++ 1	+ 0	+ 0	++ 0	- 0
11279	++ 1	++++ 1	+ 1	+ 0	+ 1
11350	+ 1	+ 1	+ 1	++ 1	+ 1
11361	+++ 1	++ 1	+ 1	++++ 1	- 0
11600	++++ 1	+ 1	+ 1	+ 0	+ 1
11603	+++ 1	+++ 0	+ 1	+++ 0	++ 1
12472	+++ 1	+ 1	+ 1	++ 1	- 1
12710	+++ 0	++ 1	+ 1	++ 1	- 1
12723	++++ 1	++ 1	+ 1	+ 1	++ 1
12831	+ 1	+ 1	+ 1	++ 1	+ 1
12866	+++ 1	- 1	- 1	+ 1	- 1
12924	++++ 1	+ 1	+ 1	+++ 1	+++ 1

12999	+++ 0	+++ 1	+ 1	+ 1	+ 1
13087	++ 1	++ 1	+ 1	+ 1	+ 1
13094	++++ 1	+++ 1	+ 1	++ 0	- 0
13150	+++ 1	+ 1	+ 1	++ 1	- 1
13175	++ 1	- 1	+ 1	+ 1	+ 1
13410	++ 1	+ 1	+ 1	+ 0	- 1

In each paired analysis, SSTR mRNA expression is shown as + to ++++ based on quantitative RT-PCR. Absence of SSTR mRNA is indicated by -. The presence or absence of SSTR immunoreactivity by peroxidase immunocytochemistry in the matching samples is shown as 1 or 0 respectively. A match between SSTR mRNA and protein expression by immunocytochemistry is indicated by the shaded boxes.

TABLE 2

CORRELATION BETWEEN SSTR mRNA (by RT-PCR) and SSTR PROTEIN EXPRESSION (BY IMMUNOCYTOCHEMISTRY) IN DUCTAL NOS PRIMARY HUMAN BREAST CANCER SAMPLES (n = 19)

	Samples Displaying Concordance For mRNA and Protein Expression	
Receptor	**Number**	**%**
SSTR1	16/19	84
SSTR2	15/19	79
SSTR3	17/19	89
SSTR4	13/19	68
SSTR5	13/19	68
SSTR1-5	74/95	78

TABLE 3.

BINDING CHARACTERISTICS AND COUPLING TO ADENYLYL CYCLASE OF WILD TYPE AND MUTANT hSSTR5 RECEPTORS

RECEPTOR	Kd (nM)	Bmax (fmol/mg protein)	% inhibition of Fsk-stimulated cAMP (at 10^{-6}M SST-28)
WT hSSTR5	0.31±0.02	162±21	52±2
T333A hSSTR5	0.75±0.14	119±43	65±2
T347A hSSTR5	0.42±0.08	102±36	58±2
T351A hSSTR5	0.39±0.19	90±51	51±4
T360A hSSTR5	0.22±0.11	70±40	46±2

FIGURE LEGENDS

FIGURE 1. Incidence of SSTR mRNA in 98 primary human ductal NOS tumors. These results are based on two separate batches of frozen tumor tissue analysed for SSTR mRNA by semi-quantitative RT-PCR as described in Task 1. The upper panels show adjacent sections of a representative grade 4 ductal NOS tumor strongly positive for SSTR1, 2, and 3, weakly positive for SSTR4 and negative for SSTR5 by peroxidase immunocytochemistry.

FIGURE 2. Effect of treatment of MCF-7 cells for 4 days with antisense or sense oligonucleotides to SSTR1, 2, 3, and 5 on receptor protein expression detected by rhodamine immunofluorescence. Note the marked reduction in the level of fluorescent labelling of antisense-treated cells compared to sense-treated or control cells.

FIGURE 3. SHP-1 dependency of hSSTR3-mediated cytotoxic signalling revealed by the potentiation of D-Trp^8 SST-14-induced apoptosis by overexpression of SHP-1 and its abrogation by the dominant negative suppressive action by expression of inactive mutant SHP-1C455S. Cells were incubated with 100 nM peptide for the indicated times and apoptotic cells were labelled with the dye HOECHST 33342 and quantitated by flow cytometry (mean $\pm$ SE, n=4).

FIGURE 4. hSSTR3 signalled intracellular acidification is SHP-1-mediated. CHO-K1 cells treated with 100 nM D-Trp^8 SST-14 for 24 h were loaded with the cell permeable dye carboxy-SNARF-1 acetoxymethylester during the final hour and cell pH was measured by radiometric analysis of its fluorescence at 580 and 640 nM using a flow cytometer. VC, mock transfected cells, SHP-1, cells transfected with active SHP-1; SHP-1C455S cells transfected with the catalytically inactive mutant SHP-1. Note the abrogation of intracellular acidification by inactivation of SHP-1. (mean $\pm$ SE, n=4).

FIGURE 5. D-Trp^8 SST-14 induced reduction in mitochondrial membrane potential ($\Delta\Psi$m) in hSSTR3 expressing CHO-K1 cells. Following incubation with 100 nM peptide for 24 h, cells were loaded with the dye DiOC6(3). Reduction in mitochondrial membrane potential was assessed by the decrease in the fluorescence intensity of the dye. The catalytically inactive mutant SHP-1C455S suppressed the effect of D-Trp^8 SST-14 (mean $\pm$ SE, n=4).

FIGURE 6. The obligatory involvement of SHP-1 in hSSTR3-mediated cytotoxic signalling was also established by the inductive effect of D-Trp^8 SST-14 on caspases. Caspase-8 activity (solid bars) was measured in extracts of CHO-K1/hSSTR3 cells incubated in the absence or presence of 100 nM peptide for 6 h using the substrate IETD-AMC. Activities of caspase-9 and caspase-3 were measured using LEHD-AMC (hatched bars) and DEVD-AMC (speckled bars) respectively as substrates in cells treated for 24 h. Fluorescence intensity of the aminomethylcoumarin (AMC) was analysed by

spectrofluorimetry (mean ± SE, n=4).

FIGURE 7. hSSTR3 signaled activation of caspase-3 but not caspase-8 is acidification- dependent. CHO-K1/hSSTR3 cells were incubated with 100 nM D-Trp^8 SST-14 (hatched bars) for 24 h in the absence or presence of 25 ng nigericin (speckled bars). Nigericin-induced pH clamping abolished the activation of caspase-3 (DEVD-ase), but not caspase-8 (IETD-ase) (mean ± SE, n=4).

FIGURE 8. SHP-1-dependent induction of Rb by D-Trp^8 SST-14 in CHO-K1/hSSTR5 cells. The ability of the peptide (100 nM) to induce Rb during 4 h treatment was assessed in mock transfected cells (vector control), or cells transfected with SHP-1 or its inactive mutant SHP-1C455S. Rb was assessed by flow cytometry following staining with anti Rb antibody and FITC-conjugated secondary antibody. The effectiveness of the peptide was increased by > 50% by overexpressed SHP-1 and was abrogated by the inactive SHP-1 mutant (mean ± SE, n=4).

FIGURE 9. Induction of apoptosis by selective nonpeptide SST agonists in CHO-K1 cells expressing individual SSTRs. Apoptosis was detected by TUNEL assay. Note the large number of rounded TUNEL-positive cells in SSTR3 expressing cells. There was minimal or no apoptosis in SSTR1,2,4, and 5 expressing cells.

FIGURE 10. Induction of apoptosis in MCF-7 cells by SSTR subtype-selective nonpeptide agonists. Apoptosis was detected by TUNEL assay. The lower panel shows a histogram of the mean (± SE) percent of apoptotic cells induced by treatment with SSTR1, SSTR2, SSTR3, SSTR4, and SSTR5 selective nonpeptide agonists compared with control, SST-14, and the SSTR1-selective peptide agonist SCH275.

FIGURE 11. Schematic depiction of wild type, mutant and chimeric SSTR3/SSTR5 receptors. ΔC-SSTR3, C-tail deletion mutant of hSSTR3; palm-SSTR3, mutant with a cys residue inserted 12 amino acids downstream from the 7th transmembrane domain to create a putative palmitoylation anchor; SSTR3/R5C, chimeric receptor substituting the C-tail of hSSTR5 in hSSTR3; SSTR5/R3C, chimeric receptor substituting the C-tail of hSSTR3 in hSSTR5.

FIGURE 12. Binding and signalling profiles of wild type, mutant and chimeric SSTR3/SSTR5 receptors. All of the mutant receptors were functionally coupled to adenylyl cyclase as determined by their ability to show dose-dependent inhibition of forskolin-stimulated cAMP levels by SST.

FIGURE 13. Somatostatin-induced inhibition of growth of HEK293 cells expressing wild type, mutant and chimeric SSTR3/SSTR5 receptors. Cell growth was assessed by MTT assay (mean ± SE, n=4).

FIGURE 14. SST-14 induced apoptosis of HEK293 cells expressing wild type, mutant and chimeric SSTR3/SSTR5 receptors. Percent apoptotic cells was analysed by TUNEL assay at day 2 (mean ± SE, n=4).

FIGURE 15. Representative HOECHST dye and TUNEL-stained HEK293 cells expressing wild type mutant and chimeric SSTR3/SSTR5 receptors. Note the pronounced nuclear shrinkage (HOECHST labelling) and *in situ* DNA fragmentation detected by TUNEL labelling in the case of wild type SSTR3 and the SSTR5 chimera substituted with the SSTR3 C-tail (SSTR5/R3 receptor).

FIGURE 16. Schematic depiction of hSSTR5 C-tail sequence showing putative phosphorylation sites on Serine and Threonine residues. Point mutations were created by substituting Alanine (A) for each of the Serine (S) and Threonine (T) residue.

FIGURE 17. Requirement of Thr phosphorylation in the C-tail of hSSTR5 for cytostatic signalling. The ability of D-Trp^8 SST-14 to induce Rb was compared in CHO-K1 cells expressing wild type hSSTR5 or its point mutants substituting T → A at residues 333, 347, 351, and 360. A 4-fold reduction in D-Trp^8 SST-14-induced increase in Rb immunofluorescence was seen with the T351A mutant. T → A substitutions at 333, 347, and 360 residues resulted in complete loss of Rb induction (mean ± SE, n=4).

FIGURE 18. Requirement of Thr phosphorylation in the C-tail of hSSTR5 for cytostatic signalling. The ability of D-Trp^8 SST-14 to induce cell cycle arrest was compared in CHO-K1 cells expressing wild type hSSTR5 or point mutants substituting T → A at residues 333, 347, 351, and 360. The increase in Gi/S ratio (expressed as fold change compared to that in the respective untreated cells taken as 1) which gives an index of cell cycle arrest was seen only in agonist-treated cells expressing the wild type receptor. The C-tail mutants showed complete (T333A, T347A, T360A) or partial (T351A) escape from SST-induced cytostasis. The Gi/S ratios in untreated and treated CHO-K1/hSSTR5 cells were 6.5 ± 0.86 and 15.6 ± 1.9 respectively (mean ± SE, n=4).

APPENDIX

1) Rocheville, M., D. Lange, U. Kumar, R. Sasi, R.C. Patel, and Y.C. Patel. Subtypes of the somatostatin receptor assemble as functional homo- and heterodimers. J. Biol. Chem. 275:7862-7869, 2000.

2) Liu, D., G. Martino, M. Thangaraju, M. Sharma, F. Halwani, S-H Shen, Y.C. Patel, and C.B. Srikant. Caspase-8-mediated intracellular acidification preceeds mitochondrial dysfunction in somatostatin-induced apoptosis. J. Biol. Chem. 275:9244-9250, 2000.

3) Patel, Y.C. Somatostatin. In Principles & Practice of Endocrinology and Metabolism, Becker, K. (Ed), Third Edition, J.B. Lippincott Co., 2000 (in press).

4) Papotti, M., Kumar, U., Volante, M., Pecchioni, C., and Patel, Y.C. Immunohistochemical detection of somatostatin receptor types 1-5 in medullary carcinoma of the thyroid. Clinical Endocrinology 2000 (in press).

5) Liu, D., Martino, G., Thangaraju, M., Sharma, M., Halwani, F., Shen, S-H, and Patel, Y.C. SHP-1-dependent, caspase-8-mediated, acidification and apoptosis are not dependent on mitochondrial dysfunction. Program Annual Meeting American Association For Cancer Research, San Francisco, CA., April 1-5, 2000 (Abstr. #987).

6) Patel, Y.C., Rocheville, M., Semaan, L., Sasi, R., Srikant, C.B., Khare, S., Chan, M., and Patel, Y.C. Apoptotic signalling by somatostatin receptor type 3 (SSTR3) requires molecular signals in the receptor C-tail. Department of Defense Breast Cancer Research Program Meeting: Era of Hope, Atlanta, Georgia, June 8-12, 2000.

7) Srikant, C.B., Sharma, K., Thangaraju, M., Liu, D., Patel, Y.C., and Shen, S-H. hSSTR subtype-selectivity for cytotoxic and cytostatic antiproliferative signalling. Department of Defense Breast Cancer Research Program Meeting: Era of Hope, Atlanta, Georgia, June 8-12, 2000.

8) Rocheville, M., Kumar, U., Semaan, L., Sasi, R., Srikant, C.B., Khare, S., Chan, M., and Patel, Y.C. Apoptotic signalling by somatostatin receptor type 3 (SSTR3) requires molecular signals in the receptor C-tail. Program Annual Meeting U.S. Endocrine Society, Toronto, Canada, June 21-24, 2000.

9) Rocheville, M., Kumar, U., and Patel, Y.C. Multiple somatostatin receptor subtypes (SSTRs) can induce apoptosis through formation of hetero-oligomers with SSTR3. Program 11th International Congress of Endocrinology, Sydney, Australia, October 29-November 2, 2000.

10) Srikant, C.B., Sharma, K., Thangaraju, M., Liu, D., Martino, G., Patel, Y.C., and Shen, S-H. Cytotoxic and cytostatic antiproliferative actions of somatostatin. Program 11th International Congress of Endocrinology, Sydney, Australia, October 29-November 2, 2000.

EXPRESSION OF SSTR1-5 IN PRIMARY DUCTAL NOS BREAST CANCER SAMPLES

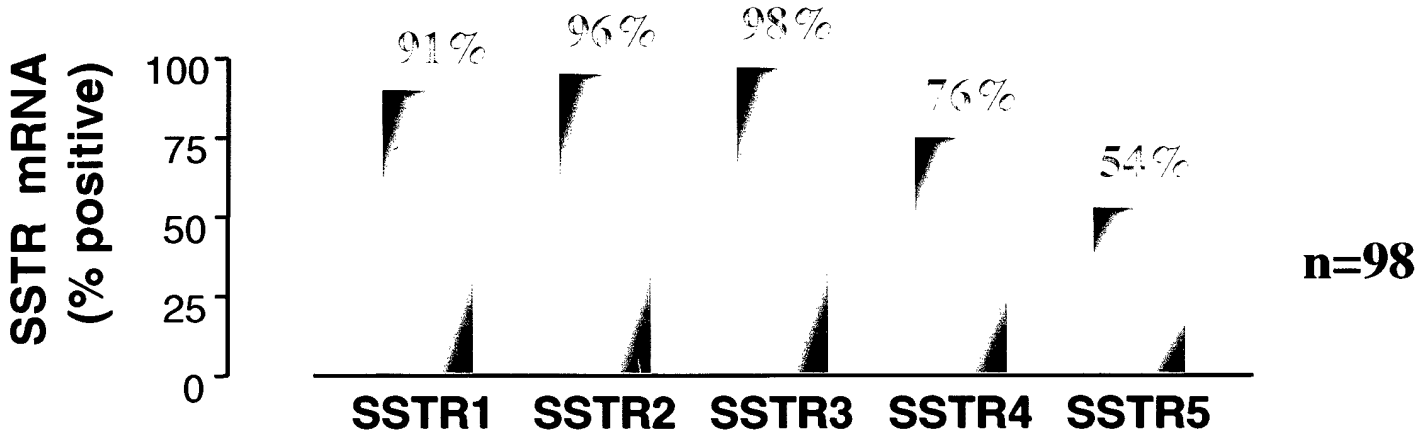

FIGURE 1.

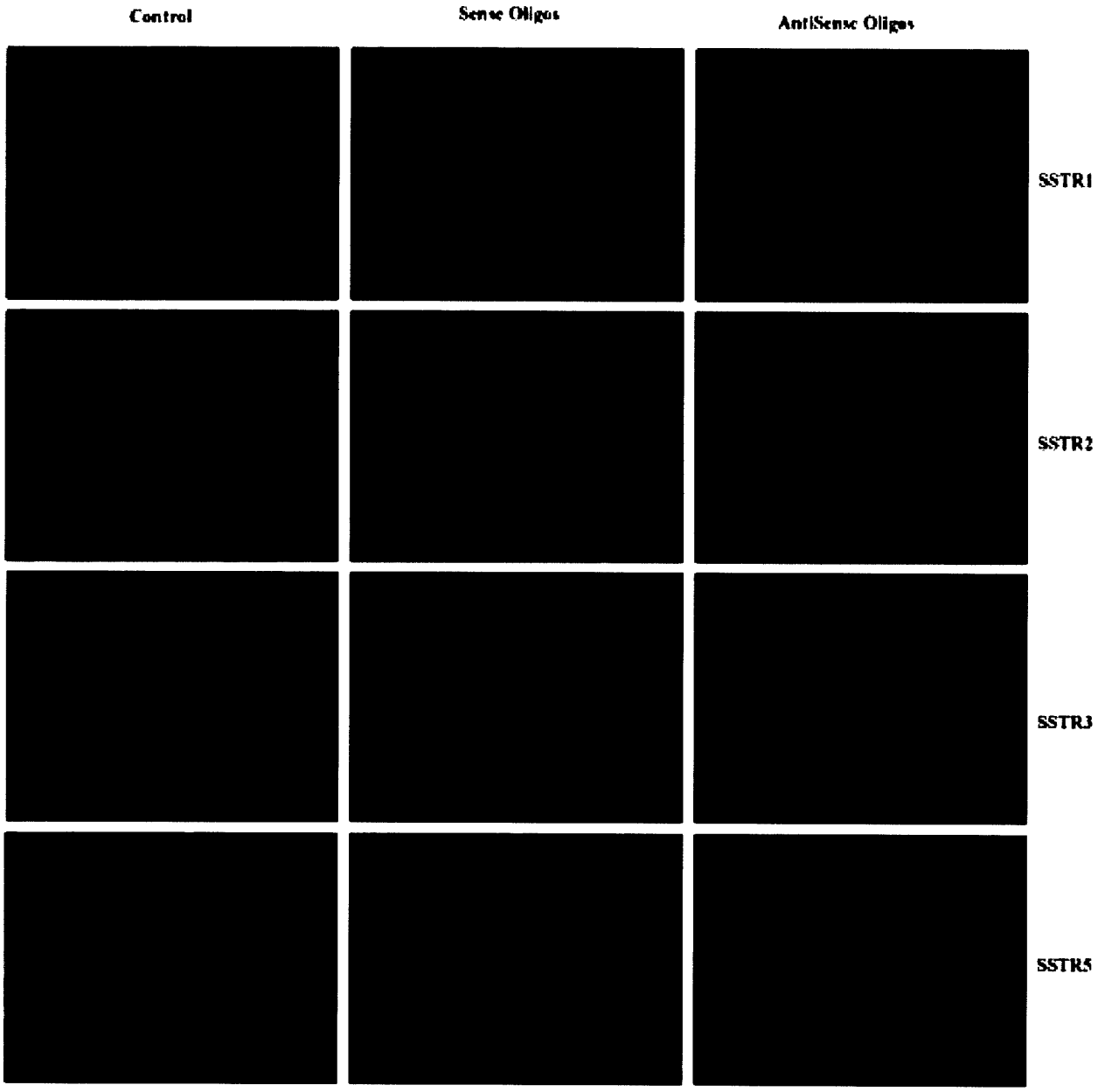
Control
Sense Oligos
AntiSense Oligos
SSTR1
SSTR2
SSTR3
SSTR5

FIGURE2.

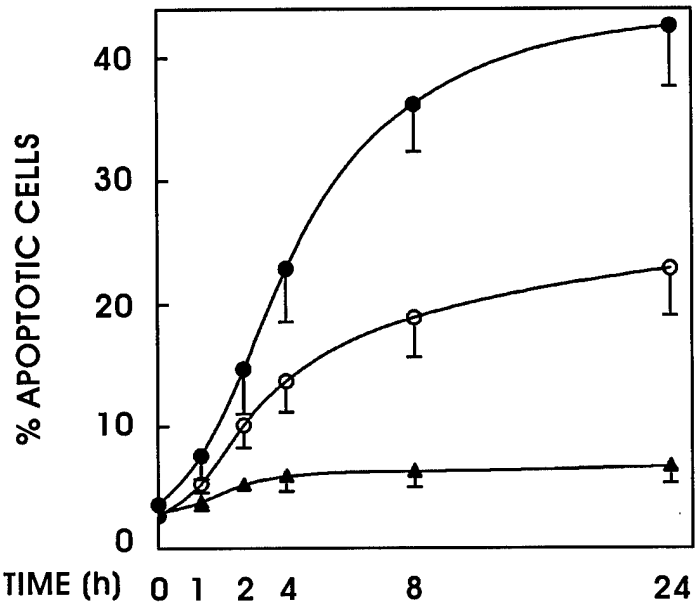

SHP-1 dependency of SSTR3-mediated cytotoxic signaling.
Time course of D-Trp8 SST-14-induced apoptosis measured by Hoechst 33342 positivity.
The number of cells displaying increased dye uptake was quantitated by flow cytometry.

CHO-K1 SSTR3 cells (Open circles)
CHO-K1 SSTR3 cells overexpressing SHP-1(closed circles)
CHO-K1 SSTR3 cells overexpressing SHP-1C455S (closed squares)

Figure 3.

SHP-1 dependency of SSTR3 signaled cell acidification

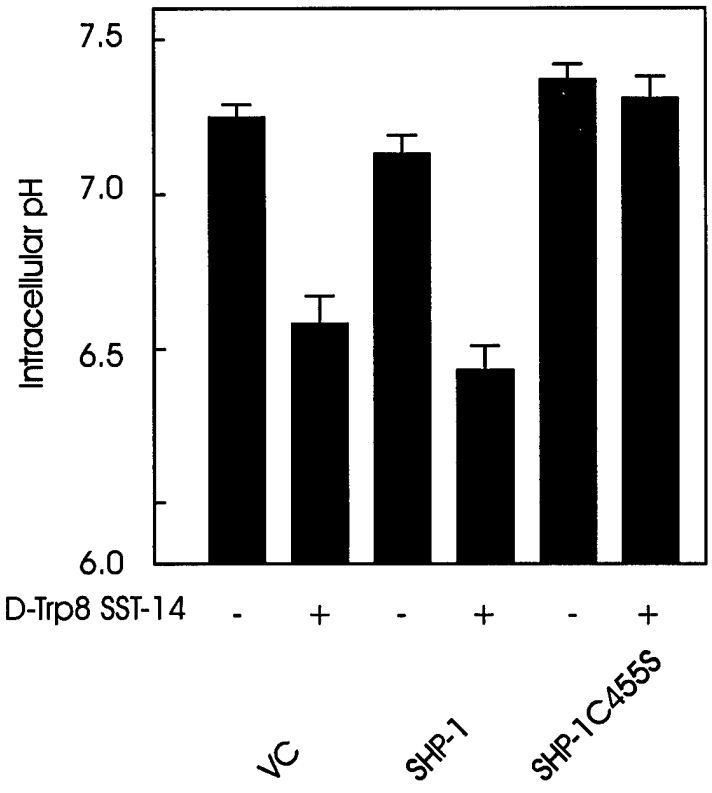

Figure 4.

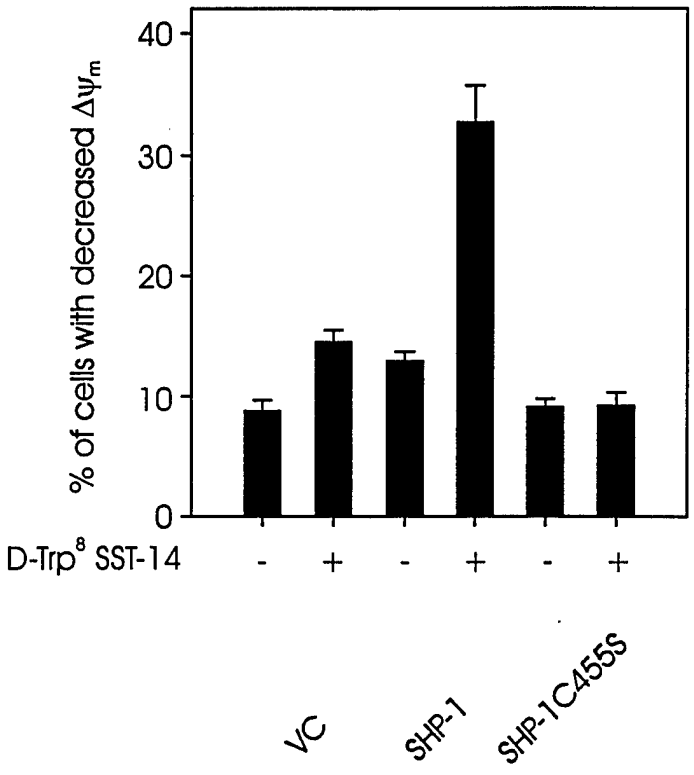
40
30
20
10
0
% of cells with decreased $\Delta\psi_m$
D-Trp^8 SST-14
- + - + - +
VC
SHP-1
SHP-1C455S

Figure 5.

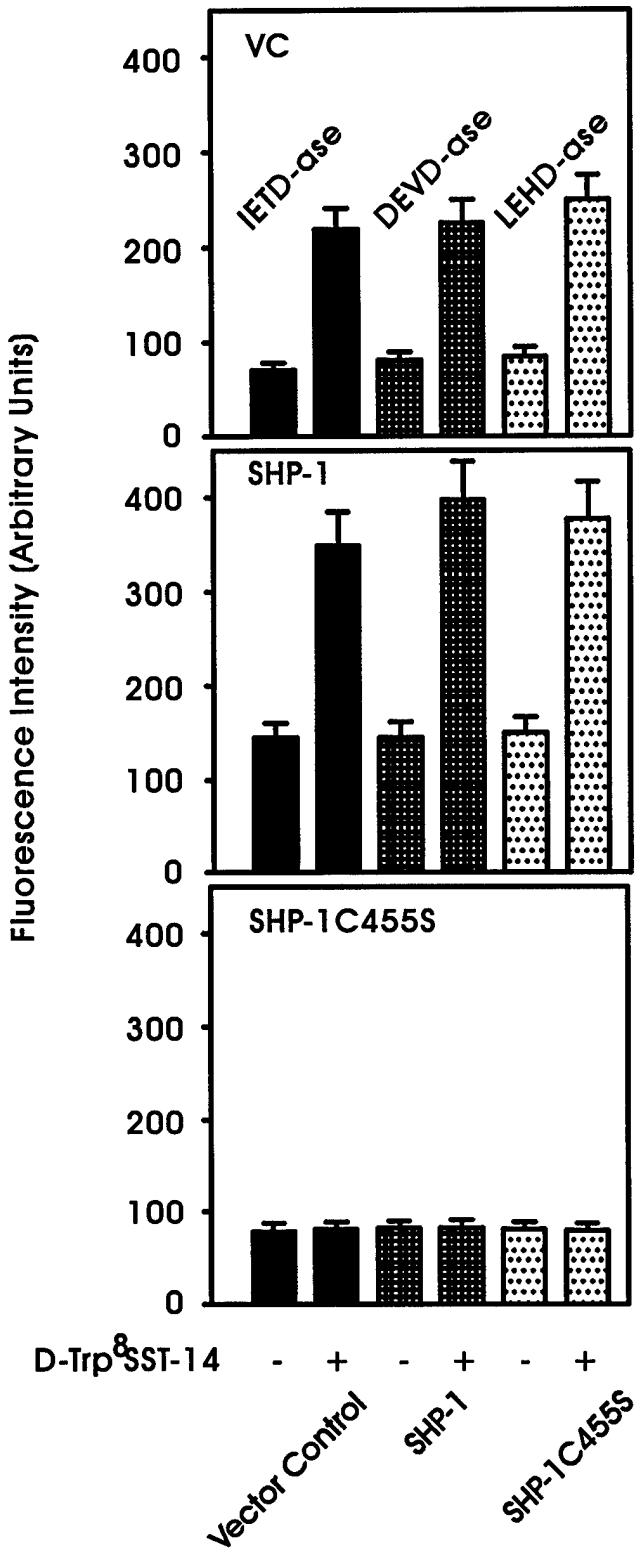
VC
IETD-ase
DEVD-ase
LEHD-ase
SHP-1
SHP-1C455S
Fluorescence Intensity (Arbitrary Units)
400
300
200
100
0
D-Trp8SST-14 - + - + - +
Vector Control
SHP-1
SHP-1C455S

Figure 6.

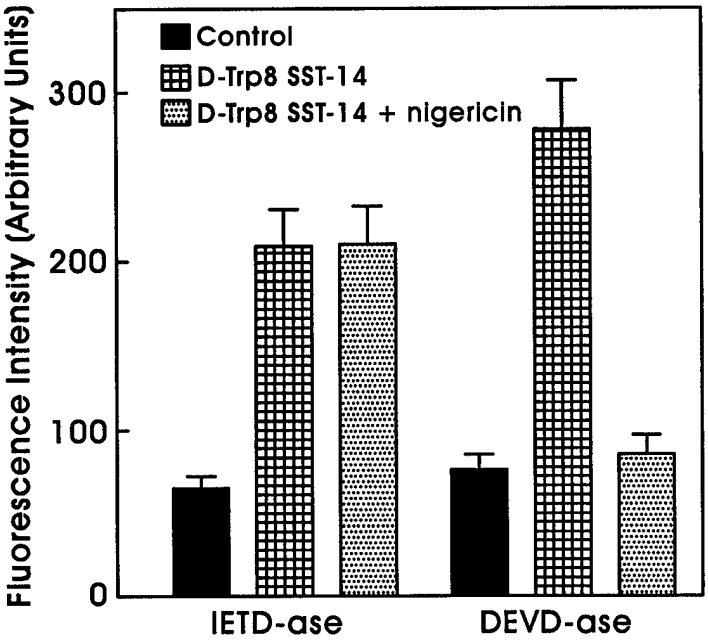
Control
D-Trp8 SST-14
D-Trp8 SST-14 + nigericin
Fluorescence Intensity (Arbitrary Units)
300
200
100
0
IETD-ase
DEVD-ase

Figure 7.

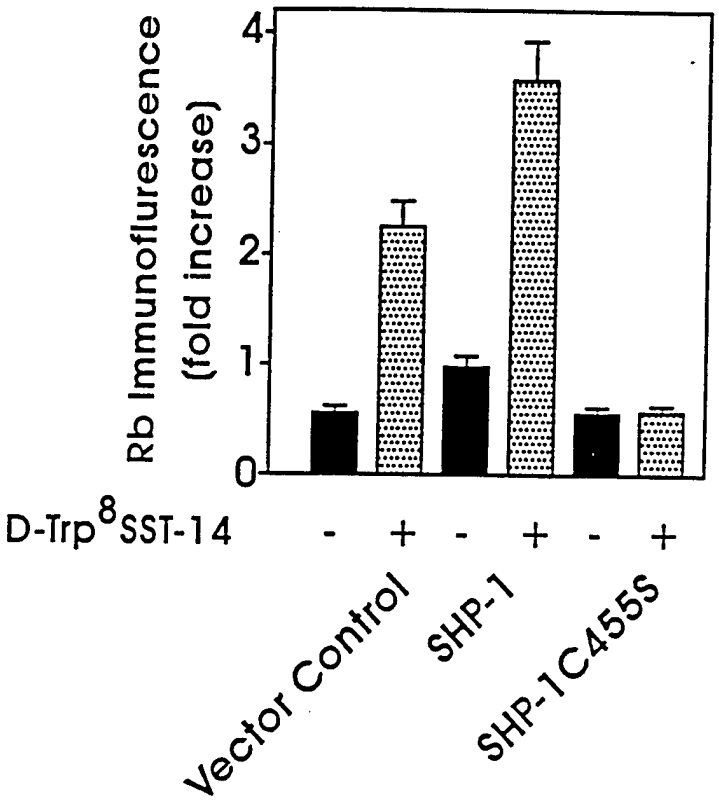
Rb Immunoflurescence
(fold increase)
4
3
2
1
0
D-Trp^{8}SST-14
- + - + - +
Vector Control
SHP-1
SHP-1C455S

Figure 8.

INDUCTION OF APOPTOSIS BY SELECTIVE SST AGONISTS * IN CHO-K1 CELLS EXPRESSING INDIVIDUAL SSTRs

* Provided by Merck [Rohrer et al *Science* 282: 737, 1998]

FIGURE 9.

INDUCTION OF APOPTOSIS IN MCF-7 CELLS BY THE SSTR-SELECTIVE NONPEPTIDE AGONISTS

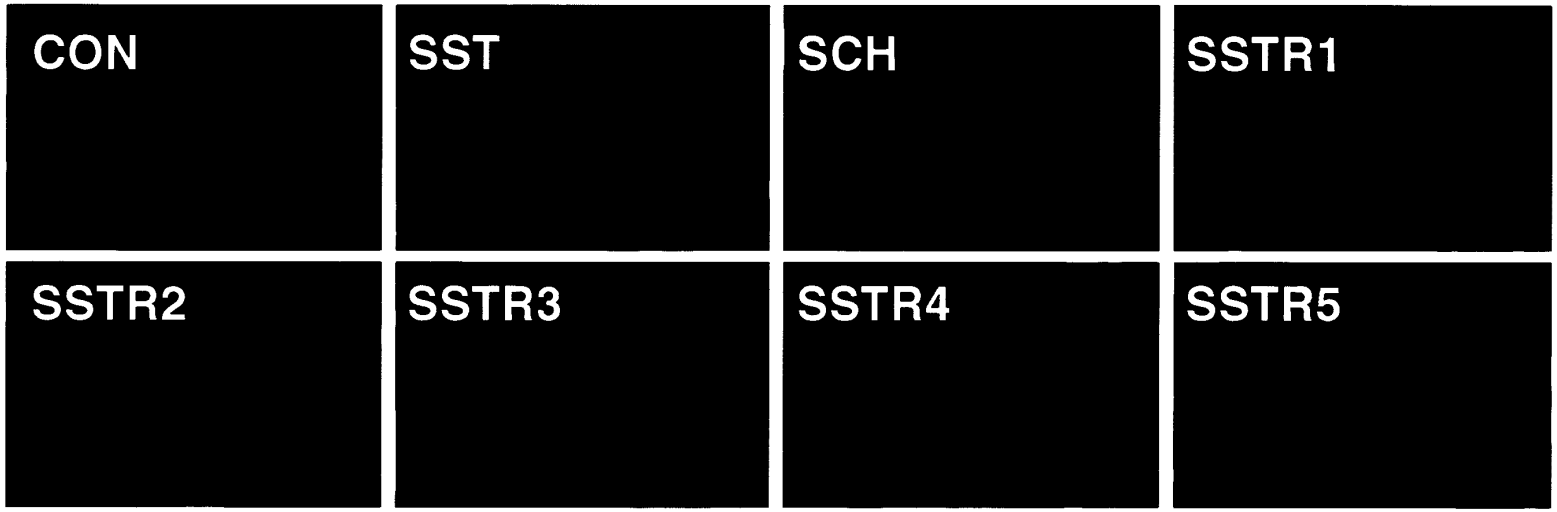

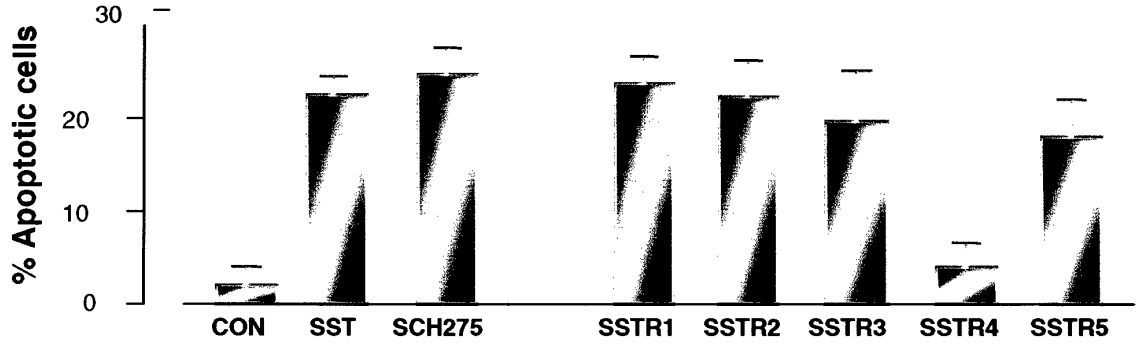

FIGURE 10.

SCHEMATIC DEPICTION OF WILD TYPE, MUTANT AND CHIMERIC SSTR3/SSTR5

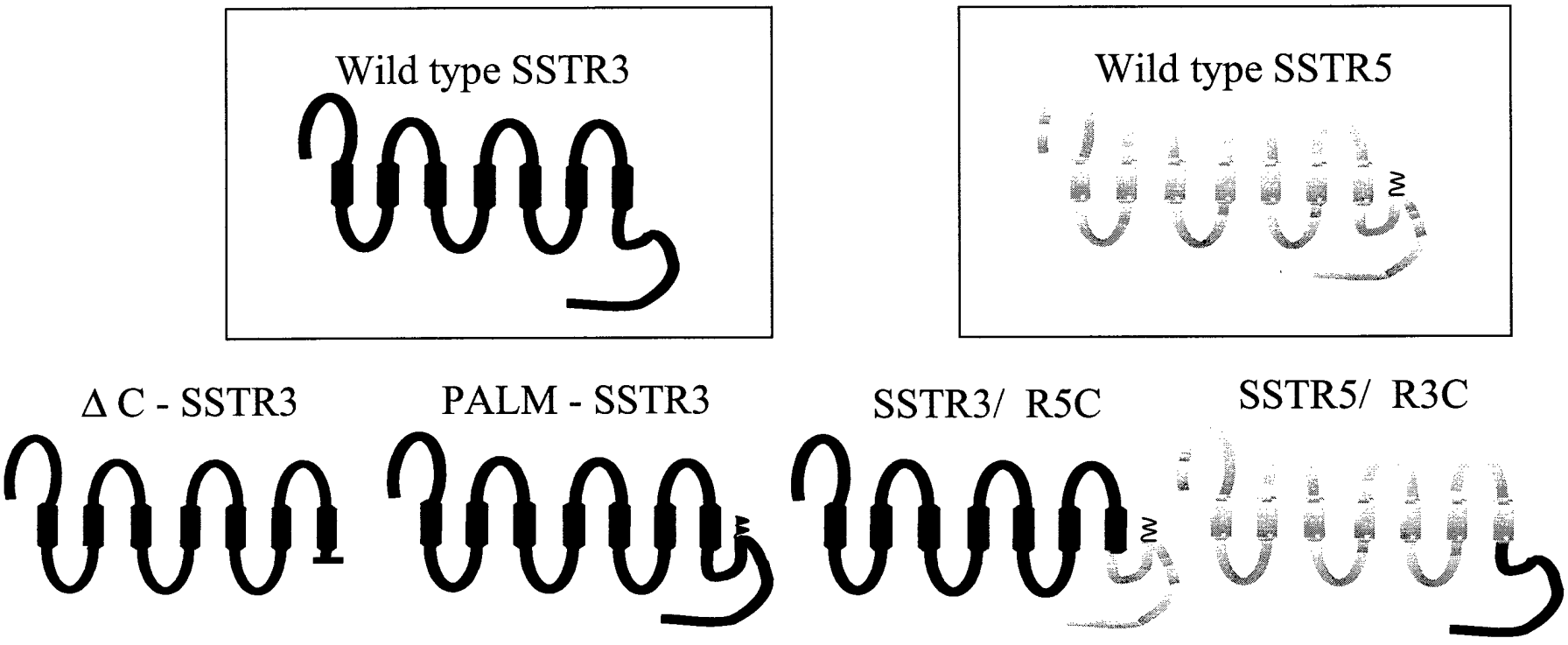

Figure 11.

BINDING AND SIGNALLING PROFILES FOR WILD TYPE, MUTANT AND CHIMERIC SSTR3/SSTR5

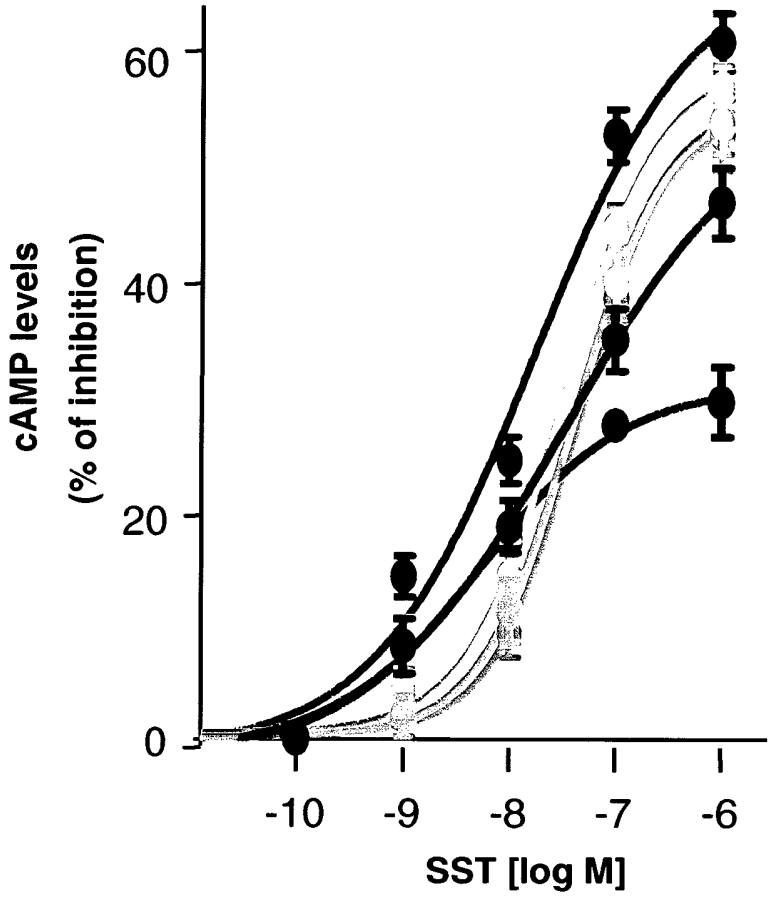

	K_D (nM)	B_{max} (pMol/mg
Wild type SSTR5	0.45±0.20	1.0±0.2
Wild type SSTR3	0.82±0.25	1.2±0.2
	0.76±0.25	1.0±0.2
PALM-SSTR3	1.10±0.30	1.1±0.2
	0.90±0.30	0.9±0.2
SSTR5/ R3-C-TAIL	0.55±0.20	0.7±0.3

FIGURE 12.

SOMATOSTATIN-INDUCED INHIBITION OF GROWTH BY HEK293 CELLS EXPRESSING WILD TYPE, MUTANT AND CHIMERIC SSTR3 / SSTR5 RECEPTORS

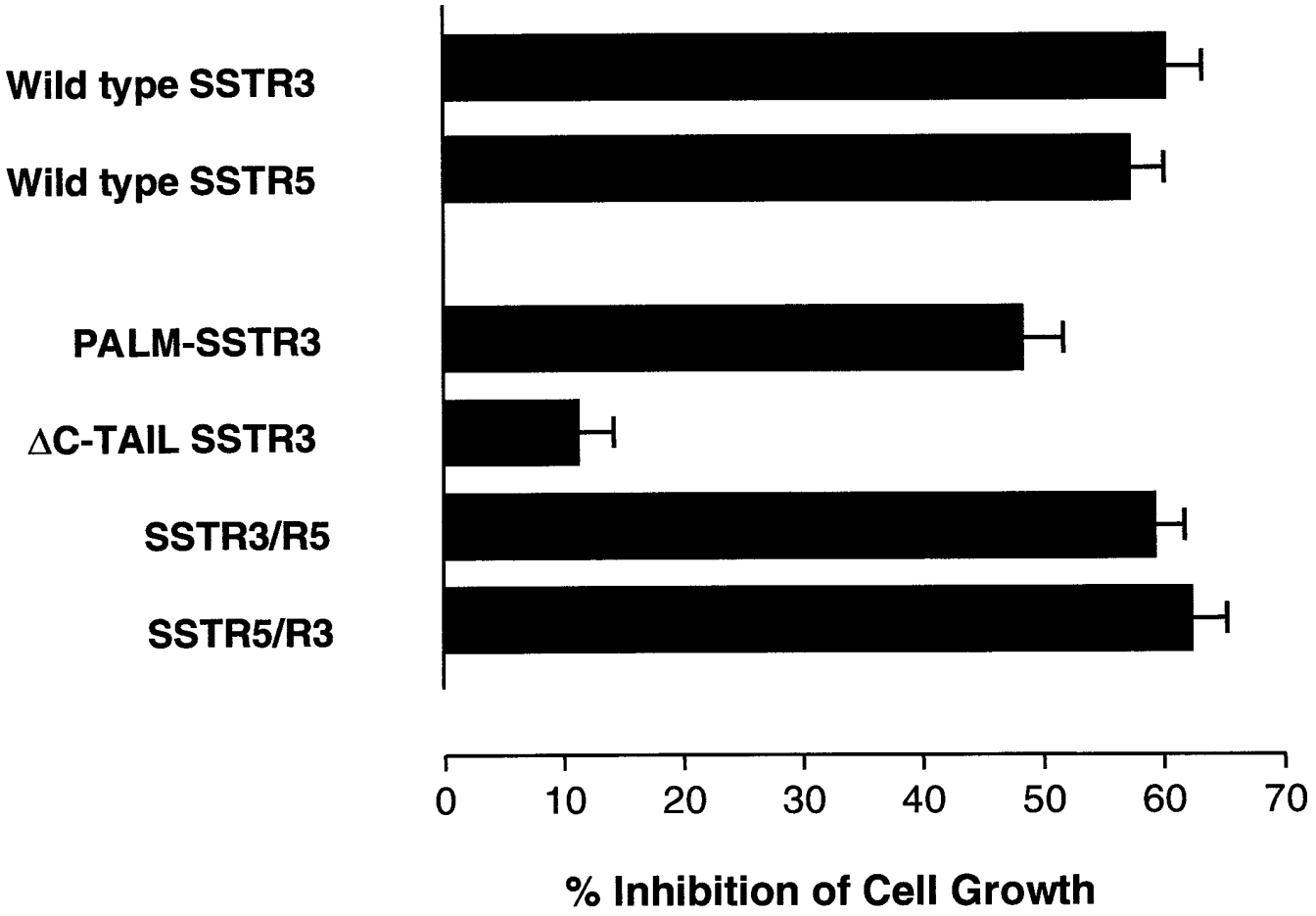

Figure 13.

SOMATOSTATIN-INDUCED APOPTOSIS OF HEK293 CELLS EXPRESSING WILD TYPE, MUTANT AND CHIMERIC SSTR3/SSTR5 RECEPTORS

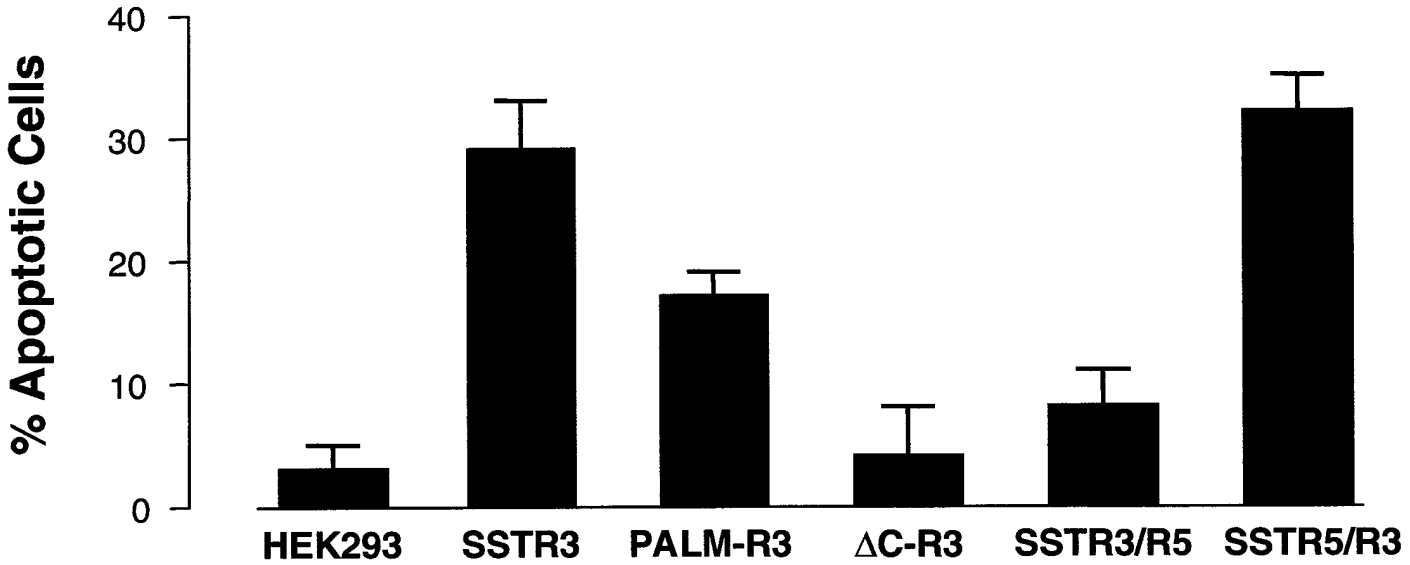

Figure 14.

SOMATOSTATIN-INDUCED APOPTOSIS OF HEK293 CELLS EXPRESSNG WILD TYPE, MUTANT AND CHIMERIC SSTR3/SSTR5 RECEPTORS

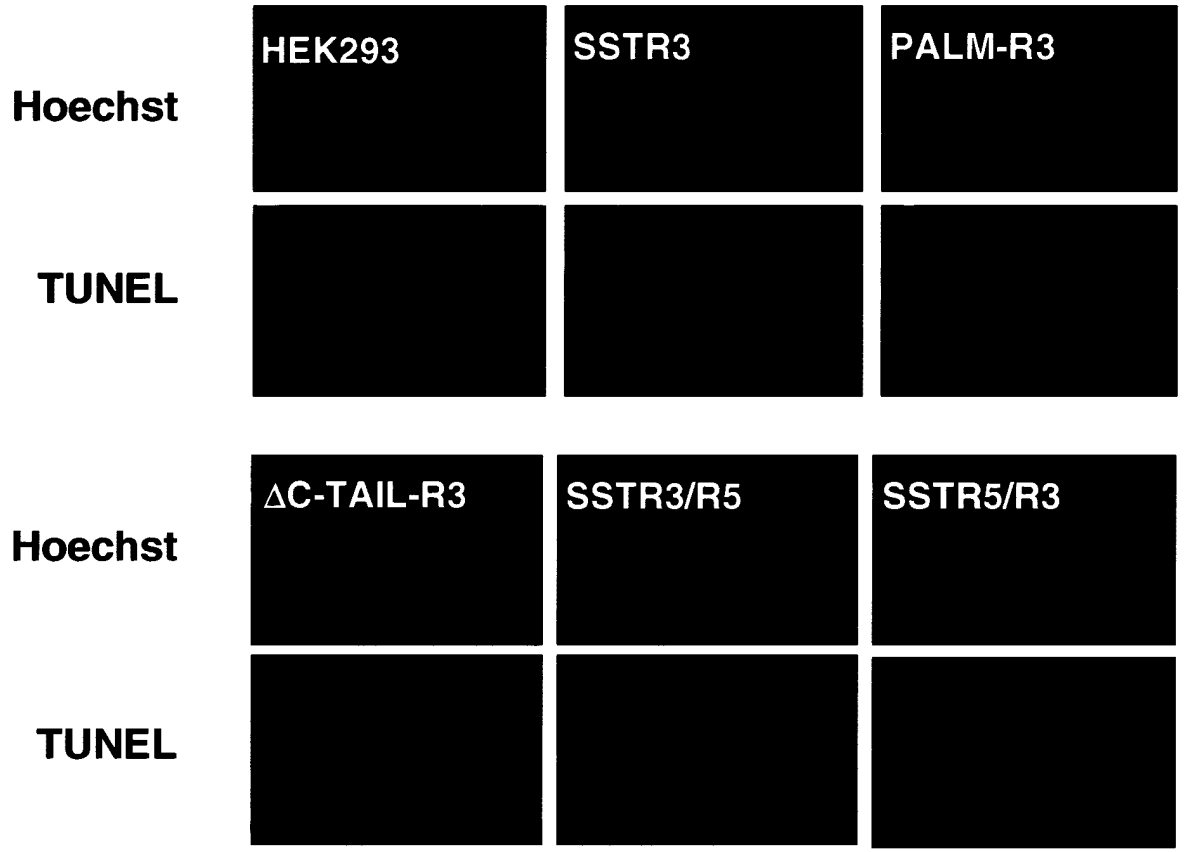

FIGURE 15.

DIAGRAM OF POINT MUTANTS WITHIN hSSTR5 C-TAIL

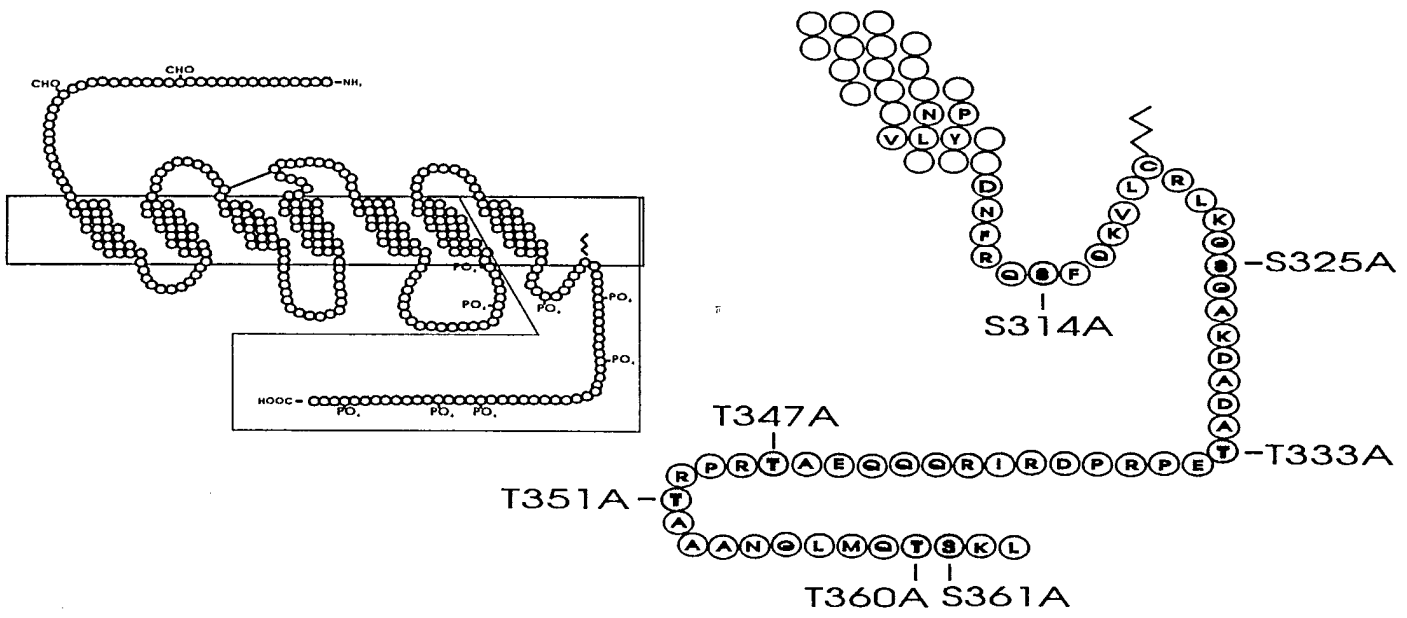

Figure 16.

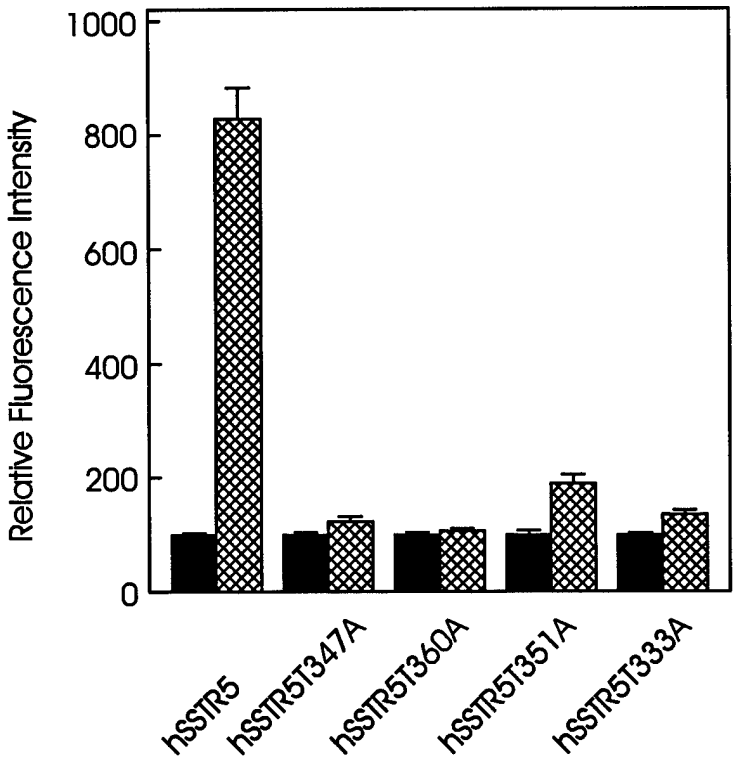
Relative Fluorescence Intensity
1000
800
600
400
200
0
hSSTR5
hSSTR5T347A
hSSTR5T360A
hSSTR5T351A
hSSTR5T333A

Figure 17.

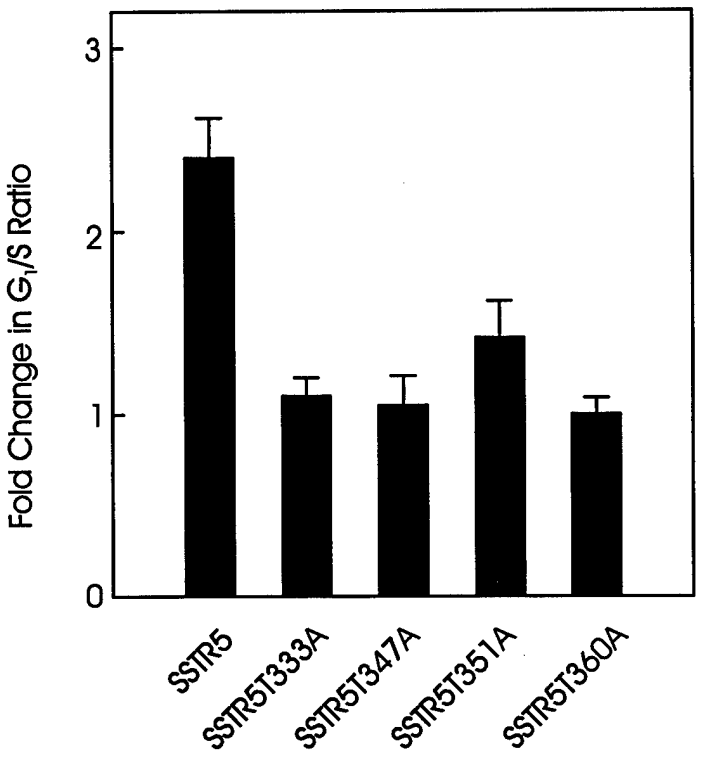
Fold Change in G1/S Ratio
3
2
1
0
SSTR5
SSTR5T333A
SSTR5T347A
SSTR5T351A
SSTR5T360A

Figure 18.

THE JOURNAL OF BIOLOGICAL CHEMISTRY
Vol. 275, No. 11, Issue of March 17, pp. 7862–7869, 2000

Printed in U.S.A.

Subtypes of the Somatostatin Receptor Assemble as Functional Homo- and Heterodimers*

(Received for publication, September 20, 1999, and in revised form, December 8, 1999)

Magalie Rocheville‡§, Daniela C. Lange‡¶, Ujendra Kumar‡, Ramakrishnan Sasi‡, Ramesh C. Patel¶, and Yogesh C. Patel‡‖

From the ‡Fraser Laboratories, Departments of Medicine, Pharmacology and Therapeutics, and Neurology and Neurosurgery, McGill University and Royal Victoria Hospital, Montreal, Quebec H3A 1A1, Canada and the ¶Department of Physics and Chemistry, Clarkson University, Potsdam, New York 13676

The existence of receptor dimers has been proposed for several G protein-coupled receptors. However, the question of whether G protein-coupled receptor dimers are necessary for activating or modulating normal receptor function is unclear. We address this question with somatostatin receptors (SSTRs) of which there are five distinct subtypes. By using transfected mutant and wild type receptors, as well as endogenous receptors, we provide pharmacological, biochemical, and physical evidence, based on fluorescence resonance energy transfer analysis, that activation by ligand induces SSTR dimerization, both homo- and heterodimerization with other members of the SSTR family, and that dimerization alters the functional properties of the receptor such as ligand binding affinity and agonist-induced receptor internalization and up-regulation. Double label confocal fluorescence microscopy showed that when SSTR1 and SSTR5 subtypes were coexpressed in Chinese hamster ovary-K1 cells and treated with agonist they underwent internalization and were colocalized in cytoplasmic vesicles. SSTR5 formed heterodimers with SSTR1 but not with SSTR4 suggesting that heterodimerization is a specific process that is restricted to some but not all receptor subtype combinations. Direct protein interaction between different members of the SSTR subfamily defines a new level of molecular cross-talk between subtypes of the SSTR and possibly related receptor families.

Many membrane proteins such as ion channels, receptor tyrosine kinases, and receptors for growth hormone and cytokines associate as functional oligomeric complexes (1–4). Although G protein-coupled receptors (GPCRs)[1] are generally believed to operate as monomers, several recent lines of evidence based on thermodynamic, biochemical, and functional studies suggest that this class of membrane proteins may also associate as dimers (5–21). However, the question of whether dimerization is a general property of GPCRs and whether it is necessary for GPCR function remains controversial (9, 10, 15, 16, 21). The GABA-B receptor associates as a heterodimer via the cytoplasmic C-tail in the endoplasmic reticulum and is targeted to the plasma membrane as a preformed dimer, independent of agonist regulation (11–14, 21). Whether other GPCR dimers are similarly preformed or whether they undergo dimerization at the plasma membrane in response to agonist activation is unclear (9, 10, 15, 16, 21). Dopamine and muscarinic receptors have been postulated to exist on the membrane as preformed dimers that are stabilized by ligand binding (9, 19). The β-adrenergic receptor on the other hand undergoes ligand-dependent dimerization and activation, whereas agonists at the δ opioid receptor have been suggested to favor monomer formation that is required for agonist-induced internalization (10, 16). In the case of somatostatin (SST) receptors (SSTRs), there are five distinct subtypes that bind the two natural ligands, SST-14 and SST-28, with comparable low nanomolar affinity (22). The five subtypes also share common signaling pathways such as the ability to inhibit adenylyl cyclase and to activate phosphotyrosine phosphatase (22–24). Furthermore, individual target cells typically express more than one SSTR subtype and often all five isoforms (25–28) raising the question of whether multiple SSTRs in the same cell are redundant or whether they interact for greater functional diversity. By using pharmacological, biochemical, and physical methods, here we show that SSTRs associate as dimers, both as homodimers or heterodimers with other members of the SSTR family, and that dimerization alters the functional properties of the receptor such as ligand binding affinity, signaling, and agonist-induced regulation. We provide the first direct evidence based on the sensitive fluorescence resonance energy transfer (FRET) analysis that hSSTR5 exists as a monomer in the basal state and undergoes dose-dependent increase in dimerization when treated with SST-14 suggesting that dimerization is induced by agonist binding.

EXPERIMENTAL PROCEDURES

Peptides and Antisera—Peptides and antisera were obtained as follows: SST-14, SST-28 (Bachem); Leu^8-D-Trp^{22}, Tyr^{25}, SST-28 (LTT-SST-28) (Peninsula); SMS-(201–995) and Tyr^3 SMS (Sandoz, Basel, Switzer-

* This work was supported by grants from the Canadian Medical Research Council, National Institutes of Health Grant NS32160-04, and the United States Department of Defense. The costs of publication of this article were defrayed in part by the payment of page charges. This article must therefore be hereby marked "*advertisement*" in accordance with 18 U.S.C. Section 1734 solely to indicate this fact.

This paper is dedicated to the memory of Monique Pellerin Rocheville.

§ Recipient of studentship support from the Fonds De La Recherche En Sante Du Quebec (FRSQ) and from the Royal Victoria Hospital Research Institute.

‖ Distinguished Scientist of the Canadian Medical Research Council. To whom correspondence should be addressed: Royal Victoria Hospital, Rm. M3-15, 687 Pine Ave. West, Montreal, Quebec H3A 1A1, Canada. Tel.: 514-842-1231 (ext. 5042); Fax: 514-849-3681; E-mail: yogesh.patel@muhc.mcgill.ca.

[1] The abbreviations used are: GPCR, G protein-coupled receptor; SST, somatostatin; SMS, octapeptide SMS-(201–995); SCH275, des-AA^{1,2,5}[D-Trp^8,IAMP^9]SRIF; LTT-SST-28, Leu^8-D-Trp^{22}, Tyr^{25}, SST-28; SCH288, des-AA^{1,5}[Tyr^2-D-Trp^8,IAMP^9]SRIF; SSTR, somatostatin receptor; wt hSSTR1, wild type human somatostatin receptor type 1; wt hSSTR4, wild type human somatostatin receptor type 4; HA-SSTR5, hemagglutinin-tagged somatostatin receptor type 5; ECL2, second extracellular loop segment; ECL3, third extracellular loop segment; C-tail, cytoplasmic carboxyl-terminal segment; CHO, Chinese hamster ovary; mAb, monoclonal antibody; pbFRET, photobleaching fluorescence resonance energy transfer.

land); des-AA^{1,2,5}[D-Trp^8,IAMP^9]SRIF (SCH275) and des-AA^{1,5}[Tyr^2-D-Trp^8,IAMP^9]SRIF (SCH288) (J. Rivier, Salk Institute); anti-HA mouse monoclonal antibody (12CA5) and fluorescein- and rhodamine-conjugated monoclonal antibodies against HA (Roche Molecular Biochemicals).

SSTR Constructs and Transfections—The Δ318 hSSTR5 C-tail deletion mutant and the second extracellular loop (ECL2) hSSTR5 mutant in which 7 of the 10 COOH-terminal residues of the second ECL were conservatively altered have been described previously (29, 30). Stable CHO-K1 cells overexpressing full-length HA-tagged hSSTR5 were obtained from K. Koller (31). Stable CHO-K1 cotransfectants expressing wt hSSTR1-pCDNA (32), wt hSSTR4-pRC/CMV (32), HA-hSSTR5 in α + 12CA5-KH (31), Δ318 hSSTR5-pTEJ8 or ECL2/Δ318 hSSTR5 mutants in pTEJ8 were prepared by Lipofectin transfection (Life Technologies, Inc.). Neomycin-resistant clones were selected and maintained in F12 medium with 10% fetal bovine serum and 700 μg/ml G418.

Binding Assays, Internalization, and Up-regulation Experiments—Binding studies were carried out for 30 min at 37 °C with cell membrane protein or whole cells with ^{125}I-labeled LTT-SST-28 radioligand or subtype-selective ligands as previously reported (29, 30, 32, 33). Receptor coupling to adenylyl cyclase was tested by incubating cells for 30 min with 1 mM forskolin with or without SST (10^{-10}–10^{-6} M) at 37 °C as described previously (30). Cells were then scraped in 0.1 N HCl and assayed for cAMP by radioimmunoassay (30, 33). Internalization experiments were carried out by incubating cells overnight at 4 °C with radioligand with or without SST (0.1 mM) (30, 32, 33). After washing, cells were warmed to 37 °C for 15, 30, and 60 min to initiate internalization. At the end of each incubation, surface-bound radioligand was removed by acid wash, and internalized radioligand was measured as acid-resistant counts in 0.1 N NaOH extracts of acid-washed cells (30, 32, 33). The ability of long term treatment with SST to up-regulate surface SSTR binding was studied in cells cultured with 1 μM SST or SMS for 22 h as described previously (32, 33). After acid wash to remove surface-bound SST, whole cell binding assays were performed to determine total and nonspecific binding. Residual surface binding was calculated as the difference between control and experimental groups (32, 33).

Western Blots—CHO-K1 cells expressing HA-SSTR5 were analyzed for receptor protein by Western blots as reported previously (27). Membranes were incubated with or without SST-14 (10^{-6} M) for 30 min at 37 °C and then solubilized in sample buffer containing 62.5 mmol/liter Tris-HCl, pH 6.8, 2% SDS, 10% glycerol, and 50 mmol/liter dithiothreitol. 50-μg samples of membrane protein were fractionated by electrophoresis on 10% SDS-polyacrylamide gels as described by Laemmli (34). The fractionated proteins were transferred by electrophoresis to nitrocellulose membranes in a transfer buffer containing 0.025 mol/liter Tris, 0.192 mol/liter glycine, and 15% methanol. The membranes were then probed for HA-SSTR5 using the mouse monoclonal antibody and the lumilight$^+$ Western blotting Kit (Roche Molecular Biochemicals) (27). Blots were analyzed semi-quantitatively using the computer scanning software Masterscan.

Photobleaching (pb) FRET Microscopy—Generally, FRET efficiencies are determined indirectly by measuring changes in the quantum yield of any competitive donor deactivation process upon introduction of an acceptor molecule (35–39). Donor photobleaching represents such a competitive process that can be exploited in pbFRET microscopy. The effective FRET efficiency E is calculated from the photobleaching time constants of the donor (D) obtained in the absence (τ_{D-A}) and presence (τ_{D+A}) of acceptor (A) according to Equation 1.

$$E = 1 - \frac{\tau_{D-A}}{\tau_{D+A}} \quad \text{(Eq. 1)}$$

In a two-state model, the minimal amount of receptor dimerization (α_{min}) is related to the fraction of acceptor labeled receptor (f_A) and E as shown in Equation 2,

$$\alpha_{min} = \frac{8E}{f_A(2+E)^2} \quad \text{(Eq. 2)}$$

where f_A is determined from the relative affinities of fluorescein- and rhodamine-conjugated mAbs and the concentration ratio used for incubation (39). pbFRET experiments were performed on CHO-K1 cells stably expressing HA-hSSTR5 using a Leica DMBL fluorescence microscope equipped with epi-illumination. An OSRAM HBO 100-watt mercury lamp was used as excitation light source. In order to separate fluorescein excitation from emission as well as to optimize fluorescein excitation while simultaneously blocking rhodamine excitation, the following filters were used: Leitz BP 450–490 (excitation), RKP510 (dichroic mirror), and BP 515–535 (emission). Digital images (8-bit) were generated with an Electrim-1000U CCD camera with a spatial resolution of 1134 × 486 pixels of size 7.8 × 13.6 μm. Exposure as well as time delays were software controlled. IGOR Pro 3.13 (Wavemetrics, OR) was used for image analysis. Images were corrected for dark current, background, and flatness.

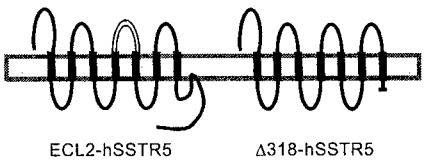

FIG. 1. **Schematic depiction of binding-deficient second extracellular loop (ECL2-hSSTR5) and signaling-deficient C-tail deletion (Δ318-hSSTR5) mutants of hSSTR5.**

Immunocytochemistry—Expression of SSTRs in transfected CHO-K1 cells was determined by immunocytochemistry. Rabbit polyclonal anti-peptide antibodies directed against sequences in the amino-terminal segment of hSSTR1 (diluted 1:300) or mouse monoclonal anti-HA antibodies (diluted 1:300) were used as primary antibodies followed by reaction with rhodamine or fluorescein-conjugated secondary antibody as described previously (33). To demonstrate colocalization of hSSTR1 with hSSTR5, CHO cells stably cotransfected with wt hSSTR1 and HA-hSSTR5 were treated with 1 μM SMS for 12 h at 4 °C. For receptor localization on the plasma membrane, cells were fixed at 4 °C in 3.7% formalin for 15 min. For receptor localization in vesicles, cells were incubated for an additional 60 min at 37 °C to allow internalization, fixed, and permeabilized in methanol/acetone at −10 °C for 15 min. The fixed cells in both instances were processed for double label confocal fluorescence immunocytochemistry. Cells were mounted with immunofluor and viewed under a Zeiss LSM 410 confocal microscope. Images were obtained as single optical sections taken through the middle of cells and averaged over 32 scans/frame.

Statistical Analysis—Results are presented as mean ± S.E.

RESULTS

Agonist-dependent Homodimerization of hSSTR5—We first demonstrated SSTR homodimerization by functional complementation of two partially active mutants of human SSTR5 (hSSTR5) that we have previously described (29, 30) (Fig. 1). One is a conservative segment exchange mutant of the second extracellular loop, ECL2 hSSTR5 which fails to bind SST-14/SST-28 but which is correctly targeted to the plasma membrane as shown by immunocytochemistry (29). The other is a cytoplasmic tail (C-tail) deletion mutant Δ318 hSSTR5 that displays complete loss of adenylyl cyclase coupling while retaining full agonist binding potency and the ability to undergo agonist-dependent internalization (30). We wondered whether loss of adenylyl cyclase coupling by the C-tail deletion mutant could be rescued by cotransfection, whereby the binding competent mutant would associate and signal through the C-tail of the binding-deficient mutant. The two mutants were stably cotransfected in CHO-K1 cells (B_{max} 119 ± 36 fmol/mg protein) and compared with individual Δ318 hSSTR5 (B_{max} 126 ± 43 fmol/mg protein) or ECL2 hSSTR5 (no binding) stable monotransfectants. Coupling to adenylyl cyclase was determined by the ability of SST-28 to inhibit forskolin-stimulated cAMP. In the cotransfectant, SST-28 produced dose-dependent inhibition of forskolin-stimulated cAMP (31 ± 2.5% at 1 μM agonist) which was completely abolished by pertussis toxin treatment (Fig. 2*B*). This suggests that the two mutant receptors assemble as homodimers to constitute a functional G protein-linked effector complex. Competition analysis showed a significant 4-fold increase in the binding affinity of SST-14 for the putative Δ318-hSSTR5/ECL2-hSSTR5 dimeric receptors (K_i 3.1 ± 1.9 nM) compared with Δ318 hSSTR5 alone (K_i 12.1 ± 2.5 nM) suggesting physical association leading to a change in receptor conformation (Fig. 2*A*). We next investigated the effect of coexpression of the mutant receptors on receptor internalization

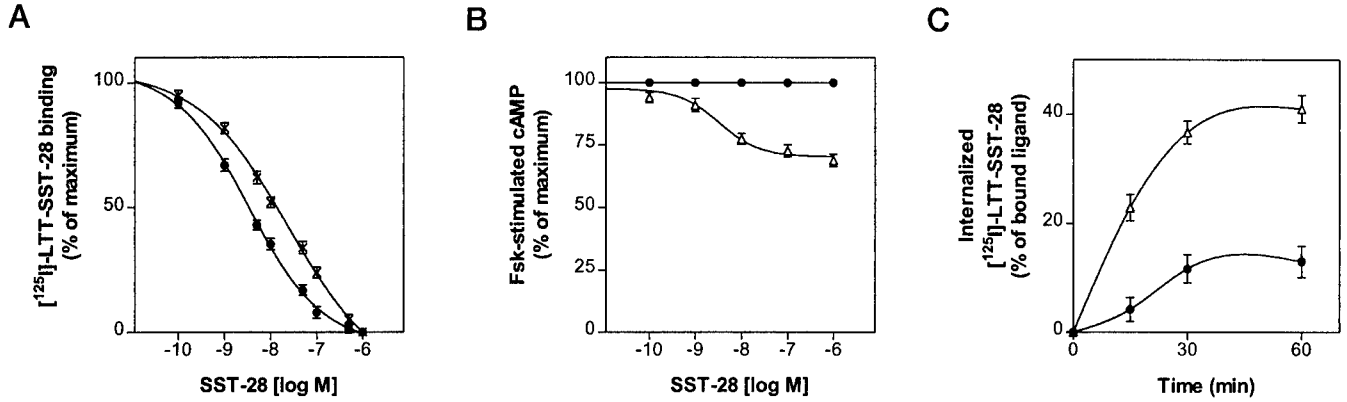

FIG. 2. **Homodimerization of hSSTR5.** Effect of cotransfecting ECL2-hSSTR5 and Δ318-hSSTR5 mutants on ligand binding affinity, adenylyl cyclase coupling, and internalization. *A*, displacement analysis of Δ318-hSSTR5 alone (○) (K_i, 12.1 ± 2.5 nM) compared with that of cotransfectants (●) (K_i, 3.1 ± 1.9 nM). *B*, SST-28 produces dose-dependent inhibition of forskolin-stimulated cAMP (△) that is abolished by 100 ng/ml pertussis toxin pretreatment (●). *C*, percent internalization of ^{125}I-LTT-SST-28 by cells expressing Δ318- hSSTR5 alone (△) compared with Δ318-hSSTR5/ECL2 hSSTR5 cotransfectants (●). For comparative purposes, wt hSSTR5 monotransfected in CHO-K1 cells displayed B_{max} 180 ± 28 fmol/mg protein and K_d 0.31 ± 0.03 nM, 70 ± 6% maximum inhibition of forskolin-stimulated cAMP at 1 μM SST-14 and maximum 66 ± 7% internalization of ^{125}I-LTT-SST-28 at 60 min (33). Mean ± S.E. of 3 experiments.

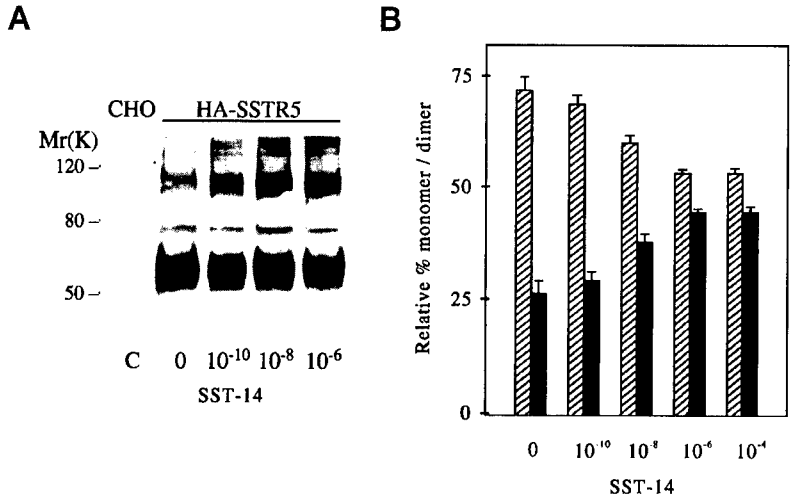

FIG. 3. **Representative Western blot of HA-hSSTR5 showing ligand-induced homodimerization.** Membranes from nontransfected (control) or HA-hSSTR5 transfected CHO-K1 cells were incubated with different amounts of SST-14 for 30 min and analyzed by Western blots using HA monoclonal antibody. *A*, hSSTR5 exists as a mixture of broad monomeric 55–65-kDa and dimeric 105–115-kDa bands. Treatment with SST-14 results in a dose-dependent increase in the proportion of dimers. A sharp nonspecific band at 77 kDa is observed in control and transfected cells. *B*, semiquantitative analysis of the percent of monomer and dimer species using computer scanning software MasterScan. The nonspecific band was used as an internal standard for protein estimation. Mean ± S.E. of 3 independent experiments.

(Fig. 2*C*). CHO-K1 cells expressing either Δ318 hSSTR5 or Δ318 hSSTR5 and ECL2 hSSTR5 mutants were incubated at 37 °C for different times with ^{125}I-labeled LTT-SST-28 (a nonselective radioligand for all five SSTR subtypes) with or without 0.1 μM SST-28 (30, 32). The Δ318 hSSTR5 mutant displayed time-dependent internalization with a maximum of 41 ± 2.8% at 60 min (Fig. 2*C*). Coexpression of the ECL2 mutant markedly inhibited internalization of the putative dimeric complex to only 13 ± 3.9% at 60 min. This suggests that the association of the ECL2 hSSTR5 mutant with the binding competent Δ318 hSSTR mutant, although promoting ligand binding affinity, impairs internalization of the dimeric receptor complex perhaps because only one of the receptor subunits is in a ligand-bound state. Physical association of SSTRs was investigated by Western blot analysis of CHO-K1 cell membranes expressing full-length hSSTR5 tagged at the amino terminus with a nonapeptide of the hemagglutinin (HA) sequence (31). These cells expressed a high level of membrane hSSTR5 (B_{max} 800 ± 90 fmol/mg protein) that existed in the basal state as a mixture of broad monomeric 55–65-kDa and dimeric 105–115-kDa bands (ratio 73 ± 3%: 27 ± 3%) (Fig. 3). Treatment with SST-14 resulted in a dose-dependent saturating increase in the proportion of dimers (monomer:dimer ratio 54 ± 1%:46 ± 1% with 1 μM ligand). The dose-response curve for hSSTR5 dimerization paralleled that for ligand-induced receptor signaling (Fig. 2*B*).

Agonist-dependent Homodimerization of hSSTR5 in Intact Cells by Photobleaching FRET Analysis—To obtain direct evidence for the association of SSTRs in intact cells, we probed for receptor homodimerization by pbFRET microscopy (35–39). HA hSSTR5 was visualized in CHO-K1 cells using fluorescein (donor)- and rhodamine (acceptor)-conjugated monoclonal antibody (mAb) against HA. Both fluorophore-tagged antibodies exhibited clear plasma membrane staining (Fig. 4*I*, *a–c*) as well as competitive antigen binding (Fig. 4*I*, *d*), from which their relative affinities could be determined. The decrease in donor fluorescence intensity due to photobleaching during prolonged exposure to excitation light was monitored in the absence (Fig. 4*II*, *a*) or presence (Fig. 4*III*, *a*) of acceptor, *i.e.* in the potential presence of an additional donor deactivation process, FRET. The photobleaching decay was analyzed for the plasma membrane regions, both on a pixel-by-pixel basis (Fig. 4, *IIb* and *IIIb*) as well as averaged over each image (Fig. 4*II*, *c* and *d*). We observed a significant slow down of the photobleaching process (as described by an increase in the photobleaching time constant) upon addition of rhodamine-labeled antibody to the cells suggesting that a large proportion of rhodamine molecules are in close enough proximity to fluorescein to act as acceptors for energy transfer. Given that the two fluorophores are associated with different receptor molecules, this finding suggests receptor association. In the basal state, we found effective FRET efficiencies of approximately 11 and 15% for donor:acceptor

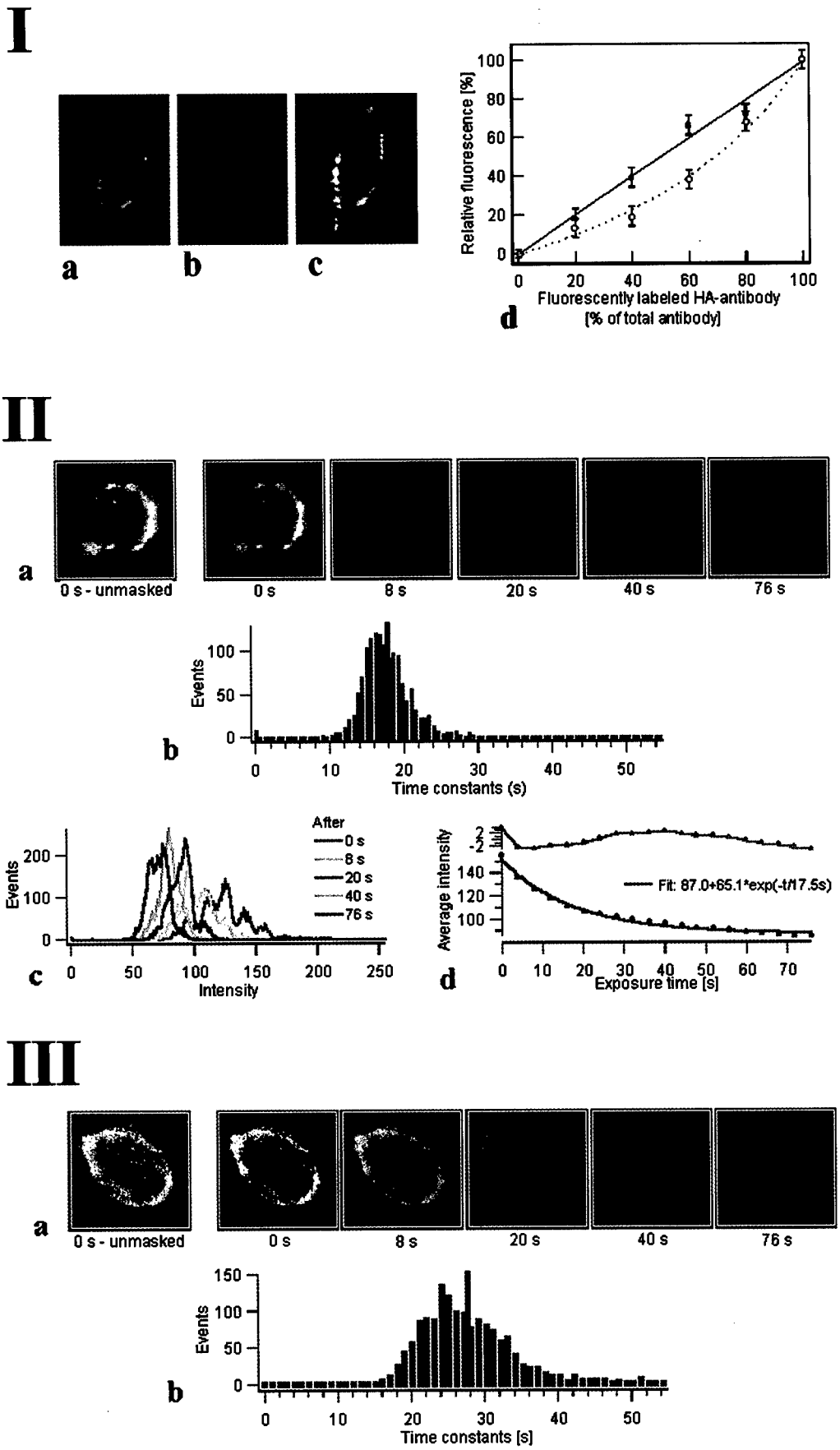

FIG. 4. *I*, confocal microscope images showing fluorescently labeled monoclonal anti-HA-antibody bound to the plasma membrane of CHO-cells transfected with HA-hSSTR5. *a*, fluorescein-conjugated mAb; *b*, rhodamine-conjugated mAb; *c*, colocalization of fluorescein- and rhodamine-conjugated mAb (*yellow*); *d*, competitive binding of native-, fluorescein-, and rhodamine-conjugated mAb. Cells were incubated with 2.5 μg/ml mAb (total concentration) in various ratios of fluorescein/unlabeled (○) and rhodamine/unlabeled (●) mAb. The relative fluorescence intensity (averaged

TABLE I

The symbols used are as follows: *D:A*, concentration ratio donor/acceptor; $D - A$ and $D + A$, corresponding to donor in absence and presence of acceptor, respectively; τ_{avg}, mean of n photobleaching time constants (each being the pixel-based average of a cell membrane), ± S.E.; n, number of cells analyzed (with an average number of ~1500 pixels per cell); σ_{n-1}, standard deviation of τ_{avg}; E, average effective FRET efficiency; α_{min}, corresponding minimal amount of receptor dimerization. Absolute photobleaching time constants are not comparable between different data sets as they were measured on different days and were therefore affected by the decrease in excitation intensity of the UV lamp.

sst-14 concentration	*D:A* ratio		τ_{avg}	n	σ_{n-1}	E	α_{min}
			s		*s*	%	
			Low expression cell line				
0 (basal state)	1:1	$D - A$,	35.6 ± 1.1	33	6.1		
		$D + A$,	36.0 ± 1.0	32	5.5	1 ± 4	3 ± 11
	1:2	$D - A$,	36.0 ± 1.2	31	6.4		
		$D + A$,	35.6 ± 0.8	25	4.0	≈0 ± 4	0 ± 10
10^{-10} M	1:1	$D - A$,	14.4 ± 0.2	40	1.2		
		$D + A$,	15.2 ± 0.4	27	2.2	5 ± 3	14 ± 8
10^{-9} M	1:1	$D - A$,	31.6 ± 0.5	46	3.7		
		$D + A$,	36.4 ± 1.0	33	5.8	13 ± 3	33 ± 7
5×10^{-8} M	1:1	$D - A$,	30.4 ± 1.2	27	6.2		
		$D + A$,	36.4 ± 0.8	21	3.6	16 ± 4	40 ± 8
10^{-6} M	1:1	$D - A$,	26.8 ± 0.8	27	4.3		
		$D + A$,	33.6 ± 0.8	36	4.8	20 ± 3	48 ± 6
	1:2	$D - A$,	28.8 ± 1.0	30	5.6		
		$D + A$,	37.6 ± 1.9	22	8.9	23 ± 5	45 ± 8
			High expression cell line				
0 (basal state)	1:2	$D - A$,	21.0 ± 0.7	37	4.5		
		$D + A$,	23.5 ± 0.4	40	2.3	11 ± 3	24 ± 6
	1:3	$D - A$,	22.4 ± 0.5	46	3.7		
		$D + A$,	26.3 ± 0.8	34	4.5	15 ± 3	30 ± 5
10^{-6} M	1:2	$D - A$,	19.9 ± 0.6	22	2.7		
		$D + A$,	25.3 ± 0.5	29	2.8	21 ± 3	42 ± 5
	1:3	$D - A$,	20.1 ± 0.4	54	3.1		
		$D + A$,	27.4 ± 0.6	48	3.9	27 ± 2	48 ± 3

ratios of 1:2 and 1:3, respectively (Table I). For a two-state model, *i.e.* for receptors existing either in a monomeric or dimeric state, as suggested by the Western blot data (Fig. 3), these FRET efficiencies relate to a minimal amount of receptor dimerization of 24 and 30%, respectively (39). Treatment with agonist resulted in increased FRET efficiencies of 21 and 27%, corresponding to higher levels of dimerization of at least 42 and 48% under saturation conditions (Table I), in good agreement with values obtained by Western blot.

To determine whether the high level of basal dimerization was caused by receptor overexpression, and to explain the relationship between monomers and dimers, we took advantage of the high sensitivity of FRET analysis for detecting dimerization to investigate a second CHO-K1 cell line expressing a 5-fold lower concentration of HA-hSSTR5 receptors (B_{max} 160 ± 30 fmol/mg protein). In contrast to cells overexpressing HA-hSSTR5, these cells displayed insignificant effective FRET efficiencies of 0–1% in the basal state suggesting that monomers predominate in the absence of agonist when the receptor is expressed at levels in the range of endogenous SSTR concentrations (Table I) (40). Treatment with SST resulted in a dose-dependent increase in FRET efficiencies (Fig. 5) suggesting that dimerization is induced by agonist binding.

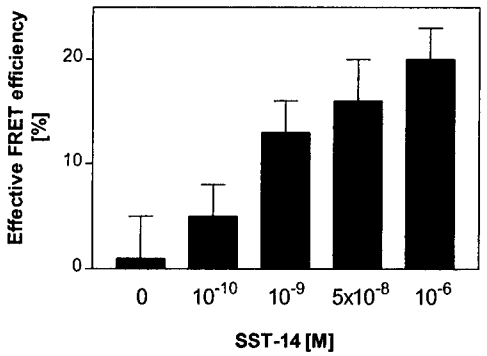

FIG. 5. **Dose-dependent increase in effective FRET efficiency by SST-14 in CHO-K1 cells expressing relatively low density of HA-hSSTR5 (see Table I for *D:A* = 1:1).**

Agonist-dependent Heterodimerization of hSSTR5 with hSSTR1—We next investigated SSTR heterodimerization and selected hSSTR1 and hSSTR5 to take advantage of their different pharmacological properties. Both receptors bind SST-14 and SST-28, but only SSTR5 and not SSTR1 binds the octapeptide SMS-(201–995) (SMS, Octreotide) (22). SSTR5 is internalized by acute agonist exposure, whereas hSSTR1 is resistant to internalization and is instead up-regulated at the membrane by prolonged agonist treatment (30, 32, 33). As previously

over 25 cells) was plotted against the proportion of fluorescently labeled mAb. Binding affinity of the rhodamine-labeled mAb was identical to that of the unlabeled mAb (*solid line*), whereas it was reduced by a factor of 0.44 for the fluorescein-labeled mAb (*dotted line*). This relative affinity was used for determining the minimum level of receptor dimerization as function of FRET efficiency (Equation 2). *II,* photobleaching of fluorescein (donor) in absence of rhodamine (acceptor). In this example, cells were treated with 1 μM SST-14, and the ratio of donor labeled to unlabeled mAb was 1:2. *a,* during donor photobleaching, a sequence of 20 images was acquired, one image every 4 s with exposure time 3 s (only selection shown). For analysis of the photobleaching decay, only the high intensity membrane region was considered; the low intensity background and intracellular regions were masked (*black*). *Leftmost,* unmasked image of initial donor fluorescence. *b,* the decrease of fluorescence intensity was analyzed for each pixel of the unmasked region and fitted to a single exponential decay. The resulting time constants were plotted in the *histogram* shown. The average time constant of 18.0 s (*black bar*) was taken as τ_{D-A} (see Equation 1). *c,* histograms of fluorescence intensities for the selection of images in *a. d,* average fluorescence intensity of each image *versus* exposure time to excitation light. The monoexponential fit (*red*) as well as the residue (*green*) demonstrate the good approximation of the photobleaching decay by a single exponential. *III, a,* photobleaching of fluorescein presence of rhodamine. The protocol was the same as in *B*, except that rhodamine-conjugated mAb was used in place of unlabeled mAb. *b,* the presence of rhodamine led to larger donor photobleaching time constants, with an average, τ_{D+A}, of 27.6 s, reflecting FRET between fluorescein and rhodamine.

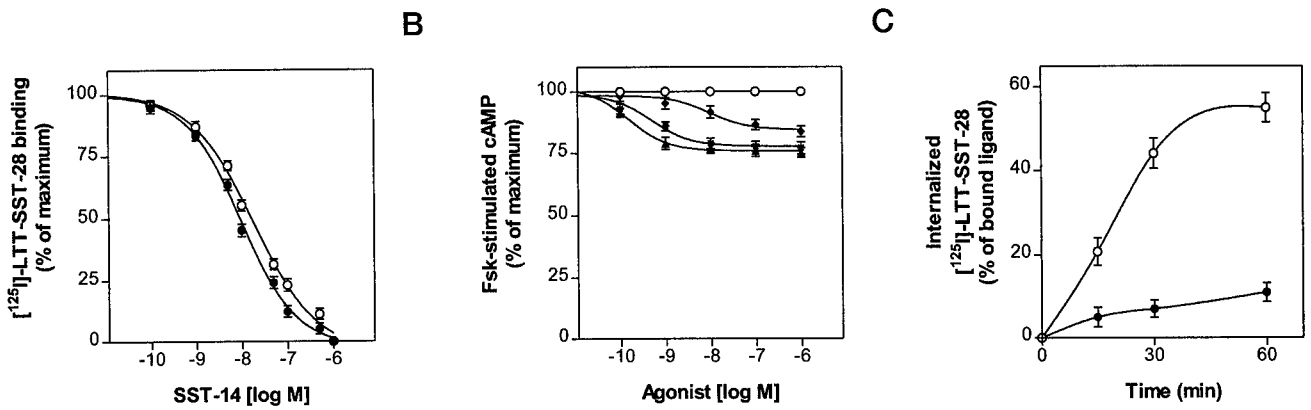

FIG. 6. **Heterodimerization of SSTR5 and SSTR1.** Effect of cotransfecting Δ318-hSSTR5 mutant with wt hSSTR1 on ligand binding affinity, adenylyl cyclase coupling, and internalization. *A,* displacement analysis of Δ318-hSSTR5 alone (○) (K_i, 15.6 ± 2 nM) compared with that of Δ318-hSSTR5/wt hSSTR1 cotransfectants (●) (K_i, 8.6 ± 0.2 nM). *B,* effect of SST agonists on forskolin-stimulated cAMP levels. Cotransfected cells were treated with SMS (♦), SST-14 (*), or SCH-275 (▲) and compared with Δ318-hSSTR5 monotransfectants treated with SST-14 (○). *C,* percent internalization of ^{125}I-Tyr^3 SMS by cells expressing Δ318-hSSTR5 alone (○) compared with Δ318-hSSTR5/wt hSSTR1 cotransfectants (●). For comparative purposes, wt hSSTR1 monotransfected in CHO-K1 cells displayed B_{max} 229 ± 10 fmol/mg protein and K_d 0.62 ± 0.13 nM, 68 ± 4% maximum inhibition of forskolin stimulated cAMP at 1 μM SST-14 and no internalization of ^{125}I-LTT-SST-28 radioligand (33). Mean ± S.E. of at least 3 experiments.

reported, up-regulation of SSTR1 is time- and temperature-dependent, reaches saturation at 22 h, and is dependent on molecular signals in the cytoplasmic C-tail of the receptor (33). To test for heterodimerization, the Δ318 hSSTR5 mutant which binds SMS was cotransfected with wt hSSTR1, which does not bind SMS (Δ318 hSSTR5, B_{max} 112 ± 12 fmol/mg protein; wt hSSTR1, B_{max} 96 ± 17 fmol/mg protein). We wondered whether the C-tail of hSSTR1 in this case would confer adenylyl cyclase responsiveness to the C-tail deletion mutant. Immunocytochemistry with antipeptide antibodies directed against the amino-terminal segment of hSSTR1 and hSSTR5 confirmed the expression of both receptor proteins in the plasma membrane of the majority of transfected cells (data not shown). Binding analysis showed a small but significant increase in the binding affinity of SST-14 for the cotransfectants (Fig. 6*A*). In contrast to the Δ318 hSSTR5 mutant that shows no adenylyl cyclase coupling, the hSSTR1/Δ318 hSSTR5 cotransfectants displayed significant dose-dependent maximum 17 ± 1.6% inhibition of forskolin-stimulated cAMP with 1 μM SMS (Fig. 6*B*). A slightly greater 23 ± 2.4% maximum inhibition was seen when SST-14, a common agonist, was applied. The reduced effect of SMS compared with SST-14 may be explained by putative Δ318 hSSTR5 dimers that would be expected to bind but not inhibit adenylyl cyclase. The SSTR1-selective agonist SCH275 (41) inhibited adenylyl cyclase to a similar extent to SST-14 suggesting that the C-tail of hSSTR1 is the limiting factor in effecting maximum forskolin-stimulated cAMP response. In contrast to the ability of hSSTR1 to rescue adenylyl cyclase coupling of the Δ318 hSSTR5 mutant, the related SSTR subtype hSSTR4, which is also SMS-insensitive (22), failed to heterodimerize with Δ318 hSSTR5 in similar cotransfection experiments. This suggests that heterodimerization of SSTRs is a specific process that is restricted to some but not all receptor subtype combinations.

Agonist-dependent Internalization of hSSTR1 through Heterodimerization with hSSTR5—We next looked at the internalization of hSSTR1/Δ318 hSSTR5 cotransfectants using as ligands ^{125}I-Tyr^3 SMS, which binds Δ318 hSSTR5 but not hSSTR1, and ^{125}I-SCH288, which is selective for SSTR1 (41). Compared with 55 ± 5.6% internalization of ^{125}I-Tyr^3 SMS at 60 min by the Δ318 hSSTR5 mutant alone, the cotransfectants showed 11 ± 3.8% internalization of this ligand (Fig. 6*C*). hSSTR1 when expressed alone showed no internalization of its selective ligand ^{125}I-SCH288 consistent with the known inability of this receptor to undergo agonist-induced internalization as a monotransfectant (32, 33). hSSTR1 cotransfected with Δ318 hSSTR5, however, displayed 15 ± 5% internalization of ^{125}I-SCH288 at 60 min. Since hSSTR1 alone cannot internalize ^{125}I-SCH288, the presence of this radioligand intracellularly must reflect internalization of hSSTR1/Δ318 hSSTR5 heterodimers. This was further demonstrated by confocal fluorescence immunocytochemistry using CHO-K1 cells cotransfected with wt hSSTR1 and HA-hSSTR5. Both receptors were colocalized on the plasma membrane of nonpermeabilized cotransfected cells (Fig. 7, *a–c*). As previously reported, hSSTR1 was predominantly localized over the cell surface when expressed alone in CHO-K1 cells (Fig. 7*g*) (33). The hSSTR1 cells permeabilized after 60 min treatment at 37 °C with agonist SST-14 (1 μM) showed very poor labeling of cytoplasmic vesicular structures (Fig. 7*h*) (33). In contrast, when hSSTR1 was cotransfected with HA-hSSTR5, it underwent internalization in the presence of agonist and was indeed colocalized with hSSTR5 in cytoplasmic vesicles of permeabilized cells (Fig. 7, *d–f*). These results suggest that although hSSTR1 does not internalize when expressed alone, it does so when coexpressed with an appropriate partner, in this case hSSTR5.

Agonist-dependent Up-regulation of hSSTR1 through Heterodimerization with hSSTR5—We further investigated agonist-induced up-regulation of hSSTR1 through heterodimerization with Δ318 hSSTR5. hSSTR1 is up-regulated at the membrane by prolonged (22 h) exposure to SST-14 (33). SMS does not bind and therefore does not up-regulate this receptor (Fig. 8*A*). The Δ318 hSSTR5 mutant bound both SST-14 and SMS, but neither induced up-regulation. Treatment of the coexpressed receptors with SMS 1 μM for 22 h induced 110 ± 16% up-regulation of cell surface binding comparable with that obtained with 1 μM SST-14 (113 ± 23%). Pharmacological analysis of the up-regulated receptors with radioligand selective for SSTR1 (^{125}I-SCH288) or SSTR5 (^{125}I-Tyr^3 SMS) showed 92 ± 12.5% increase in ^{125}I-SCH288 binding without any change in ^{125}I-Tyr^3 SMS binding, thereby identifying hSSTR1 as the receptor subtype that was up-regulated at the cell surface by chronic SMS treatment (Fig. 8*B*). Since SMS does not bind SSTR1, its ability to up-regulate this receptor must be through binding to Δ318 hSSTR5 and association with hSSTR1. Although cross-talk between the receptors at the level of signaling cannot be entirely excluded, this appears unlikely since deletion of the C-tail of hSSTR5 blocks signaling, at least via

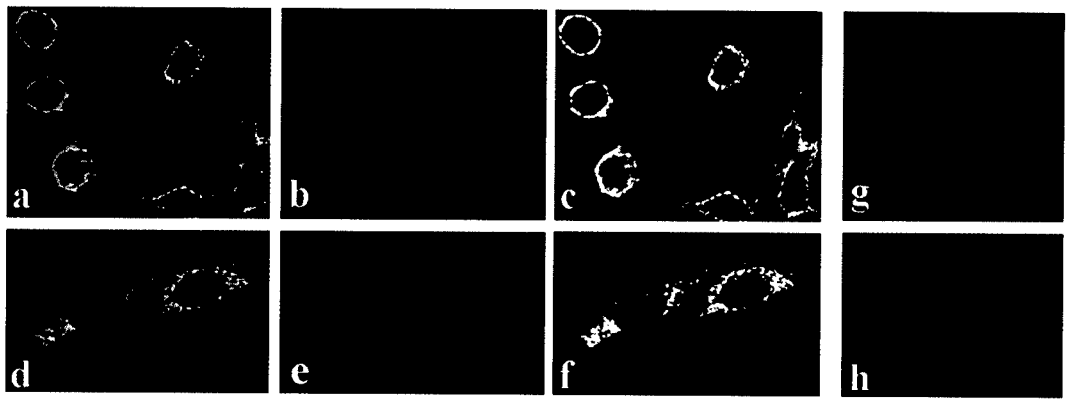

FIG. 7. **Confocal immunofluorescence analysis of wt hSSTR1 and HA-hSSTR5 stably cotransfected in CHO-K1 cells demonstrating receptor distribution on plasma membrane of nonpermeabilized cells (*a–c*) and in cytoplasmic vesicles in permeabilized cells after treatment with SMS 1 μM (*d–f*).** *a*, fluorescein immunofluorescent images showing HA-hSSTR5 localized on the plasma membrane (*green*). *b*, rhodamine immunofluorescent images of wt hSSTR1 localized on the plasma membrane (*red*). *c*, merged image to show colocalization of the two receptors on the plasma membrane (*yellow*). *d–f*, in permeabilized cells, hSSTR5 (*d, green label*) and hSSTR1 (*e, red label*) are colocalized (*f, yellow image*) in cytoplasmic vesicular structures. *g* and *h*, rhodamine fluorescence of hSSTR1 expressed alone in CHO-K1 cells. hSSTR1 is distributed on the plasma membrane (*g*) but does not appear in cytoplasmic vesicles in agonist-treated permeabilized cells (*h*). hSSTR1 is therefore localized intracellularly with hSSTR5 when coexpressed but not alone.

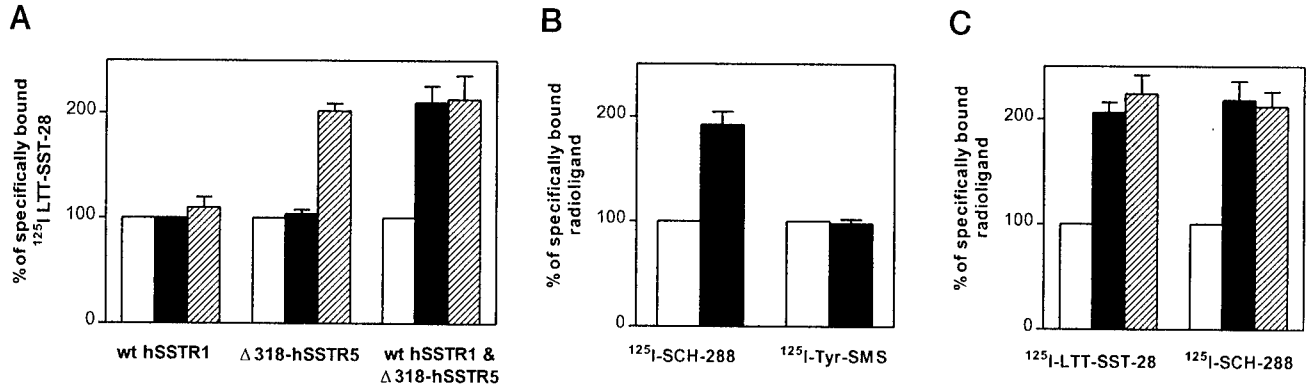

FIG. 8. **Agonist-induced up-regulation of hSSTR1 through heterodimerization.** Cells expressing either wt hSSTR1, Δ318 hSSTR5, or both receptors together were incubated with control medium (*open bars*) or medium containing 1 μM SMS (*black bars*) or SST-14 (*hatched bars*) for 22 h and subjected to acid wash followed by whole cell binding with different radioligands. *A*, binding of ^{125}I-LTT-SST-28 to mono- and cotransfected cells. *B*, binding of ^{125}I-SCH288 and ^{125}I-Tyr^3 SMS to cotransfectants. *C*, up-regulation of endogenous hSSTR1 in MCF7 cells by treatment with SMS assessed by ^{125}I-LTT-SST-28 and ^{125}I-SCH-288 radioligands. Mean ± S.E. of 3 experiments.

adenylyl cyclase (30). The ability of a ligand that interacts selectively with one SSTR subtype to induce up-regulation of another, noninteractive subtype was also demonstrated in the case of endogenous SSTRs (Fig. 8*C*). MCF-7 human breast cancer cells were found (by RT-PCR) (28) to express mRNA for several SSTRs with the following relative abundance (compared with actin mRNA): SSTR1 (+++), SSTR2 (+), SSTR3 (±), SSTR4 (−), and SSTR5 (+++). Confocal fluorescence immunocytochemistry (26, 27) confirmed the protein expression of SSTR1,2,3,5 (but not SSTR4) in these cells. Treatment of MCF-7 cells with 1 μM SMS for 22 h induced a significant 109 ± 15% increase in membrane SSTRs assessed by whole cell binding with ^{125}I-LTT-SST-28. Analysis of the up-regulation response with ^{125}I-SCH288 indicated surface recruitment of hSSTR1 (118 ± 22% increase in binding) (Fig. 8*C*). Since SMS binds only to SSTR2,3,5, these results, taken together with those from the hSSTR1/Δ318 hSSTR5 cotransfection experiments, suggest functional cross-talk in MCF7 cells between SSTR1 and SSTR5 (and likely between SSTR1 and SSTR2) through receptor dimerization.

DISCUSSION

The existence of receptor dimers has been proposed for several GPCRs, based on studies of cross-linked or solubilized receptors or on functional complementation of mutant and chimeric receptors (5–10, 19–21). However, the question of whether GPCR dimers are necessary for activating or modulating normal receptor function has remained unclear (16, 21). By using FRET to monitor dimerization directly, as well as pharmacological and biochemical studies of both mutant and wild type receptors, here we provide strong evidence that members of the SSTR family, undergo agonist-dependent homo- and heterodimerization and that dimeric association alters SSTR functions such as ligand binding affinity, internalization, and up-regulation. We show that hSSTR5 forms heterodimers with hSSTR1 but not with hSSTR4 suggesting that heterodimerization of SSTRs is a specific process that is restricted to some but not all receptor subtype combinations.

The density of endogenous SSTR expression in receptor-rich tissues such as the brain, pituitary, pancreas, and adrenals in the rat measured with a nonspecific radioligand such as ^{125}I-LTT-SST-28 (which detects all five SSTR subtypes) ranges between 220 and 360 fmol/mg protein (40). In addition, because these tissues express all five SSTR isoforms, the concentration of individual subtypes is likely to be a fraction of this amount. To determine whether the level of receptor expression influences dimerization, we initially studied recombinant hSSTR5 overexpressed in CHO-K1 cells and found significant dimerization of this receptor in the basal state, both by Western blots and FRET analysis. At lower levels of transfection corresponding to endogenous SSTR concentrations, however, hSSTR5 oc-

curred only as a monomer in the basal state as determined by FRET. Activation by ligand induced receptor homodimerization in a dose-dependent manner. The parallel dose-response curves for ligand-induced dimerization and signaling by hSSTR5 suggest that dimerization is obligatory for receptor activation. Furthermore, hSSTR5 formed heterodimers with hSSTR1. This means that a given SSTR exists in different states as a monomer (probably inactive), a homodimer, or a heterodimer with one or more SSTR subtypes. Our results suggest that the use of high density receptor expression systems for detecting dimers by Western blots in several earlier studies may account for the high level of basal dimerization as an artifact of receptor overexpression and may help to explain some of the difficulties in interpreting the functional relationship between monomers and dimers (9, 10, 19, 20). The structural requirements for GPCR dimerization are unknown although several dimerization interfaces have been proposed such as the extracellular amino-terminal domain for the glutamate and calcium-sensing receptors (42, 43), the intracellular third loop and the VIth transmembrane domain for the β-adrenergic and dopamine receptors (9, 15, 16), and the C-tail for the GABA-B receptor (11–14, 21). In the case of SSTRs, the C-tail is clearly not required given the ability of SSTR1 and SSTR5 to form homo- and heterodimers with the C-tail deletion mutant of hSSTR5.

There are a number of functional consequences of dimerization by SSTR and other GPCRs. A given agonist may bind with different affinities to a given SSTR depending on its oligomeric configuration. A receptor may undergo regulatory responses in the absence of ligand, for instance by an agonist that binds selectively to one subtype and that modulates the internalization or up-regulation responses of another subtype(s) through heterodimerization. hSSTR1 internalized only as a heterodimer but not when expressed alone suggesting that coexpression of this receptor with hSSTR5 or possibly another subtype(s), as occurs endogenously, is a crucial determinant of its agonist-dependent regulatory responses. The ability of SMS to up-regulate endogenous hSSTR1 by binding to hSSTR5 as shown here may explain the clinical observation of why prolonged treatment of individuals with SMS leads to an escape from the acute effects of the drug (44). This is because up-regulation of receptors such as hSSTR1 may compensate for the desensitized responses of other subtypes interacting with SMS to maintain normal SST responsiveness in target cells such as those in the pituitary and islets that coexpress all of these subtypes (26, 27). Such direct protein interaction between different members of the SSTR subfamily, and possibly between SSTR and related receptor families, defines a new level of molecular cross-talk between GPCRs for greater functional diversity.

Acknowledgments—We thank K. Koller (Affymax Research Institute) for providing HA-tagged hSSTR5 cells, J. Rivier for SCH288 and SCH275 peptides, and Sandoz Basel for SMS and Tyr^3 SMS peptides. We also thank Wei-Yi for technical assistance and M. Correia for secretarial help.

REFERENCES

1. Katsuwada, T., Kashiwabuchi, N., Mori, H., Sakimura, K., Kushiya, E., Araki, K., Meguro, H., Masaki, H., Kumanishi, T., Arakawa, M. & Mishina, M. (1992) *Nature* **358,** 36–41
2. Ullrich, A. & Schlessinger, J. (1990) *Cell* **61,** 203–212
3. Cunningham, B. C., Ultsch, M., de Vos, A. M., Mulkerrin, M. G., Clauser, K. R. & Wells, J. A. (1991) *Science* **254,** 821–825
4. Greenlund, A. C., Schreiber, R., Goeddel, D. V. & Pennica, D. (1993) *J. Biol. Chem.* **268,** 18103–18110
5. Maggio, R., Vogel, Z. & Wess, J. (1993) *Proc. Natl. Acad. Sci. U. S. A.* **90,** 3103–3107
6. Hebert, T. E., Moffett, S., Morello, J.-P., Loisel, T. P., Bichet, D. G., Barrett, C. & Bouvier, M. (1996) *J. Biol. Chem.* **271,** 16384–16392
7. Monnot, C., Bihoreau, L., Conchon, S., Curnow, K. M., Corvol, P. & Clauser, E. (1996) *J. Biol. Chem.* **271,** 1507–1513
8. Osuga, Y., Hayaski, M., Kudo, M., Conti, M., Kobilka, B. & Hsueh, A. J. W. (1997) *J. Biol. Chem.* **272,** 25006–25012
9. George, S. R., Lee, S. P., Varghese, G., Zeman, P. R., Seeman, P., Ng, G. Y. K. & O'Dowd, B. F. (1998) *J. Biol. Chem.* **273,** 30244–30248
10. Cvejic, S. & Devi, L. A. (1997) *J. Biol. Chem.* **272,** 26959–26964
11. Kuner, R., Kohr, G., Grunewald, S., Eisenhardt, G., Bach, A. & Kornau, H.-C. (1999) *Science* **283,** 74–77
12. Jones, K. A., Borowsk, B., Tamm, J. A., Craig, D. A., Durkin, M. M., Dai, M., Yao, W. J., Johnson, M., Gunwaldsen, C., Huang, L. Y., Tang, C., Shen, Q., Salon, J. A., Morse, K., Laz, T., Smith, K. E., Nagarathnam, D., Noble, S. A., Branchek, T. A. & Gerald, C. (1998) *Nature* **396,** 674–678
13. Kaupmann, K., Malitschek, B., Schuler, V., Heid, J., Froestl, W., Beck, P., Mosbacher, J., Bischoff, S., Kulik, A., Shigemoto, R., Karschin, A. & Bettler, B. (1998) *Nature* **396,** 683–687
14. White, J. H., Wise, A., Main, M. J., Green, A., Fraser, N. J., Disney, G. H., Barnes, A. A., Emson, P., Foord, S. M. & Marshall, F. H. (1998) *Nature* **396,** 679–682
15. Gouldson, P. R. & Reynolds, C. A. (1997) *Biochem. Soc. Trans.* **25,** 1066–1071
16. Hebert, T. E. & Bouvier, M. (1998) *Biochem. Cell Biol.* **76,** 1–11
17. Onaran, H. O. & Gurdel, H. (1999) *Trends Pharmacol. Sci.* **20,** 274–278
18. Jordan, B. A. & Devi, L. A. (1999) *Nature* **399,** 697–700
19. Zeng, F.-Y., Hopp, A., Soldner, A. & Wess, J. (1999) *J. Biol. Chem.* **274,** 16629–16640
20. AbdAlla, S., Zaki, E., Lother, H. & Quitterer, U. (1999) *J. Biol. Chem.* **274,** 26079–26084
21. Marshall, F. H., Jones, K. A., Kaupmann, K. & Bettler, B. (1999) *Trends Pharmacol. Sci.* **20,** 396–399
22. Patel, Y. C. (1999) *Front. Neuroendocrinol.* **20,** 157–198
23. Reardon, D. B., Dent, P., Wood, S. L., Kong, T. & Sturgill, T. W. (1997) *Mol. Endocrinol.* **11,** 1062–1069
24. Sharma, K., Patel, Y. C. & Srikant, C. B. (1999) *Mol. Endocrinol.* **13,** 82–90
25. Patel, Y. C., Panetta, R., Escher, E., Greenwood, M. & Srikant, C. B. (1994) *J. Biol. Chem.* **269,** 1506–1509
26. Kumar, U., Laird, D., Srikant, C. B., Escher, E. & Patel, Y. C. (1997) *Endocrinology* **138,** 4473–4476
27. Kumar, U., Sasi, R., Suresh, S., Patel, A., Thangaraju, M., Metrakos, P., Patel, S. C. & Patel, Y. C. (1999) *Diabetes* **48,** 77–85
28. Khare, S., Kumar, U., Sasi, R., Puebla, L., Calderon, L., Lemstrom, K., Hayry, P. & Patel, Y. C. (1999) *FASEB J.* **13,** 387–394
29. Greenwood, M. T., Hukovic, N., Kumar, U., Panetta, R., Hjorth, S. A., Srikant, C. B. & Patel, Y. C. (1997) *Mol. Pharmacol.* **52,** 807–814
30. Hukovic, N., Panetta, R., Kumar, U., Rocheville, M. & Patel, Y. C. (1998) *J. Biol. Chem.* **273,** 21416–21422
31. Koller, K. J., Whitehorn, E. A., Tate, E., Ries, T., Aguilar, B., Chernov-Rogan, T., Davis, A. M., Dobbs, A., Yen, M. & Barrett, R. W. (1997) *Anal. Biochem.* **250,** 51–60
32. Hukovic, N., Panetta, R., Kumar, U. & Patel, Y. C. (1996) *Endocrinology* **137,** 4046–4049
33. Hukovic, N., Rocheville, M., Kumar, U., Sasi, R., Khare & Patel, Y. C. (1999) *J. Biol. Chem.* **274,** 24550–24558
34. Laemmli, U. K. (1970) *Nature* **227,** 680–685
35. Forster, T. (1948) *Naturwissenschaften* **6,** 166–175
36. Hirschfeld, T. (1976) *Appl. Optics* **15,** 3135–3139
37. Jovin, T. M. & Arndt-Jovin, D. J. (1989) in *Cell Structure and Function by Microspectrofluorometry* (Kohen, E. & Hirschberg, J. G., eds) pp. 99–117, Academic Press, New York
38. Clegg, R. M. (1996) in *Fluorescence Imaging Spectroscopy and Microscopy* (Wang, X. F. & Herman, B., eds) pp. 179–252, Wiley-Interscience, New York
39. Gadella, T. W. J. & Jovin, T. M. (1995) *J. Cell Biol.* **129,** 1543–1558
40. Srikant, C. B. & Patel, Y. C. (1987) in *Somatostatin: Basic and Clinical Status* (Reichlin, S., ed) pp. 89–102, Plenum Publishing Corp., New York
41. Liapakis, G., Hoeger, C., Rivier, J. & Reisine, T. (1996) *J. Pharmacol. Exp. Ther.* **276,** 1089–1094
42. Romano, C., Yang, W.-L. & O'Malley, K. L. (1996) *J. Biol. Chem.* **271,** 28612–28616
43. Bai, M., Trivedi, S. & Brown, E. M. (1998) *J. Biol. Chem.* **273,** 23605–23610
44. Lamberts, S. W. J., Vander Lely, A. J. & de Herder, W. W. (1996) *N. Engl. J. Med.* **334,** 246–254

THE JOURNAL OF BIOLOGICAL CHEMISTRY
Vol. 275, No. 13, Issue of March 31, pp. 9244–9250, 2000
Printed in U.S.A.

Caspase-8-mediated Intracellular Acidification Precedes Mitochondrial Dysfunction in Somatostatin-induced Apoptosis*

(Received for publication, October 4, 1999, and in revised form, December 21, 1999)

Danni Liu‡, Giovanni Martino‡, Muthusamy Thangaraju‡, Monika Sharma‡, Fawaz Halwani§, Shi-Hsiang Shen¶, Yogesh C. Patel‡, and Coimbatore B. Srikant‡‖

From the ‡Fraser Laboratories, Department of Medicine, and the §Department of Pathology, McGill University and Royal Victoria Hospital, Montreal, Quebec H3A 1A1 and the ¶Pharmaceutical Sector, N.R.C. Biotechnology Research Institute, Montreal, Quebec H4P 2R2, Canada

Activation of initiator and effector caspases, mitochondrial changes involving a reduction in its membrane potential and release of cytochrome *c* (cyt *c*) into the cytosol, are characteristic features of apoptosis. These changes are associated with cell acidification in some models of apoptosis. The hierarchical relationship between these events has, however, not been deciphered. We have shown that somatostatin (SST), acting via the Src homology 2 bearing tyrosine phosphatase SHP-1, exerts cytotoxic action in MCF-7 cells, and triggers cell acidification and apoptosis. We investigated the temporal sequence of apoptotic events linking caspase activation, acidification, and mitochondrial dysfunction in this system and report here that (i) SHP-1-mediated caspase-8 activation is required for SST-induced decrease in pH_i. (ii) Effector caspases are induced only when there is concomitant acidification. (iii) Decrease in pH_i is necessary to induce reduction in mitochondrial membrane potential, cyt *c* release and caspase-9 activation and (iv) depletion of ATP ablates SST-induced cyt *c* release and caspase-9 activation, but not its ability to induce effector caspases and apoptosis. These data reveal that SHP-1-/caspase-8-mediated acidification occurs at a site other than the mitochondrion and that SST-induced apoptosis is not dependent on disruption of mitochondrial function and caspase-9 activation.

Apoptosis is a physiological process of cell death indispensable for the maintenance of multicellular organisms. This process drives the cell into self-destruction via a common execution pathway. The cellular machinery utilized for this process creates distinct apoptotic features of cell shrinkage, cytoplasmic and nuclear condensation, membrane blebbing, chromatin compaction, and fragmentation of chromosomal DNA into 180-base pair multimers. A central event in the process of apoptosis is the activation of cysteine aspartate proteases (caspases) (1). Active caspases consist of dimeric complexes of ~20- and 10-kDa fragments derived from the procaspases that exist as inactive zymogens by internal proteolytic cleavage at cysteine-aspartate sites (2). Mammalian caspases can be divided into initiator (*e.g.* caspases 2, 8, 9, 10) and effector (caspases 3, 4, 5, 6, 7, 11, 12, and 13) enzymes. A feature of apoptosis that impinges on caspases is altered mitochondrial function characterized by a reduction in the electrochemical gradient across the mitochondrial membrane ($\Delta\psi_m$)[1] and release of mitochondrial cyt *c* into the cytoplasm (3–15). Cyt *c* is necessary for caspase-9 activation (16, 17). Caspase-9 can function as an initiator caspase when mitochondrial dysfunction is the primary event in apoptosis, whereas it serves to amplify the apoptotic signaling of other initiator caspases under conditions in which disruption of mitochondria is a late event (16–19).

In some models of apoptosis activation of caspases is associated with intracellular acidification (20–23). The question of whether intracellular acidification is necessary for inducing caspases or occurs merely as a consequence of caspase activation has remained an issue of debate (24–32). For instance, contradictory reports suggest that the pan-caspase inhibitor z-VAD-fmk prevents decrease in pH_i, whereas acidification *per se* was found to activate z-VAD-fmk-sensitive caspases (27, 32). Since z-VAD-fmk inhibits both initiator and effector caspases, its use does not allow differentiation between caspases that may be activated in a pH_i-sensitive and -insensitive manner during apoptosis associated with acidification. The temporal relationship between mitochondrial dysfunction and acidification has not been definitively established, although it was reported recently that loss of $\Delta\psi_m$ may trigger a decrease in intracellular pH (pH_i) in hematopoietic cells (27, 32).

Somatostatin (SST) receptor (SSTR)-mediated cytotoxic signaling triggers acidification and apoptosis in MCF-7 and T47D breast cancer cells: prevention of acidification by pH clamping inhibited its ability to induce apoptosis (33–35). Translocation of the tyrosine phosphatase SHP-1 from the cytosol to the membrane is an early and essential event in SST-induced cell acidification and apoptosis (34–36). When ectopically expressed, SHP-1 lowered the resting pH_i of MCF-7 cells (pH_i = 7.07 *versus* 7.25 in cells transfected with the empty vector), and amplified not only the cytotoxic action of SST, but also acidification-induced apoptosis. Moreover, agonist-induced acidification and acidification-induced apoptosis were both inhibited by the dominant negative suppressive effect SHP-1C455S (35). In the present study we undertook to delineate the temporal sequence of activation of different caspases in relation to cellular acidification and mitochondrial dysfunction during SST-induced apoptosis in MCF-7 cells. We present evidence demonstrating that caspase 8 activation is necessary for intracellular acidification to occur during SST-induced apoptosis and that the effector caspases are induced only as a consequence of the

* This work was supported by Canadian Medical Research Council Grant MT-12603 and the U. S. Department of Defense Breast Cancer Program. The costs of publication of this article were defrayed in part by the payment of page charges. This article must therefore be hereby marked "*advertisement*" in accordance with 18 U.S.C. Section 1734 solely to indicate this fact.

‖ To whom correspondence should be addressed: M3.15, Royal Victoria Hospital, 687 Pine Ave. W., Montreal, Quebec H3A 1A1, Canada. Tel.: 514-842-1231 (ext. 5359); Fax: 514-849-3681; E-mail: mdcs@musica.mcgill.ca.

[1] The abbreviations used are: $\Delta\psi_m$, mitochondrial membrane potential; cyt *c*, cytochrome *c*; $DiOC_6(3)$, 3,3′-dihexyloxacarbocyanine iodide; NHE, Na^+/H^+ exchanger; pH_i, intracellular pH; SST, somatostatin.

decrease in pH_i. Moreover, the reduction in $\Delta\psi_m$ and the release of cyt *c* into the cytosol from the mitochondria also occur distal to acidification. Depletion of ATP prevented the activation of caspase-9 but only partially inhibited its ability to activate the terminal caspases and induce apoptosis. These data suggest that SST-induced, acidification-dependent, apoptosis is not dependent on mitochondrial dysfunction.

MATERIALS AND METHODS

The MCF-7 cell line (clone HTB22) was obtained from ATCC. Special reagents were obtained from the following sources: [D-Trp^8]SST-14 (Bachem, Torrance, CA); annexin-V labeling kit (Roche Diagnostics, Montreal, CA); nigericin (ICN, Costa Mesa, CA). Carboxy-SNARF-1 acetoxymethyl ester and 3,3′-dihexyloxacarbocyanine iodide ($DiOC_6(3)$) (Molecular Probes, Eugene, OR). Aminomethylcoumarin derivatives (caspase substrates) and aldehyde derivatives (caspase inhibitors) of tetrapeptide sequences that are recognized by distinct caspases: IETD (caspase-8), LEHD (caspase-9), and DEVD (caspases-3/-7) (BioMol Research Laboratories, Plymouth Meeting, PA). Antibodies against the different caspases and cyt *c* were purchased from Pharmingen (San Diego, CA). All other reagents used were of analytical grade and were obtained from regular commercial sources.

Cell Culture and Incubation Conditions—Cells were plated in 75-cm^2 culture flasks and grown in minimal essential medium containing nonessential amino acids and supplemented with 10% fetal bovine serum. Cells were incubated in the presence or absence of 100 nM [D-Trp^8]SST-14 for different time periods as indicated. To examine the effect of direct acidification, cells were incubated in medium supplemented with 140 mM K^+ and 10 nM nigericin. Caspase inhibitors were dissolved in dimethyl sulfoxide and used at 1:1000 dilution to yield a final concentration of 50 mg/ml. Depletion of intracellular ATP was achieved in glucose-deprived cells by inhibiting F_0/F_1-ATPase with oligomycin (37). Briefly, cells were incubated with 10 mM oligomycin in glucose-free Dulbecco's modified Eagle's medium (Canadian Life Technologies, Guelph, Ontario) supplemented with 50 mM malic acid, 2 mM glutamate, 1 mM sodium pyruvate, 10 mM HEPES/Na^+ (pH 7.4), 0.05 mM β-mercaptoethanol, and 10% dialyzed fetal bovine serum as described by Eguchi *et al.* (38) prior to peptide treatment. Cellular ATP was measured using a commercial luciferase luminescence assay kit (Sigma). The ATP concentration decreased by >83 ± 6% (n = 4) following oligomycin treatment (data not shown).

Detection of Apoptosis—Apoptosis was determined by annexin-V positivity using the annexin-V-FLUOS kit (Roche Diagnostics, Montreal, Canada) or by the presence of oligonucleosomal DNA fragments as described previously (34, 35, 39). Cells labeled with fluorescein isothiocyanate-conjugated annexin-V and propidium iodide were analyzed by flow cytometry in a Becton Dickinson Vantage Plus flow cytometer. A 5-watt argon laser generating light at 351–363 nm was used as the excitation source and fluorescein isothiocyanate fluorescence was detected with a 560-nm short pass dichroic filter while propidium iodide fluorescence was detected using a 610-nm long pass filter. At least 10,000 gated events were recorded for each sample and the data analyzed by Winlist software (Verity Software House, ME). To assess DNA fragmentation, DNA was extracted twice with phenol/chloroform and once with chloroform from cells incubated in lysis buffer (500 mM Tris-HCl (pH 9) containing 2 mM EDTA, 10 mM NaCl, 1% SDS, and 1 mg/ml proteinase K) at 48 °C for 30 h. DNA extracts were incubated with 300 μg/ml bovine pancreatic RNase A at 37 °C for 1 h and 10-μg aliquots of DNA samples containing 10 μg/ml ethidium bromide were subjected to electrophoresis on 1.2% (w/v) agarose gels using the Hoefer Switchback™ pulse controller and visualized under UV light.

Measurement of Intracellular pH—For measuring intracellular pH, cells were loaded with 10 μM acetoxymethylester derivative of SNARF-1 for the final hour of incubation in the absence or presence of 100 nM [D-Trp^8]SST-14 at 37 °C (39). The cells were then scraped, washed, and maintained at 37 °C. Intracellular carboxy SNARF-1 was excited at 488 nm and emission was recorded at both 580 and 640 nm with 5-nm band pass filters with linear amplifiers in a Becton-Dickinson FACStar Vantage cytometer. The ratio of the emissions at these wavelengths was electronically calculated and used as a parameter indicative of pH_i. The intracellular pH values were estimated by comparison of the mean ratios of the samples to a calibration curve of intracellular pH generated by incubation of carboxy-SNARF-1 loaded cells in buffers ranging in pH from 8.0 to 6.25 and containing the proton ionophore nigericin (33). Cells with fluorescence of <50 units were excluded in the calculation of the ratio of the emissions at 580 and 640 nm.

Measurement of Mitochondrial Membrane Potential—$DiOC_6(3)$ (50 nM final concentration) was added to the cells 15 min prior to the completion of incubation. The cells were then washed to remove excess fluorochrome, scraped, and maintained at 37 °C. $DiOC_6(3)$ fluorescence was measured in a EPICS 750 series Flow Cytometer (Coulter Electronics, Hialeah, FL) with the excitation and emission wavelengths set at 488 and 520 nm, respectively. At least 10,000 events were recorded for each sample and the data analyzed by WinList Program (Verity Software House, Topsham, ME).

Subcellular Fractionation and Western Blotting—Cells were washed in phosphate-buffered saline and resuspended in 500 ml of a buffer containing 25 mM Hepes-KOH buffer (pH 7.4) containing 10 mM KCl, 1.5 mM $MgCl_2$, 5 mM EDTA, 1 m M EGTA, 2 mM dithiothreitol, 250 mM sucrose, 0.2% Triton X-100, and protease inhibitor mixture (Roche Diagnostics, Montreal, CA). The cells were homogenized in a Pyrex homogenizer using a type B pestle. Cell debris and nuclei were removed by centrifugation at 1,000 × *g* for 10 min at 4 °C. Mitochondrial fraction was then pelleted by centrifugation at 10,000 × *g* for 20 min. The supernatant obtained at this stage was re-centrifuged at 40,000 × *g* for 1 h to obtain cytosolic fraction.

Thirty micrograms of cytosolic fractions prepared from cells incubated under different experimental conditions were subjected to SDS-polyacrylamide gel electrophoresis. The separated proteins were blotted onto nitrocellulose membranes and subjected to immunoblot analysis for cyt *c*, or caspases-8, -9, -3, and -7.

Measurement of Caspase Activity—Activities of caspases were measured in the lysates measuring the *in vitro* hydrolysis of DEVD-AMC (caspases-3 and -7), IETD-AMC (caspase-8), and LEHD-AMC (caspase-9) (40, 41). The fluorescence of the aminomethylcoumarin released from the substrates was measured in a Perkin-Elmer spectrofluorimeter with the excitation and emission wavelengths set at 380 and 460 nm, respectively. Enzyme activity was quantitated against a standard fluorescence curve generated using aminomethylcoumarin over a concentration range of 0–1000 nM.

RESULTS

In order to determine the hierarchy of caspase activation during acidification-dependent apoptosis we measured the time course of [D-Trp^8]SST-14-induced changes in enzyme activities using substrates that display specificity for initiator and effector caspases *in vitro*: IETD-AMC (caspase-8) and DEVD-AMC (caspases-3/-7) respectively. In cells incubated with 100 nM [D-Trp^8]SST-14 a concentration which induced maximal apoptosis (35, 39), the IETD-AMC hydrolyzing activity was maximal by 3 h (6-fold increase over the basal value of 0.5 nmol/mg protein, Fig. 1), but had fallen to basal levels by 24 h. By contrast, DEVD-specific caspase activity increased by <3-fold during SST treatment but continued to increase and remained elevated even at 24 h (1.21 ± 0.14 and 3.61 ± 0.7, respectively, compared with 0.45 ± 0.05 nmol/mg protein in untreated control cells). When acidification was prevented by pH clamping by the inclusion of nigericin, SST-induced increase in IETDase was unaffected whereas its ability to induce DEVDase activity was completely inhibited (Fig. 2). We next examined the effect of selective inhibitors of these caspases on SST-induced acidification and apoptosis. IETD-CHO (the tetrapeptide aldehyde inhibitor of caspase-8) prevented the decrease pH_i in SST-treated cells whereas DEVD-CHO (the caspase-3/-7 inhibitor) was without effect (Fig. 3*A*). By contrast, the ability of SST to induce apoptosis was suppressed by both inhibitors as confirmed by DNA fragmentation analysis (Fig. 3*B*) and by annexin-V positivity (not shown). The temporal sequence of activation of the different caspases during [D-Trp^8]SST-14-induced apoptosis was confirmed by measuring the effect of each of the caspase inhibitors on the activities of other caspases (Fig. 4). IETD-specific caspase activation by SST was unaffected by DEVD-CHO (Fig. 4*A*) but the inductive effect of SST on DEVD-specific caspase activity was totally inhibited by IETD-CHO (Fig. 4*B*).

Mitochondrial dysfunction characterized by a reduction in its transmembrane potential ($\Delta\Psi_m$) and release of cyt *c* into the cytosol, are characteristic features of apoptosis (6, 9, 10, 42, 43). An important arm of apoptotic signaling involves cyt *c*-depend-

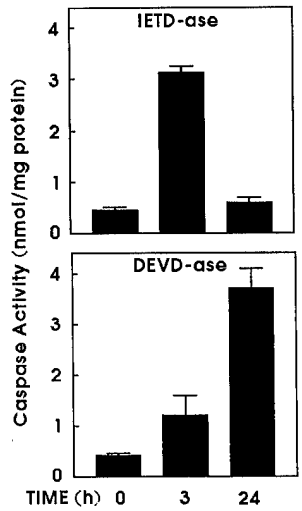

FIG. 1. **[D-Trp^8]SST-14-induced activation of caspase-8 (IETD-ase) precedes that of caspases-3/-7 (DEVDase) in MCF-7 cells.** Enzyme activities were measured using the aminomethylcoumarin derivatives of the tetrapeptide substrates in extracts of cells incubated with 100 nM peptide at the indicated times. IETDase activity was maximal at 3 h, and declined to basal level by 24 h (*top panel*). By contrast, DEVDase activity was maximal at 24 h (*bottom panel*). Values represent nanomole of aminomethylcoumarin liberated from the substrates during 30 min incubation with cell extracts *in vitro* and was quantitated against the fluorescence readings of serially diluted aminomethylcoumarin as described under "Materials and Methods" (mean ± S.E., n = 6).

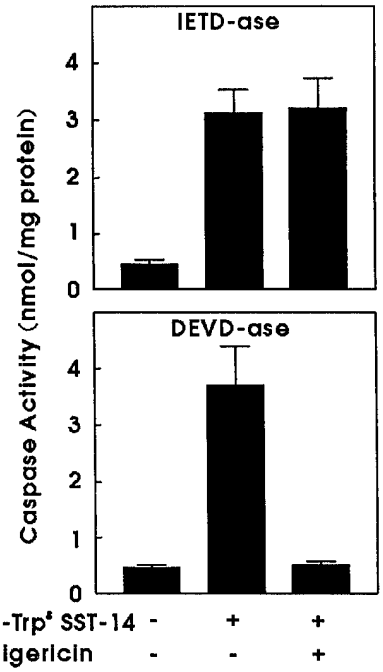

FIG. 2. **Effect of pH clamping on caspase activation.** [D-Trp^8]SST-14 induced increase in caspase-8 (IETDase) activity was not affected by the prevention of acidification by nigericin (*top panel*) whereas pH clamping prevented the increase in caspase-3/-7 (DEVDase) activity (*bottom panel*). Enzyme activities were measured after 4 h (IETDase) or 24 h (DEVDase) treatment (mean ± S.E., n = 6).

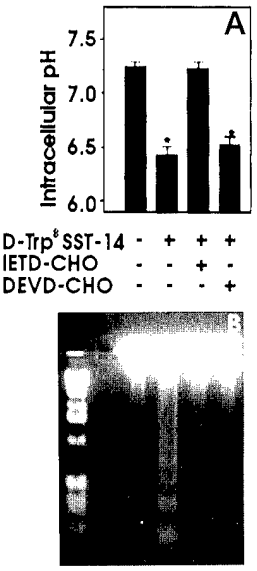

FIG. 3. **Differential effects of caspase-inhibitors on [D-Trp^8]SST-14-induced acidification, but not on apoptosis in MCF-7 cells.** *A*, the decrease in pH_i in cells incubated with 100 nM peptide for 24 h was prevented by the caspase-8 inhibitor IETD-CHO, but not by the caspase-3/-7 inhibitor, DEVD-CHO (mean ± S.E., n = 6). *B*, oligonucleosomal DNA fragmentation in peptide-treated cells was completely inhibited by both IETD-CHO and DEVD-CHO (figure representative of four different experiments).

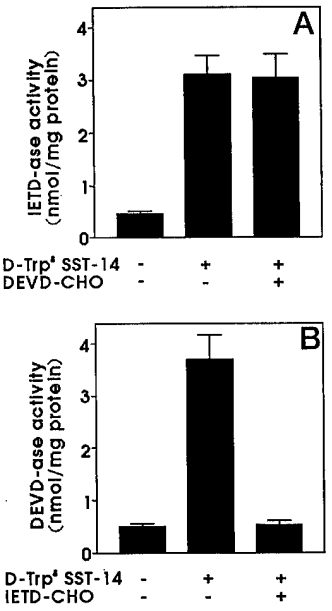

FIG. 4. **Inhibition of DEVDase does not prevent [D-Trp^8]SST-14-induced activation of IETDase, whereas inhibition of IETD-ase abrogates induction of DEVDase.** *A*, extracts of cells incubated with 100 nM peptide ± DEVD-CHO for 4 h were assayed for IETDase activity or for 24 h ± IETD-CHO for DEVDase assay (mean ± S.E., n = 6).

ent activation of caspase-9. Cyt *c* released from the mitochondria complexes with APAF-1 (the mammalian homolog of the pro-apoptotic protein CED-4 of *Caenorhabditis elegans*) and procaspase-9. Such activation of caspase-9 has been reported to be necessary for the full expression of nuclear apoptotic events (44). To determine whether mitochondrial dysfunction precedes or follows acidification, we compared the effects of pH clamping and different caspase inhibitors on $\Delta\psi_m$, cyt *c* release, and caspase-9 activation in SST-treated cells. SST induced a decrease in $\Delta\psi_m$ in MCF-7 cells (Fig. 5*A*). Inhibition of acidification by pH clamping totally abrogated the ability of SST to decrease $\Delta\psi_m$. Maximal effect was seen at 6 h when 48 ± 7% of SST-treated cells displayed a significant reduction in $\Delta\psi_m$ compared with the untreated control (Fig. 5*B*). Additionally, loss of $\Delta\psi_m$ during SST treatment was prevented almost completely by IETD-CHO but was decreased only by 23 ± 3% by DEVD-CHO (Fig. 5*B*). A marked increase in cytosolic cyt *c* content was seen in SST-treated cells (Fig. 6). Such an increase did not

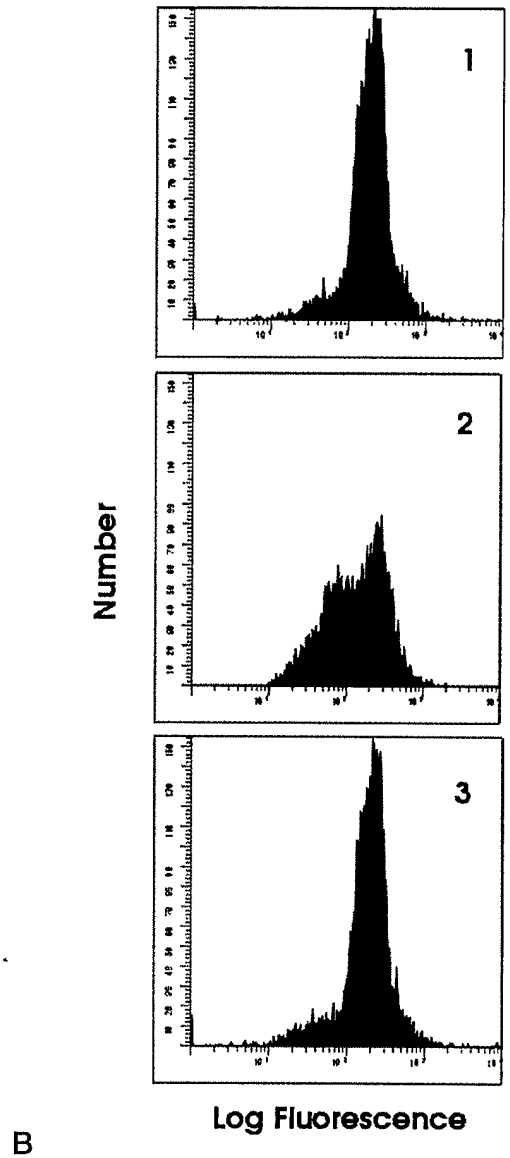

FIG. 5. **[D-Trp^8]SST-14-induced reduction in $\Delta\psi_m$ is acidification-dependent.** *A*, cells were incubated for 6 h in the absence (*panel 1*) or presence of 100 nM peptide (*panel 2*) in regular medium or with the peptide in nigericin containing medium (*panel 3*), labeled with $DiOC_6(3)$ and analyzed by flow cytometry. Representative recordings of six separate measurements are shown. The reduction in $\Delta\psi_m$ in peptide-treated cells is evident from the decrease in the number of cells with the resting potential as well as from the appearance of the distinct peak of cells with lower $DiOC_6(3)$ fluorescence (*panel 2*). Inhibition of acidification prevented the ability of [D-Trp^8]SST-14 to decrease $\Delta\psi_m$ (compare *panels 3* and *1*). *B*, quantitation of the effect of pH clamping, IETD-CHO and DEVD-CHO on D-Trp^8-induced reduction in $\Delta\psi_m$ (mean ± S.E., n = 6). The effect of the peptide was only partially inhibited by DEVD-CHO, whereas it was completely abolished in the presence of IETD-CHO similar to that seen in cells clamped at physiological pH in the presence of nigericin. *, $p < 0.001$; **, $p < 0.01$.

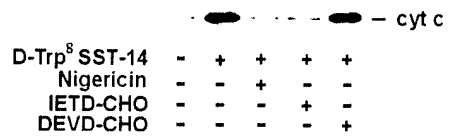

FIG. 6. **[D-Trp^8]SST-14-induced increase in cytosolic cyt *c* precedes the activation of DEVDase.** 30-mg protein aliquots from cytosolic extracts of cells incubated in the absence and presence of 100 nM [D-Trp^8]SST-14 alone or with the indicated inhibitors were subjected to immunoblot analysis following electrophoresis and membrane transfer. Nigericin and IETD-CHO, but not DEVD-CHO, prevented [D-Trp^8]SST-14-induced increase in cyt *c*.

occur when acidification was prevented by pH clamping. SST-induced increase in cytosolic cyt *c* was completely suppressed by IETD-CHO but was not inhibited by inhibition of effector caspases by DEVD-CHO. We measured the caspase-9 activity in extracts of cells incubated with SST using the tetrapeptide substrate LEHD-AMC, a substrate with reported caspase-9 selectivity (41). LEHD-specific caspase activity was induced by SST in MCF-7 cells in an acidification-dependent manner (Fig. 7). Inhibition of caspase-9 activity with LEHD-CHO did not affect SST-induced loss of $\Delta\psi_m$ or the release of cyt *c* into the cytosol (not shown).

Cyt *c*- and APAF-1-mediated activation of caspase-9 is an energy-dependent process requiring ATP (45, 46). In order to establish the extent to which SST-signaled apoptosis is mediated via ATP-dependent caspase-9 activation, we tested the effect of depleting intracellular ATP on the cytotoxic signaling of SST. In ATP-depleted cells, SST failed to activate LEHDase (Fig. 8*A*). ATP depletion also inhibited SST-induced increase in cytosolic cyt *c* (Fig. 8B). By contrast, ATP depletion decreased the inductive effect of SST on DEVDase activity only by 9 ± 1% (Fig. 8*C*). Likewise ATP depletion had minimal effect on the extent of apoptosis. Following 4 h treatment with SST, the number of annexin-V positive cells was 8.8 ± 1.5% in ATP-depleted and 12.1 ± 1.1% in ATP-replete MCF-7 cells. Precise quantitation of the long term effect of ATP depletion on SST-induced apoptosis was not possible because of significant necrosis (as determined by the presence of cells labeled with both propidium iodide and annexin V (data not shown)).

Immunoblot analysis confirmed the pH-independent generation of active caspase-8 (IETD-AMC-specific) by the formation of the 20-kDa caspase-8 fragment from the 50-kDa procaspase-8 in [D-Trp^8]SST-14-treated cells. Inhibition of acidification by pH clamping did not prevent activation of caspase-8 (Fig. 9). By contrast, generation of the 20-kDa fragments of caspase-3 and caspase-7 (DEVD-AMC-specific proteases) from procaspase-3 (32 kDa) and procaspase-7 (35 kDa) and of caspase-9 (LEHD-AMC-specific) from procaspase-9 (48 kDa) occurred only if acidification was present.

The present finding that caspase-8 precedes the onset of acidification prompted us to assess the importance of SHP-1 in the activation of IETDase and DEVDase by [D-Trp^8]SST-14 and by direct acidification. IETDase activity was higher in [D-Trp^8]SST-14 SST-treated cells expressing SHP-1 compared with the empty vector (3.75 ± 0.5 ± 3.1 ± 0.4 nmol/mg protein, Fig. 10, *top panel*). Likewise, agonist-induced increase in DEV-

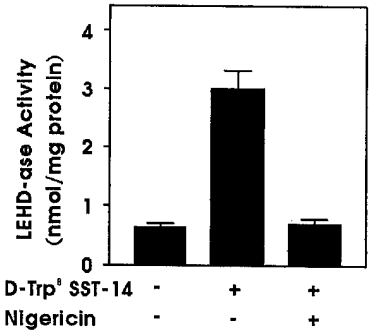

FIG. 7. **Activation of caspase-9 (LEHDase) by [D-Trp^8]SST-14 is attenuated by inhibition of acidification.** Cells were incubated as described in the legend for Fig. 2*B* (mean ± S.E., n = 6).

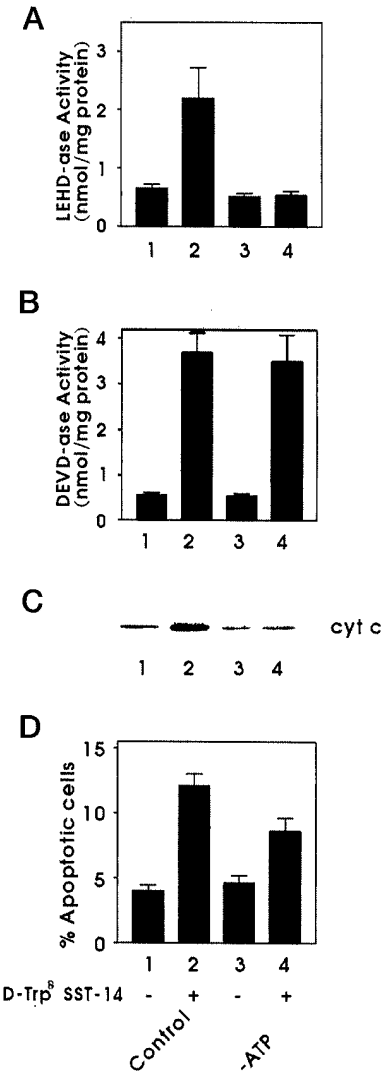

FIG. 8. **Effect of ATP depletion on [D-Trp^8]SST-14-induced cytotoxic signaling.** ATP-depleted cells were prepared by incubating with oligomycin in glucose-free medium for 1 h. Control and ATP-depleted cells were incubated for 4 h in the absence (*lanes 1* and *3*) or presence of 100 nM peptide (*lanes 2* and *4*). *A*, LEHDase activation by the peptide seen in control cells was completely abolished by ATP-depletion (compare *lanes 2* and *4*). *B*, [D-Trp^8]SST-14-induced increase in cytosolic cyt *c* was also inhibited by ATP depletion.

Dase activity was also higher in cells expressing SHP-1 (3.72 ± 0.43 *versus* 2.45 ± 0.36 nmol/mg protein in control vector-transfected cells, Fig. 10, *bottom panel*). As shown in this figure, SHP-1C455S suppressed the ability of [D-Trp^8]SST-14 SST

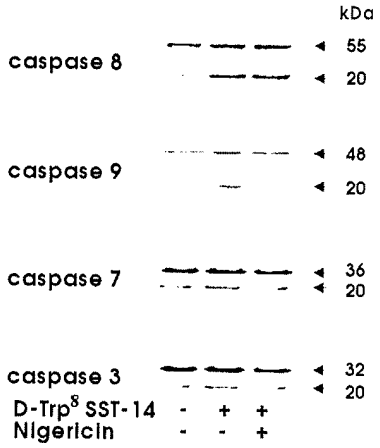

FIG. 9. **Immunoblot analysis demonstrating differential pH sensitivity of caspase activation.** Formation of the 20-kDa active caspase from the inactive procaspase-8 induced by [D-Trp^8]SST-14-mediated cytotoxic signaling was pH-independent. By contrast, the formation of the 20-kDa fragments from procaspases-9, -7, and -3 in peptide-treated cells was prevented by inhibition of acidification by nigericin (data representative of four independent experiments).

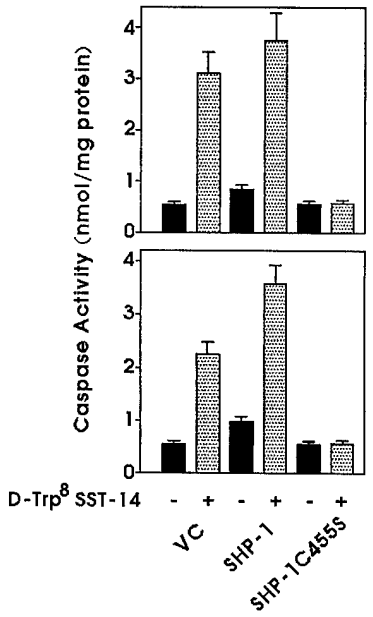

FIG. 10. **SHP-1 dependence of caspase activation by [D-Trp^8]SST-14 in MCF-7 cells.** The ability of the peptide to induce both IETDase (*top panel*) and DEVDase (*bottom panel*) during the 4-h incubation was higher in SHP-1 expressing cells compared with the empty vector control (*VC*) cells, and was abolished by the dominant negative effect of SHP-1C455S. Mean ± S.E., n = 3).

to activate both enzymes. Interestingly, basal activities of IETDase and DEVDase (0.85 ± 0.07 and 0.93 ± 0.1 nmol/mg protein, respectively) were slightly higher in cells overexpressing the wild type SHP-1. When subjected to direct acidification, IETDase activity was minimal in all three cell types (Fig. 11). In SHP-1 expressing cells, IETDase activity was lower than that seen under basal conditions at pH 7.2 (0.63 ± 0.07 *versus* 1.12 ± 0.14 nmol/mg of protein, respectively, compare Figs. 10 and 11). By contrast, DEVDase activity was higher in both vector control and SHP-1-transfected cells (2.45 ± 0.3 and 3.57 ± 0.5 nmol/mg of protein, respectively). The dominant negative effect of SHP-1C455S completely abolished the acidification-induced increase in DEVDase activity. Finally we assessed the role of SHP-1 in [D-Trp^8]SST-14-induced reduction in $\Delta\psi_m$. While the maximum number of cells that displayed decreased

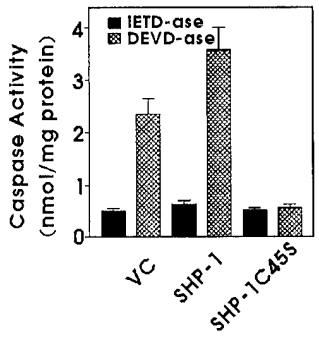

FIG. 11. **Acidification-induced activation of DEVDase (*speckled bars*) in SHP-1-expressing MCF-7 cells was higher than that in control vector (*VC*)-transfected cells.** SHP-1C455S suppressed acidification-induced increase in DEVDase activity. Acidification had no effect on IETDase activity (*solid bars*) in all three cell types.

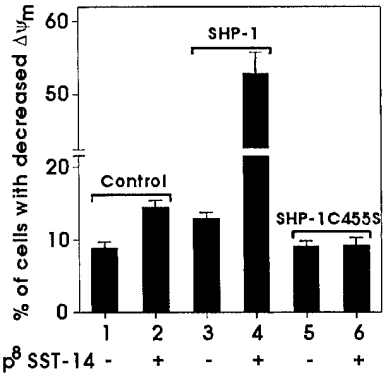

FIG. 12. **SHP-1 dependence of [D-Trp^8]SST-14-induced reduction in $\Delta\psi_m$.** Cells were incubated with 100 nM peptide for 90 min prior to measurement of $\Delta\psi_m$. [D-Trp^8]SST induced reduction in in $\Delta\psi_m$ was seen in 53 ± 4% of SHP-1 expressing cells whereas only 12.8 ± 1% of vector control (*VC*) cells displayed a reduction mitochondrial membrane potential. In cells expressing SHP-1C455S, the peptide failed to trigger the loss of mitochondrial membrane potential (mean ± S.E., n = 4).

$\Delta\psi_m$ was the same in both control vector and SHP-1 transfected cells following incubation with [D-Trp^8]SST-14, the rate of reduction in $\Delta\psi$ was increased by ectopically expressed SHP-1 reaching maximal level by 90 min, a time point at which only 12% of the control vector-transfected cells displayed decrease in $\Delta\psi_m$ (Fig. 12). In SHP-1C455S-transfected cells no decrease in $\Delta\psi_m$ occurred even after 24 h treatment with [D-Trp^8]SST-14.

DISCUSSION

In this study we demonstrated that the cytotoxic signaling of SST in MCF-7 cells activates multiple caspases and that SHP-1-dependent activation of caspase-8 precedes the decrease in pH_i whereas acidification is necessary for the induction of the effector caspases. In accordance with this was the finding that inhibition of SST-induced acidification by pH clamping with nigericin did not affect SST-induced activation of caspase-8 while it completely abrogated the induction of the other caspases. Likewise, inhibition of caspase-8 by IETD-CHO prevented SST-induced acidification and activation of terminal caspases. By contrast, LEHD-CHO and DEVD-CHO did not prevent a SST-induced increase in caspase-8 activity and the decrease in pH_i. Moreover, SST-induced increase in caspase-8 activity peaked by 3 h and declined thereafter paralleling the previously reported time course of acidification (35). The distal caspases, in contrast, displayed sustained increase in activity. These data demonstrate that caspase-8 activation is required for SST-induced acidification and, additionally, that its activity is pH_i sensitive. This is supported by the finding that the 20-kDa fragment derived from procaspase-8 was present in cells with acidic pH_i during SST treatment. By contrast, the generation of caspases-9, -3, and -7 from the respective procaspases occurred only when there was acidification. The detection of caspase-3 in the HTB22 clone of MCF-7 cells used in the present study contrasts with its reported absence in other clones of this cell line due to a 47-base pair deletion within the exon 3 of the caspase-3 gene (47, 48).[2] We found that acidification *per se* was sufficient to activate the effector caspases in the absence of a detectable increase in caspase-8 activity. While this suggests that acidification may trigger the activation of the effector caspases directly, the possibility that transient activation of caspase-8 during rapid acidification may suffice to induce these caspases cannot be ruled out. The finding that SHP-1 is required not only for the induction of IETDase by SST but also of DEVDase by cell acidification reinforces the idea that SHP-1 modulates the apoptotic events both before and after cell acidification (34). The phosphatase-dependent processes that lead to caspase activation remain to be delineated.

[2] R. U. Janicke, personal communication.

Caspase-8 can activate caspases-3 and -7 directly and/or through induction of caspase-9 (17, 18, 45, 49). In order to assess the relative importance of caspase-9 in the cytotoxic signaling of SST, we compared the effect of SST in control and ATP-depleted MCF-7 cells. SST was unable to activate caspase-9 in ATP-depleted cells, but was still capable of activating DEVDase and inducing apoptosis. Thus, SST-induced apoptosis in MCF-7 cells involves caspase-8-mediated direct activation of terminal caspases as well as an amplifying effect mediated through mitochondrial dysfunction and consequent activation of caspase-9. These data support the concept that caspase-8 can activate apoptotic pathways involving effector caspases through both mitochondria-dependent and -independent pathways (17, 44, 50–54). The extent of SST-induced apoptosis was 34 ± 5% lower in ATP-depleted cells, an effect that could be accounted for by the loss of caspase-9-mediated activation of the terminal caspases and/or the loss of effector caspase-mediated activation of caspase-9. We found that DEVD-CHO only partially suppressed the effect of SST on $\Delta\psi_m$ and cyt *c* release suggesting that mitchondrial dysfunction may be caused to some extent by the action of the effector caspases as demonstrated previously in an *in vitro* model (10).

We showed that intracellular acidification precedes the onset of reduction in $\Delta\psi_m$ in MCF-7 cells exposed to the cytotoxic action of SST. Likewise, release of cyt *c* from the mitochondria and LEHDase activation was observed in cells subjected to direct acidification (details not shown). This is in contrast to the report that mitochondrial permeability transition causes acidification during valinomycin-induced apoptosis in hematopoetic cells (55). It is possible that the cause and effect relationship between mitochondrial dysfunction and cell acidification may be cell type-dependent. Indeed the existence of two cell types in which caspase-8 can trigger apoptosis without invoking mitochondrial dysfunction (type I cells) and those in which apoptosis is induced predominantly in a mitochondria-dependent manner (type II cells) has been described (51). The fact that mitochondrial dysfunction occurs late and is inconsequential in SST-signaled apoptosis adds credence to this idea. This is supported by the recently reported finding that ATP-dependent steps in Fas-mediated apoptosis in Type I cells are located downstream of caspase-3 (56).

The mechanism of SHP-1-/caspase-8-mediated inhibition of pH homeostasis remains to be elucidated. We have previously shown that amiloride and bafilomycin-1, which inhibit Na^+/H^+ exchanger (NHE) and H^+-ATPase, respectively, trigger acidification and apoptosis in MCF-7 cells. Inhibition of NHE low-

ered the pH_i to a greater extent than inhibition of H^+-ATPase. (34). This raises the possibility that SHP-1 and caspase-8 mediated signaling may generate or unmask molecule(s) that may disrupt proton extrusion pathways involving these channels. The finding that SST-induced acidification does not occur at the mitochondria suggests that it inhibits the regulation of proton transport through NHE and H^+-ATPase either at the cell membrane or some other subcellular locus. The existence of multiple NHE isoforms and their differential localization at the cell membrane (*e.g.* NHE-1 and NHE-2) or at the endoplasmic reticulum-nuclear envelope and endosomes (*e.g.* NHE-3) (57) raises the possibility that SST may inhibit some or all of the NHEs. Our present findings suggest that SHP-1- and caspase-8-mediated disruption of pH homeostasis may target these proton extrusion pathway(s). Studies are currently in progress to identify the subcellular site(s) and the underlying mechanism involved in SST-induced acidification.

In summary, these findings help define the temporal sequence of events that link the initiator and effector caspases with inhibition of pH homeostasis and mitochondrial dysfunction in acidification-dependent apoptosis. We demonstrated that (i) SHP-1-dependent activation of caspase-8 is required for SST-induced decrease in pH_i while SHP-1-dependent activation of effector caspases is necessary for acidification-induced apoptosis. (ii) Mitochondrial dysfunction and activation of effector caspases occur distal to acidification and (iii) caspase-9 is not essential for SST-induced apoptosis to occur but, when induced, can amplify the cytotoxic signaling of SST.

Acknowledgment—We thank Dr. J. J. Lebrun for the use of the luminometer.

REFERENCES

1. Cohen, G. M. (1997) *Biochem. J.* **326,** 1–16
2. Walker, N. P., Talanian, R. V., Brady, K. D., Dang, L. C., Bump, N. J., Ferenz, C. R., Franklin, S., Ghayur, T., Hackett, M. C., Hammill, L. D., Herzog, L., Hugunin, M., Huoy, W., Mankovich, J. A., McGuiness, L., Orlewicz, E., Paskind, M., Pratt, C. A., Reis, P., Summani, A., Terranova, M., Welch, J. P., Xiong, L., Möller, A., Tracey, D. E., Kamen, R., and Wong, W. W. (1994) *Cell* **78,** 343–352
3. Vayssiere, J. L., Petit, P. X., Risler, Y., and Mignotte, B. (1994) *Proc. Natl. Acad. Sci. U. S. A.* **91,** 11752–11756
4. Kroemer, G., Petit, P. X., Zamzami, N., Vayssiere, J.-L., and Mignotte, B. (1995) *FASEB J.* **9,** 1277–1287
5. Zamzami, N., Marchetti, P., Castedo, M., Zanin, C., Vayssiere, J.-L., Petit, P. X., and Kroemer, G. (1995) *J. Exp. Med.* **181,** 1661–1672
6. Petit, P. X., Lecoeur, H., Zorn, E., Dauguet, C., Mignotte, B., and Gougeon, M. L. (1995) *J. Cell Biol.* **130,** 157–167
7. Kroemer, G., Zamzami, N., and Susin, S. A. (1997) *Immunol. Today* **18,** 44–51
8. Kroemer, G. (1997) *Nature Med.* **3,** 614–620
9. Susin, S. A., Zamzami, N., and Kroemer, G. (1998) *Biochim. Biophys. Acta* **1366,** 151–165
10. Bossy-Witzel, E., Newmeyer, D. W., and Green, D. G. (1998) *EMBO J.* **17,** 37–49
11. Rosse, T., Olivier, R., Monney, L., Rager, M., Conus, S., Fellay, I., Jansen, B., and Borner, C. (1998) *Nature* **391,** 496–499
12. Hirsch, T., Marzo, I., and Kroemer, G. (1997) *Biosci. Rep.* **17,** 67–76
13. Marchetti, P., Hirsch, T., Zamzami, N., Castedo, M., Decaudin, D., Susin, S. A., Masse, B., and Kroemer, G. (1996) *J. Immunol.* **157,** 4830–4836
14. Marchetti, P., Castedo, M., Susin, S. A., Zamzami, N., Hirsch, T., Macho, A., Haeffner, A., Hirsch, F., Geuskens, M., and Kroemer, G. (1996) *J. Exp. Med.* **184,** 1155–1160
15. Marzo, I., Brenner, C., and Kroemer, G. (1998) *Biomed. Pharmacother.* **52,** 248–251
16. Fraser, A., and Evan, G. (1996) *Cell* **85,** 781–784
17. Gross, A., Yin, X.-M., Wang, K., Wei, M. C., Jockel, J., Milliman, C., Erdjument-Bromage, H., Tempst, P., and Korsmeyer, S. J. (1999) *J. Biol. Chem.* **274,** 1156–1163
18. Fernandes-Alnemri, T., Armstrong, R. C., Krebs, J., Srinivasula, S. M., Wang, L., Bullrich, F., Fritz, L. C., Trapani, J. A., Tomaselli, K. J., Litwack, G., and Alnemri, E. S. (1996) *Proc. Natl. Acad. Sci. U. S. A.* **93,** 7464–7469
19. Muzio, M., Salvesen, G. S., and Dixit, V. M. (1997) *J. Biol. Chem.* **272,** 2952–2956
20. Kakutani, T., Ebara, Y., Kanja, K., Hidaka, M., Matsumoto, Y., Nagano, A., and Wataya, Y. (1998) *Biochem. Biophys. Res. Commun.* **247,** 773–779
21. Zanke, B. W., Lee, C., Arab, S., and Tannock, I. F. (1998) *Cancer Res.* **58,** 2801–2008
22. Liu, D., Thangaraju, M., Shen, S.-H., and Srikant, C. B. (1999) *Annual Meeting of the Endocrine Society San Diego, CA, June, 1999,* p. 353, Abstract P2–346, Endocrine Society, San Diego, CA
23. Wolf, C. M., and Eastman, A. (1999) *Biochem. Biophys. Res. Commun.* **254,** 821–827
24. Park, H. J., Makepeace, C. M., Lyons, J. C., and Song, C. W. (1996) *Eur. J. Cancer* **32A,** 540–546
25. Newell, K., Wood, P., Stratford, I., and Tannock, I. (1992) *Br. J. Cancer* **66,** 311–317
26. Maidorn, R. P., Cragoe, E. J., Jr., and Tannock, I. F. (1993) *Br. J. Cancer* **67,** 297–303
27. Furlong, I., Ascaso, R., Rivas, A., and Collins, M. (1997) *J. Cell Sci.* **110,** 653–661
28. Angoli, D., Delia, D., and Wanke, E. (1996) *Biochem. Biophys. Res. Commun.* **229,** 681–685
29. Gottlieb, R. A., Giesing, H. A., Zhu, J. Y., Engler, R. L., and Babior, B. M. (1995) *Proc. Natl. Acad. Sci. U. S. A.* **92,** 5965–5968
30. Gottlieb, R. A., Nordberg, J., Skowronski, E., and Babior, B. M. (1996) *Proc. Natl. Acad. Sci. U. S. A.* **93,** 654–658
31. Meisenholder, G. W., Martin, S. J., Green, D. R., Nordberg, J., Babior, B. M., and Gottlieb, R. A. (1996) *J. Biol. Chem.* **271,** 16260–16262
32. Wolf, C. M., Reynolds, J. E., Morana, S. J., and Eastman, A. (1997) *Exp. Cell. Res.* **230,** 22–27
33. Sharma, K., and Srikant, C. B. (1998) *Biochem. Biophys. Res. Commun.* **242,** 134–140
34. Thangaraju, M., Sharma, K., Liu, D., Shen, S.-H., and Srikant, C. B. (1999) *Cancer Res.* **59,** 1649–1654
35. Thangaraju, M., Sharma, K., Leber, B., Andrews, D. W., Shen, S.-H., and Srikant, C. B. (1999) *J. Biol. Chem.* **274,** 29549–29557
36. Srikant, C. B., and Shen, S. H. (1996) *Endocrinology* **137,** 3461–3468
37. Lee, C., and Ernster, L. (1966) *Biochem. Biophys. Res. Commun.* **23,** 176–181
38. Eguchi, Y., Shimizu, S., and Tsujimoto, Y. (1997) *Cancer Res.* **57,** 1835–1840
39. Sharma, K., and Srikant, C. B. (1998) *Int. J. Cancer* **76,** 259–266
40. Thornberry, N. A. (1994) *Methods Enzymol.* **244,** 615–631
41. Thornberry, N. A., Rano, T. A., Peterson, E. P., Rasper, D. M., Timkey, T., Garcia-Calvo, M., Houtzager, V. M., Nordstrom, P. A., Roy, S., Vaillancourt, J. P., Chapman, K. T., and Nicholson, D. W. (1997) *J. Biol. Chem.* **272,** 17907–17911
42. Kluck, R. M., Bossy-Wetzel, E., Green, D. R., and Newmeyer, D. D. (1997) *Science* **275,** 1132–1136
43. Cai, J., Yang, J., and Jones, D. P. (1998) *Biochim. Biophys. Acta* **1366,** 139–149
44. Kuwana, T., Smith, J. J., Muzio, M., Dixit, V., Newmeyer, D. D., and Kornbluth, S. (1998) *J. Biol. Chem.* **273,** 16589–16594
45. Li, P., Nijhawan, D., Budihardjo, I., Srinivasula, S. M., Ahmad, M., Alnemri, E. S., and Wang, X. (1997) *Cell* **91,** 479–489
46. Zou, H., Henzel, W. J., Lui, X., Lutschg, A., and Wang, X. (1997) *Cell* **90,** 405–413
47. Janicke, R. U., Sprengart, M. L., Wati, M. R., and Porter, A. G. (1998) *J. Biol. Chem.* **273,** 9357–9360
48. Kurokawa, H., Nishio, K., Fukumoto, H., Tomonari, A., Suzuki, T., and Saijo, N. (1999) *Oncol. Rep.* **6,** 33–37
49. Srinivasula, S. M., Ahmad, M., Ottilie, S., Bullrich, F., Banks, S., Wang, Y., Fernandes-Alnemri, T., Croce, C. M., Litwack, G., Tomaselli, K. J., Armstrong, R. C., and Alnemri, E. S. (1997) *J. Biol. Chem.* **272,** 18542–18545
50. Chauhan, D., Pandey, P., Ogata, A., Teoh, G., Krett, N., Halgren, R., Rosen, S., Kufe, D., Kharbanda, S., and Anderson, K. (1997) *J. Biol. Chem.* **272,** 29995–29997
51. Scaffidi, C., Fulda, S., Srinivasan, A., Friesen, C., Li, F., Tomaselli, K. J., Debatin, K. M., Krammer, P. H., and Peter, M. E. (1998) *EMBO J.* **17,** 1675–1687
52. Li, H., Zhu, H., Xu, C. J., and Yuan, J. (1998) *Cell* **94,** 491–501
53. Ferrari, D., Stepczynska, A., Los, M., Wesselborg, S., and Schulze-Osthoff, K. (1998) *J. Exp. Med.* **188,** 979–984
54. Vier, J., Linsinger, G., and Hacker, G. (1999) *Biochem. Biophys. Res. Commun.* **261,** 71–78
55. Furlong, I. J., Lopez Mediavilla, C., Ascaso, R., Lopez Rivas, A., and Collins, M. K. (1998) *Cell Death Differ.* **5,** 214–221
56. Eguchi, Y., Srinivasan, A., Tomaselli, K. J., Shimizu, S., and Tsujimoto, Y. (1999) *Cancer Res.* **59,** 2174–2181
57. Orlowski, J., and Grinstein, S. (1997) *J. Biol. Chem.* **272,** 22373–22376

CHAPTER 169

SOMATOSTATIN

YOGESH C. PATEL

Somatostatin (SST) was first found in the mammalian hypothalamus as a tetradecapeptide (SST-14), which inhibited the release of growth hormone (GH). It has since come to be known as a multifunctional hormone that is also produced throughout the central nervous system and in most peripheral organs. Somatostatin acts on a diverse array of endocrine, exocrine, neuronal, and immune cell targets to inhibit secretion, to modulate neurotransmission, and to regulate cell growth. These actions are mediated by a family of G protein–coupled receptors with five distinct subtypes (termed SSTR1 through SSTR5). SST is best regarded as an endogenous inhibitory regulator of the secretory and proliferative responses of many different target cells. In addition, the peptide may be of importance in the pathophysiology of several diseases such as neoplasia, inflammation, Alzheimer and Huntington diseases, and acquired immunodeficiency syndrome (AIDS), and has found a number of clinical applications in the diagnosis and treatment of neuroendocrine tumors and various gastrointestinal disorders.[1-8]

SOMATOSTATIN GENES AND GENE PRODUCTS

Like other protein hormones, somatostatin is synthesized as part of a large precursor protein (proSST) that is processed to generate two bioactive forms, SST-14 and SST-28 (Fig. 169-1). In humans only one somatostatin gene is found, located on the long arm of chromosome 3, which encodes for both SST-14 and SST-28, whereas lower vertebrates (e.g., fish) have two somatostatin genes that separately encode for SST-14 or SST-28.[2,4,8]

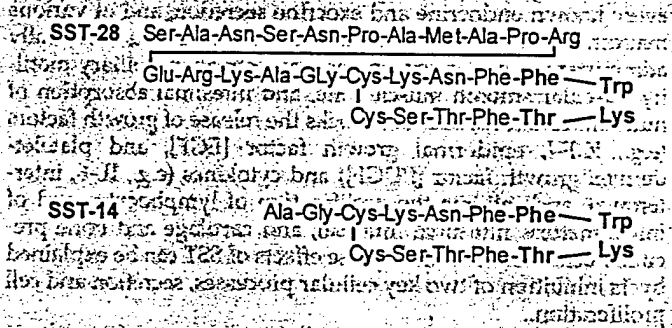

FIGURE 169-1. Structure of naturally occurring somatostatin peptides. (*SST-28*, somatostatin-28; *SST-14*, somatostatin-14; *CST-17*, human cortistatin-17.) Amino acid residues necessary for bioactivity are shown in bold. Octreotide and lanreotide are synthetic somatostatin analogs.

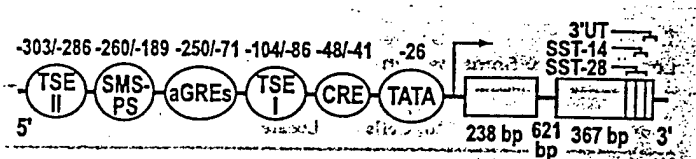

FIGURE 169-2. Schematic depiction of the rat somatostatin gene and its regulatory domains. The messenger RNA coding region consists of two exons of 238 and 367 base pairs (*bp*) separated by an intron of 621 bp. Located upstream (i.e., 5' end) from the start site of mRNA transcription (*arrow*) are the regulatory elements TATA, [AU: Q4] cyclic adenosine monophosphate response element (*CRE*), atypical glucocorticoid response element (*aGRE*), and somatostatin promoter silence element (*SMS-PS*). Tissue-specific elements (*TSE*) consisting of TAAT motifs that operate in concert with CRE to provide high-level constitutive activity are shown. (*3'UT*, [AU: Q5]; *SST-14*, somatostatin-14; *SST-28*, somatostatin-28.)

The transcriptional unit of the rat SST gene consists of exons of 238 and 367 base pairs (bp) separated by an intron of 621 bp (Fig. 169-2). The 5'-upstream region contains a number of regulatory elements for tissue-specific and extracellular signals, including a cyclic adenosine monophosphate (cAMP) response element (CRE) and two nonconsensus glucocorticoid response elements (GREs).[2,4] The SST-14 sequence has been totally conserved throughout vertebrate evolution, whereas the amino-acid structure of SST-28 has changed ~30% during evolution from fish to humans.[2,4,8] A novel second SST-like gene, *cortistatin (CST)*, which has been described in humans, yields two cleavage products, CST-17 and CST-29, which are comparable to SST-14 and SST-28 (see Fig. 169-1).[9] The CST peptides interact with all five SSTRs, but unlike with somatostatin, expression of cortistatin is restricted to the cerebral cortex and its biofunction(s) remains unknown.[3,9]

ANATOMIC DISTRIBUTION OF SOMATOSTATIN CELLS

Somatostatin-producing cells occur in high densities throughout the central and peripheral nervous systems, and in the endocrine pancreas and gut. They occur in smaller numbers in the thyroid, adrenal medulla, testes, prostate, submandibular gland, kidneys, and placenta[1,8,10] (Table 169-1). The typical morphologic appearance of an SST cell is that of a neuron with multiple branching processes, or of a secretory cell, often with short cytoplasmic extensions (D cells). In the brain, the highest concentrations of SST are found in the hypothalamus, neocortex, and basal ganglia, throughout the limbic system, and at all levels of the major sensory systems.[1,8,10-11] The approximate relative amounts of SST in the major regions of the brain are as follows: cerebral cortex, 49%; spinal cord, 30%; brainstem, 12%; hypothalamus, 7%; olfactory lobe, 1%; and cerebellum, 1%.[11]

SST cells in the pancreas are almost exclusively islet D cells and account for 2% to 3% of the total adult islet cell population.[12] Gut SST cells are of two types: D cells in the mucosa and neurons that are intrinsic to the submucous and myenteric plexuses.[13] In the thyroid, SST coexists with calcitonin in a subpopulation of C cells.[1] In addition to these typical SST-producing neuroendocrine cells, which secrete large amounts of the peptide from storage pools, inflammatory and immune cells also produce SST, usually in small amounts on activation.[14,15] In the rat, the gut accounts for ~65% of total body SST, whereas lesser amounts occur in the brain (25%), the pancreas (5%), and the remaining organs (5%). The relative proportions of SST-14 and SST-28 synthesized and secreted vary considerably in different tissues.[4] SST-14 is the predominant form in the brain, pancreas, upper gut, and enteric neurons, whereas SST-28 is an important constituent of brain and is the predominant molecular form in the intestinal mucosa.

TABLE 169-1.
Localization of Somatostatin

Body Region	Type of Cells	Locale
MAJOR SITES		
Nervous system	Neurons	Hypothalamus
		Cerebral cortex
		Limbic system
		Basal ganglia
		Major sensory systems
		Spinal cord
		Dorsal root ganglia
		Autonomic ganglia
Pancreas	D cells	Islets
Gut	D cells	Mucosal glands
	Neurons	Submucous and myenteric plexuses
MINOR SITES		
Adrenal	—	Scattered medullary cells
Placenta	—	Cytotrophoblasts in chorionic villi
Reproductive organs	—	Testis, epididymis, prostate
Submandibular gland	D cells	Scattered ductal cells
Thyroid	C cells	Scattered parafollicular cells (coexisting with calcitonin)
Urinary system	—	Scattered cells in renal glomerulus and collecting ducts

SOMATOSTATIN IN THE PLASMA AND OTHER BODY FLUIDS

Both SST-14 and SST-28 are released readily from tissues and are detected in blood.[1,4,8,16] The main source of circulating SST is the gastrointestinal tract.[17] Circulating SST is inactivated rapidly by the liver and kidneys. The plasma half-life of SST-14 is 2 to 3 minutes, whereas that of SST-28 is slightly longer.[4] Fasting plasma concentrations of SST-like immunoreactivity [AU: Q1] (SST-LI) range from 5 to 18 pmol/L. These levels double in response to the ingestion of a mixed meal.[4] The bioactive circulating forms consist of SST-14, des-Ala[1] SST-14 (a postsecretory conversion product of SST-14), and SST-28.[16] With few exceptions, fluctuations in peripheral plasma levels of SST-LI are small. The main clinical utility of plasma measurements is in the diagnosis of SST-producing tumors, which are associated with marked hypersomatostatinemia.

SST is secreted into the cerebrospinal fluid (CSF), probably from all parts of the brain.[18,19] It is stable in this medium and attains a concentration that is approximately twice that in the general circulation. Significant amounts are also excreted in the urine (4–6 pmol/L). Semen contains high levels of SST-LI, 200-fold greater than those in plasma. Amniotic fluid is rich in SST-LI originating from the fetus.

REGULATION OF SOMATOSTATIN SECRETION AND GENE EXPRESSION

Because SST cells are so widely distributed and interact with many different body systems, the fact that the secretion of SST can be influenced by a broad array of secretagogues, ranging from ions and nutrients to neuropeptides, neurotransmitters, classic hormones, and growth factors, is not surprising.[1,2,4,8] Glucagon, GH-releasing hormone (GHRH), neurotensin, corticotropin-releasing hormone (CRH), calcitonin gene–related peptide (CGRP), and bombesin are potent stimulators of SST release, whereas opioids and γ-aminobutyric acid (GABA) generally inhibit SST secretion.[1,4,8] Of the various hormones studied, thyroid hormones enhance SST secretion from the hypothalamus; their effect on secretion from other tissues has not been adequately investigated.[4,8] Glucocorticoids exert a dose-dependent biphasic effect on SST secretion; low doses are stimulatory and high doses are inhibitory.[4] Insulin stimulates hypothalamic SST release but has an inhibitory effect on the release of SST from islet and gut.[4] Finally, members of the growth factor–cytokine family such as GH, insulin-like growth factor-I (IGF-I), interleukin-1 (IL-1), tumor necrosis factor α (TNFα), and interleukin-6 (IL-6) are capable of stimulating SST secretion from brain cells.[2]

Many of the agents that influence SST secretion also regulate SST gene expression.[2,4,8] Steady-state SST messenger RNA (mRNA) levels are stimulated by growth factors and cytokines (e.g., GH, IGF-I, IGF-II, IL-1, TNFα, IL-6, interferon-γ, and interleukin-10), glucocorticoids, testosterone, estradiol, and *N*-methyl-D-aspartate–receptor agonists; and are inhibited by glucocorticoids, insulin, leptin, and transforming growth factor-β (TGF-β). Among the intracellular mediators known to modulate SST gene expression are Ca^{2+}, cAMP, cyclic guanosine monophosphate (cGMP), and nitric oxide (NO).[2,4,8] Activation of the adenylate cyclase–cAMP pathway plays an important role in the stimulation of SST secretion and gene transcription.[20] Cyclic AMP–dependent transcriptional enhancement is mediated by the nuclear protein *cAMP response element–binding protein (CREB)*, which binds to the cAMP response element on the SST gene.[20] Ca^{2+}-dependent induction of the SST gene occurs through phosphorylation of CREB by the Ca^{2+}-dependent protein kinase I and protein kinase II. GH, IGF-I, IGF-II, and glucocorticoids have all been shown to induce the SST gene by direct interaction with its promoter.[4] The molecular mechanisms underlying the effects of estrogens, testosterone, cGMP, and NO on SST mRNA levels remain to be determined.[4]

ACTIONS OF SOMATOSTATIN

SST not only has wide anatomic distribution, but it acts on multiple targets, including the brain, pituitary, endocrine and exocrine pancreas, gut, kidney, adrenal, thyroid, and immune cells[1,2,7,8] (Fig. 169-3). Its actions include inhibition of virtually every known endocrine and exocrine secretion, and of various neurotransmitters; behavioral and autonomic effects if centrally administered; and effects on gastrointestinal and biliary motility, vascular smooth muscle tone, and intestinal absorption of nutrients and ions. SST also blocks the release of growth factors (e.g., IGF-I, epidermal growth factor [EGF], and platelet-derived growth factor [PDGF]) and cytokines (e.g., IL-6, interferon-γ), and inhibits the proliferation of lymphocytes and of inflammatory, intestinal mucosal, and cartilage and bone precursor cells.[2] All of these diverse effects of SST can be explained by its inhibition of two key cellular processes, secretion and cell proliferation.

SOMATOSTATIN RECEPTORS, RECEPTOR SUBTYPES, AND SIGNAL TRANSDUCTION

Somatostatin acts through high-affinity plasma membrane receptors that are pharmacologically heterogeneous and feature several different isoforms.[2,3,5,6,21] Molecular cloning has revealed a family of five structurally related SSTR subtype genes that encode for seven transmembrane domain, G protein–coupled receptor proteins that display distinct agonist-binding profiles for natural and synthetic SST peptides[2,3,21] (Table 169-2). Receptor types 1 through 4 bind SST-14 and SST-28 approximately equally, whereas the type 5 receptor displays relative selectivity for binding of SST-28.[2,3,21] Four of the genes (the exception is SSTR2) appear to have no introns. Each of the receptor genes is located on a separate chromosome. The mRNA for individual

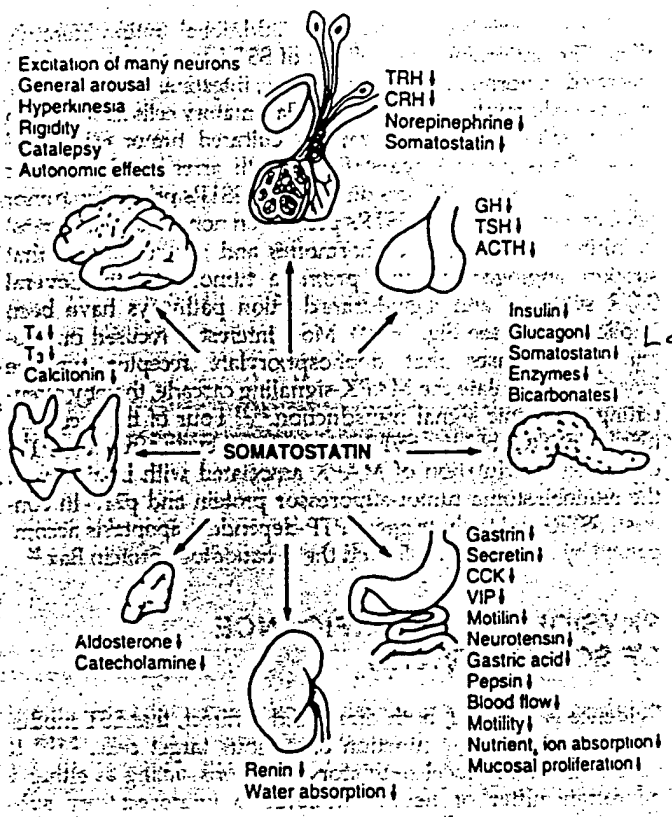

FIGURE 169-3. Principal actions of somatostatin. Somatostatin inhibits the release of dopamine from the midbrain and of norepinephrine, thyrotropin-releasing hormone (*TRH*), corticotropin-releasing hormone (*CRH*), and endogenous somatostatin from the hypothalamus. It also inhibits both the basal and the stimulated secretion of growth hormone (*GH*), thyroid-stimulating hormone (*TSH*), and islet-hormones. It has no effect on luteinizing hormone (*LH*), follicle-stimulating hormone (*FSH*), prolactin, or adrenocorticotropic hormone (*ACTH*) in normal subjects. It does, however, suppress elevated ACTH levels in Addison disease and in ACTH-producing tumors. In addition, it inhibits the basal and the TRH-stimulated release of prolactin in vitro and diminishes elevated prolactin levels in acromegaly. In the gastrointestinal tract, somatostatin inhibits the release of virtually every gut hormone that has been tested. It has a generalized inhibitory effect on gut exocrine secretion (gastric acid, pepsin, bile, colonic fluid) and suppresses motor activity generally as well as through inhibition of gastric emptying, gallbladder contraction, and small intestine segmentation. Somatostatin, however, stimulates migrating motor complex activity. The effects of somatostatin on the thyroid include inhibition of the TSH-stimulated release of thyroxine (T_4) and triiodothyronine (T_3). The adrenal effects consist of the inhibition of angiotensin II–stimulated aldosterone secretion and the inhibition of acetylcholine-stimulated medullary catecholamine secretion. In the kidneys, somatostatin inhibits the release of renin stimulated by hypovolemia and inhibits antidiuretic hormone (*ADH*)–mediated water absorption. (*CCK*, cholecystokinin; *VIP*, vasoactive intestinal peptide.) (Modified from Patel YC. General aspects of the biology and function of somatostatin. In: Weil C, Muller EE, Thorner MO, eds. Somatostatin. Basic and clinical aspects of neuroscience series, vol 4. Berlin: Springer-Verlag, 1992:1.)

TABLE 169-2.
Characteristics of Cloned Human Somatostatin Receptor (hSSTR), Types 1–5

	hSST R1	hSST R2	hSST R3	hSST R4	hSST R5
Amino acids	391	369	418	388	363
Chromosomal location	14	17	22	20	16
Agonist binding*					
SST-14	++	++	++	++	++
SST-28	++	++	++	++	+++
~~Lanreotide~~ Octreotide	–	++	+	–	++
~~Somatuline [AU: Q6a]~~ Lanreotide	–	++	+	–	++
G-protein coupling	Yes	Yes	Yes	Yes	Yes
Effector coupling					
Adenylate cyclase activity	↓	↓	↓	↓	↓
Tyrosine phosphatase activity	↑	↑	↑	↑	↑
MAPK activity	↑	↓	↓↑	↑	↓
Tissue distribution					
Brain	Yes	Yes	Yes	Yes	Yes
Pituitary	Yes	Yes	Yes		Yes
Islet	Yes	Yes	Yes	Yes	Yes
Stomach	Yes	Yes	Yes	Yes	Yes
Liver	Yes				
Lungs				Yes	
Kidneys	Yes	Yes			
Placenta				Yes	

↑, increased; ↓, decreased; *SST-14*, somatostatin-14; *SST-28*, somatostatin-28; *MAPK*, mitogen-activated protein kinase.

*Binding potency shown is based on IC_{50} [AU: Q7] value for each agonist: –, IC_{50} 150–1000 nM; +, IC_{50} 10–20 nM; ++, IC_{50} 1–10 nM; +++, IC_{50} <1 nM.

Not all tissues have been tested simultaneously;

(Data from Patel YC. Somatostatin and its receptor family. Frontiers Neuroendocrinol 1999; 20:157; Patel YC. Molecular pharmacology of somatostatin receptor subtypes. J Endocrinol Invest 1997; 20:348; Lamberts SWJ, Van Der Lely A-J, de Herder WW. Drug therapy: octreotide. N Engl J Med 1996; 334:246; and Reisine T, Bell GI. Molecular biology of somatostatin receptors. Endocr Rev 1995; 16:427.)

Concentration required for half maximal inhibition

SST receptors elicit their cellular responses through G protein–linked modulation of multiple second messenger systems (Fig. 169-4), including (a) receptor coupling to adenylate cyclase, (b) receptor coupling to K^+ channels, (c) receptor coupling to Ca^{2+} channels, (d) receptor coupling to exocytotic vesicles, (e) receptor coupling to phosphotyrosyl protein phosphatase (PTP), and (f) receptor coupling to the mitogen-activated protein kinase (MAPK) pathway.[2,3,21] The five receptors share common signaling pathways, such as the inhibition of adenylate cyclase, activation of PTP, and modulation of MAPK[2] (see Table 169-2). SSTR2, SSTR3, SSTR4, and SSTR5 are coupled to K^+ channels; SSTR1 and SSTR2, to voltage-dependent Ca^{2+} channels; SSTR2 and SSTR5, to phospholipase C; and SSTR1, to a Na^+/H^+ exchanger.[2]

human SSTR subtypes is widely expressed in brain, pituitary, pancreatic islets, stomach, jejunum, colon, lung, kidney, and liver, with a characteristic tissue-specific pattern for each receptor.[2,3,21,22] Typically, more than one subtype occurs in a given target tissue (e.g., SSTR1 through SSTR5 in the brain, stomach, pancreatic islets, and aorta; SSTR1, SSTR2, SSTR3, and SSTR5 in the pituitary). SSTR2 is the most abundantly expressed subtype, in terms of both the number of tissues that express this receptor and the level of expression. It is preferentially expressed by islet A cells and immune cells. SSTR1 and SSTR5 are the main subtypes expressed by islet B cells.[23] SSTR2 and SSTR5 are the principal subtypes found in somatotropes.

SOMATOSTATIN RECEPTOR–MEDIATED INHIBITION OF SECRETION AND CELL PROLIFERATION

The pronounced ability of SST to block regulated secretion from many different cells is due in part to receptor-induced inhibition of two key intracellular mediators, cAMP and Ca^{2+}, because of receptor-linked effects on adenylate cyclase and on K^+ and Ca^{2+} ion channels[2] (see Fig. 169-4). In addition, SST inhibits secretion stimulated by cAMP, Ca^{2+} ions, or any other known second messenger through a distal effect, which is targeted directly to secretory granules and is dependent of activation of the protein phosphatase calcineurin.[2,3,7] The antiproliferative effects of SST

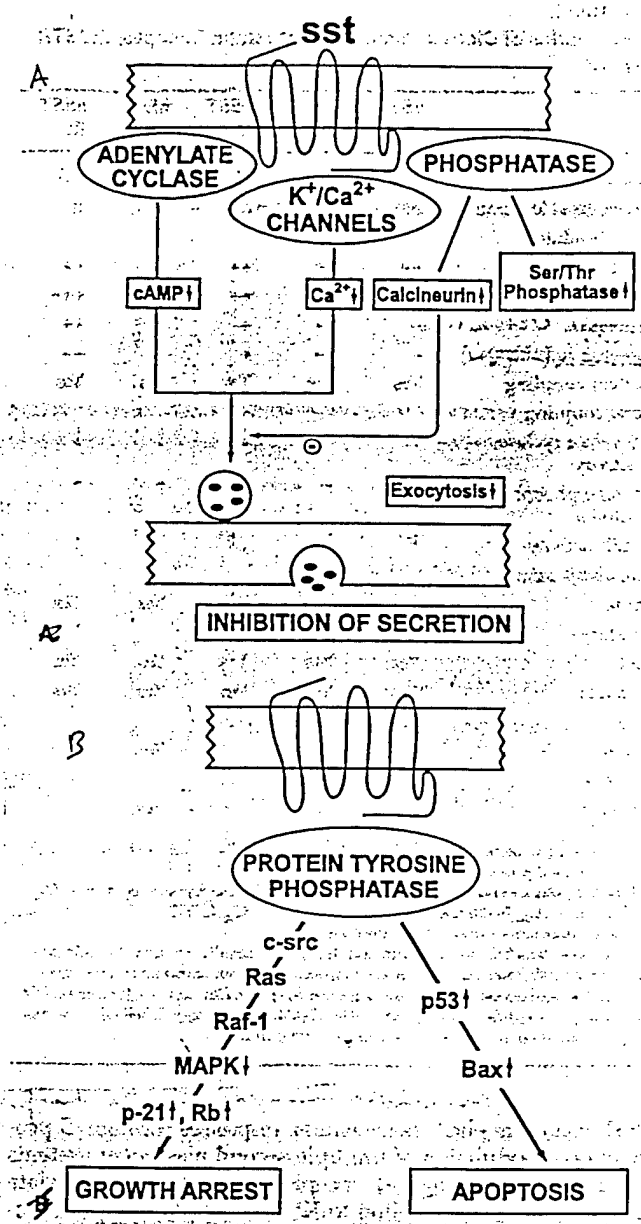

FIGURE 169-4. Schematic depiction of somatostatin-receptor (*SSTR*)–signaling pathways leading to inhibition of secretion (A) and to cell proliferation and induction of apoptosis (B). Receptor activation leads to a fall in intracellular cyclic adenosine monophosphate (*cAMP*) (due to inhibition of adenylate cyclase), a fall in Ca^{2+} influx (due to activation of K^+ and Ca^{2+} ion channels), and stimulation of phosphatases such as *calcineurin*, which inhibits exocytosis, and *serine threonine (Ser/Thr) phosphatases*, which dephosphorylate and activate Ca^{2+} and K^+ channel proteins. Blockade of secretion by somatostatin (*SST*) is in part mediated through inhibition of Ca^{2+} and cAMP (proximal effect) and through a more potent distant effect involving direct inhibition of exocytosis via SST-dependent activation of calcineurin. Induction of protein tyrosine phosphatase by SST plays a key role in mediating cell growth arrest (via SSTR1, SSTR 2, SSTR 4, SSTR 5), or apoptosis (via SSTR3). Cell growth arrest is dependent on activation of the mitogen-activated protein kinase (*MAPK*) pathway and induction of *Rb (retinoblastoma tumor-suppressor protein)*, and *p21 (cyclin-dependent kinase inhibitor)*. C-src, which associates with both the activated receptor and phosphotyrosyl protein phosphatase (*PTP*), may provide the link between the receptor, PTP, and the mitogenic signaling complex. Induction of apoptosis is associated with dephosphorylation-dependent activation of the tumor-suppressor protein p53 and the proapoptotic protein Bax. [AU: Q6] (From Patel YC. Somatostatin and its receptor family. Frontiers Neuroendocrinol 1999; 20:157.)

were recognized through the use of long-acting analogs (i.e., octreotide) for the treatment of hormone hypersecretion from pancreatic, intestinal, and pituitary tumors. SST not only blocked hormone hypersecretion from these tumors but also caused variable tumor shrinkage through an additional antiproliferative effect. The antiproliferative effects of SST have since been demonstrated in normal dividing cells (e.g., intestinal mucosal cells), in activated lymphocytes, and in inflammatory cells as well as in vivo in solid tumors and various cultured tumor cell lines.[2] These effects involve cytostatic (growth arrest) and cytotoxic (apoptotic) actions. SST acts directly (via SSTRs present on tumor cells) and indirectly (via SSTRs present on nontumor cell targets) to inhibit the secretion of hormones and growth factors that support angiogenesis and promote tumor growth. Several SSTR subtypes and signal-transduction pathways have been implicated[2,3,21] (see Fig. 169-4). Most interest is focused on protein phosphatases that dephosphorylate receptor tyrosine kinases or modulate the MAPK-signaling cascade, thereby attenuating mitogenic signal transduction.[24,25] Four of the receptors (SSTR1, SSTR2, SSTR4, SSTR5) induce cell-cycle arrest via PTP-dependent modulation of MAPK associated with induction of the retinoblastoma tumor-suppressor protein and p21.[2] In contrast, SSTR3 uniquely triggers PTP-dependent apoptosis accompanied by activation of p53 and the proapoptotic protein Bax.[26]

PHYSIOLOGIC SIGNIFICANCE OF SOMATOSTATIN

Evidence is growing, both direct and indirect, that SST modulates the physiologic function of various target cells.[1,2,4,5,8] It subserves mainly local regulatory functions, acting as either a neurotransmitter or neuromodulator; a neurosecretory substance (i.e., one released directly from nerve axons into the bloodstream as in the median eminence), or a paracrine-autocrine regulator (local cell-to-cell interaction or self-regulation). In addition, SST may act via the circulation as a true endocrine substance to influence distant targets.

Direct evidence exists of a physiologic role for hypothalamic-SST in the regulation of GH and thyroid-stimulating hormone (TSH) secretion by the pituitary.[1,8,27] A variety of physiologic GH responses are orchestrated by SST, acting either alone or in concert with GHRH.[1,8,27] SST participates in the genesis of the normal pulsatile pattern of GH secretion and in GH regulatory responses to physiologic stimuli such as stress, glucose administration, or food deprivation. GHRH and SST neurons in the hypothalamus are anatomically coupled and influence each other reciprocally.[8,27] SST inhibits GH secretion both by a direct action on the pituitary, and indirectly through suppression of GHRH release (Fig. 169-5). The secretion of SST in turn is stimulated by GHRH and is subject to positive feedback regulation by GH (*short loop*) and by IGF-I produced by GH action on the liver (*long loop*). Because of the extensive extrahypothalamic brain distribution of SST, its effects on the spontaneous electrical activity of neurons, its release from nerve endings in response to depolarization, and its behavioral effects, this peptide has been postulated to serve as a central neurotransmitter or neuromodulator.[1,5] Given the high concentration of both SST neuronal elements and SSTRs in limbic, neocortical, striatal, and sensory areas, SST appears to be particularly important in modulating functions in these regions. Within the pancreatic islets, the close anatomic proximity of SST cells to the A and B cells, the demonstration that insulin and glucagon are exquisitely sensitive to inhibition by low concentrations of SST, and the finding that inactivation of islet D-cell function augments insulin and glucagon output, all provide evidence for the possible modulation of pancreatic islet A- and B-cell function by SST[4,8] (Fig. 169-6). The suggestion has been made that islet D cells, which produce predominantly SST-14 and only negligible amounts of SST-28, regulate A cells by local action, whereas SST-28 released in the circulation from the gut in response to food ingestion modulates nutrient-stimulated insulin release by a hemocrine mechanism.[28] The diffuse distribution of SST throughout the gut, together with its pleiotropic effects and the complex regulation

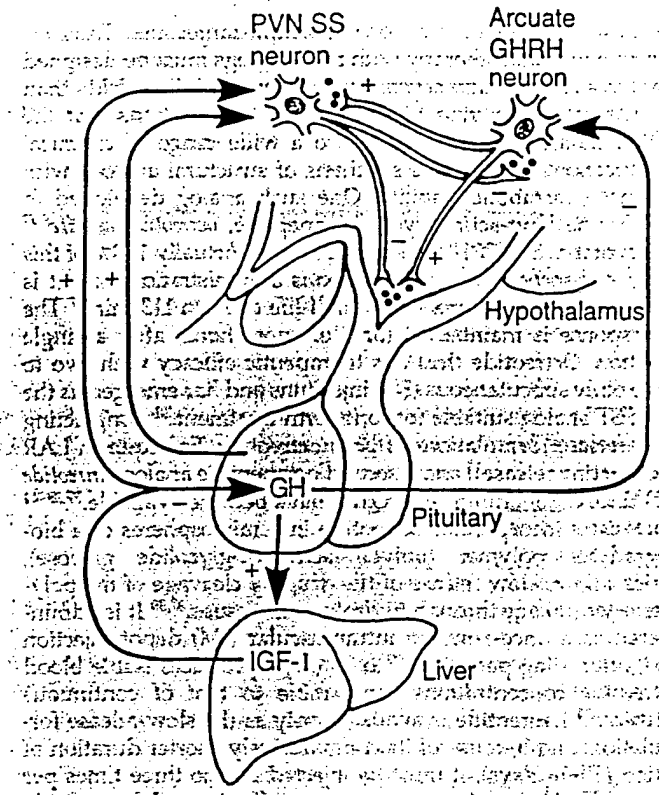

FIGURE 169-5. Schematic representation of the interaction between somatostatin (*SST*), growth hormone–releasing hormone (*GHRH*), growth hormone (*GH*), and insulin-like growth factor I (*IGF-I*) in regulating GH secretion. GH release is stimulated by GHRH (produced by GHRH neurons in the arcuate nucleus) and inhibited by SST (produced by somatostatinergic neurons in the anterior hypothalamic periventricular nucleus [*PVN*]). SST inhibits GH secretion both by direct action at the pituitary level and indirectly through suppression of GHRH release. GHRH, in turn, stimulates SST secretion. GH exerts negative feedback on its own secretion by inhibiting GHRH release, stimulating SST release, and potentiating the release of IGF-I from the liver. IGF-I, in turn, stimulates SST release and inhibits GH secretion by a direct action on the pituitary. (Modified from Patel YC. General aspects of the biology and function of somatostatin. In: Weil C, Muller EE, Thorner MO, eds. Somatostatin. Basic and clinical aspects of neuroscience series, vol 4. Berlin: Springer-Verlag, 1992:1.)

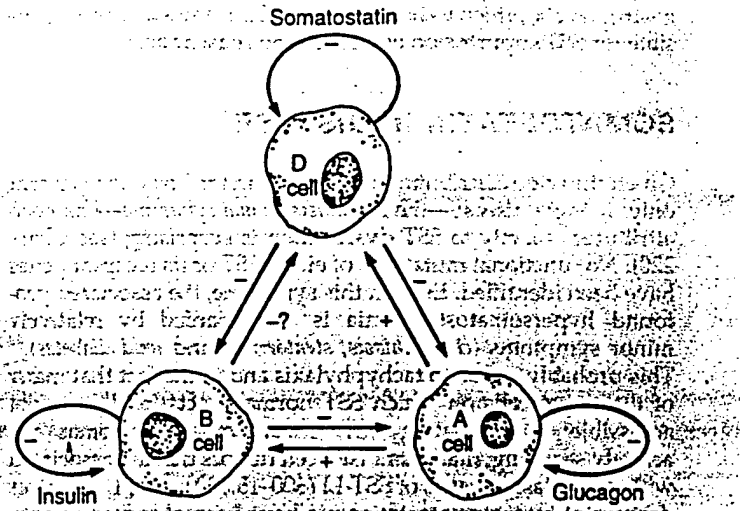

FIGURE 169-6. Effects of endogenous or exogenous somatostatin (*SST*), insulin, and glucagon on the function of pancreatic islet cells. SST inhibits insulin and glucagon release, glucagon stimulates insulin and SST release, and insulin inhibits the release of glucagon and possibly of SST. In addition, all three islet hormones inhibit their own secretion by an autocrine mechanism. Physiologically, intraislet insulin and glucagon regulate the secretion of SST, and intraislet insulin regulates glucagon release. The precise physiologic role of intraislet SST remains unclear (see text for details). (Modified from Patel YC. General aspects of the biology and function of somatostatin. In: Weil C, Muller EE, Thorner MO, eds. Somatostatin. Basic and clinical aspects of neuroscience series, vol 4. Berlin: Springer-Verlag, 1992:1.)

of its secretion, suggests that SST exerts control over many discrete cell systems involved in gastrointestinal, pancreatic, and biliary functions. SST regulates acid secretion both directly through the circulation to inhibit parietal cells and through a paracrine mechanism to suppress gastrin release.[29] Circulating SST is also a physiologic regulator of pancreatic exocrine secretion.[30] Elsewhere in the gut, evidence exists to suggest that SST controls the rate of absorption of nutrients and participates in the regulation of gut hormone secretion, gastrointestinal motor tone, blood flow, and mucosal cell proliferation.[31] Although acute changes in tissue or circulating levels of SST are accompanied by alterations in the function of target organs (e.g., the pituitary or gut), an interesting finding is that SST deficiency from birth (as in the SST knock-out mouse) does not produce any developmental defect or growth abnormality in young animals.[32] This means either that the SST gene is redundant or, more likely, that adaptive responses occur from other genes (e.g., *cortistatin*), which compensate for the loss of the SST gene.

SUBTYPE-SELECTIVE BIOACTIONS OF SOMATOSTATIN RECEPTORS

Because SST exerts its numerous bioeffects through five receptors, the question arises whether a given response is selective for one subtype or whether multiple subtypes are involved. The marked overlap in the cellular pattern of expression of the different SSTR pathways, coupled with the finding that individual target cells typically express multiple SSTR subtypes and often all five isoforms in the same cell, suggests that SSTRs may operate in concert rather than as individual members. Nonetheless, evidence exists for relative subtype selectivity for some SSTR effects. At the level of cell secretion and cell proliferation, the two general cellular effects modulated by SST, four of the subtypes (SSTR1, SSTR2, SSTR4, SSTR5) are capable of arresting cell growth, whereas SSTR3 is uniquely cytotoxic. In contrast to the case for cell proliferation, surprisingly little is known about subtype selectivity, if any, for cell secretion. Immune, inflammatory, and neoplastic cells are important targets for SST action.[2,14,15] Unlike the classic SST-producing neuroendocrine cells (e.g., in the hypothalamus or islets), which release large quantities of the peptide acutely from storage pools, SST and SST receptors in inflammatory cells (e.g., macrophages and lymphocytes) are coinduced, probably by growth factors and cytokines, as part of a general mechanism for activating the endogenous SST system for paracrine-autocrine modulation of the proliferative and hormonal responses associated with inflammatory and immune reactions. SSTR2, the main isotype expressed in lymphocytes and inflammatory cells, appears to be the functional SSTR responsible for modulating the proliferative and secretory responses of these cells.[15] Based on the pattern of SSTR subtype expression as well as the effects of selective nonpeptide agonists, SSTR2 and SSTR5 are the subtypes involved in regulating GH and TSH secretion from the human pituitary.[2,33] Similar studies in the case of islet hormones suggest a preferential effect of SSTR2 on glucagon release and of SSTR5 and possibly SSTR1 on insulin secretion.[23,34] Despite the pharmacologic evidence for the involvement of SSTR2 in pituitary GH secretion, an SSTR2-deficient mouse shows only subtle abnormalities of neuroendocrine GH feedback control. The animals grow normally both in utero and postnatally, a finding that suggests maintenance of overall GH secretion.[35] These animals display high basal gastric acid secretion in the face of normal

gastrin levels, which indicates that SSTR2 is the subtype responsible for SST suppression of endogenous gastric acid.

SOMATOSTATIN IN DISEASE

Given the wide distribution of SST cells in the body, the fact that only a single disease—the *somatostatinoma syndrome*—has been attributed directly to SST dysfunction is surprising (see Chap. 220). No functional mutations of either SST or its receptor genes have been identified. Even in this syndrome, the associated profound hypersomatostatinemia is accompanied by relatively minor symptoms (*cholelithiasis, steatorrhea,* and *mild diabetes*).[36] This probably is due to tachyphylaxis and to the fact that many of the target cells on which SST normally acts locally are not accessible to circulating SST. Most somatostatinomas are actively secreting, malignant islet cell tumors that are associated with high plasma levels of SST-LI (600–15,000 pmol/L).[36] Lesser degrees of hypersomatostatinemia have been observed in nonpancreatic SST-producing tumors, such as duodenal somatostatinoma, medullary thyroid carcinoma, pheochromocytoma, extraadrenal paraganglioma, and small-cell cancer of the lung. The serial measurement of plasma SST-LI values has proved useful as a tumor marker in the follow-up of these patients.

In several diseases, disordered SST function occurs probably as a secondary feature. Foremost among these is *Alzheimer disease,* in which a decrease in the levels of SST in the cerebral cortex and CSF is seen.[5,19] The reduction in cortical SST correlates with the number of senile plaques and neurofibrillary tangles, and although its pathophysiologic significance is unclear, it has become an important biochemical marker for the disease. Cerebrocortical SST, CSF SST, or both are also decreased in *other neuropsychiatric disorders* such as depression, Parkinson disease, and multiple sclerosis.[19] Whereas the reduction in brain or CSF SST in Alzheimer disease appears to be secondary to neurodegeneration, the SST changes that occur in depression and multiple sclerosis fluctuate with disease activity and reflect functional alterations in peptide production. In contrast to the loss of SST in Alzheimer disease, SST neurons in the striatum in *Huntington disease* are selectively resistant to neurodegeneration and show up-regulated function. Selective survival and up-regulation of SST gene expression in response to neuronal injury has also been demonstrated in the striatum in animal models of *hypoxia-ischemia* and in the cortex of monkeys and human patients with *AIDS encephalopathy.*

Plasma SST levels are elevated significantly in *hepatic cirrhosis* and in *chronic renal failure,* an elevation that reflects impaired metabolism. In experimental hyperinsulinemic diabetes and in human *type 2 diabetes,* release of gut SST in response to *meal ingestion* is impaired. Patients with *duodenal ulcers* have reduced antral SST-LI levels, which implicates local deficiency of SST in the pathogenesis of this disorder. Despite the large amounts of SST present in the gut, primary gastrointestinal disease generally is not associated with alterations in circulating SST concentrations.

CLINICAL APPLICATIONS OF SOMATOSTATIN AND ITS ANALOGS

The potent pharmacologic properties of SST have attracted much interest in the use of this substance as a therapeutic agent for the treatment of various diseases. The naturally occurring forms proved unsuitable, however, because their short half-lives made continuous intravenous administration necessary. The specificity of endogenous SST derives from the fact that it is produced mainly at local sites of action and is rapidly inactivated after release by peptidases in tissue and blood, so that unwanted systemic effects are minimized. Injections of synthetic SST, on the other hand, produce a wide array of effects due to simultaneous activation of multiple target sites. Thus, for effective pharmacotherapy with SST, analogs must be designed that have *more selective actions* and *greater metabolic stability* than the naturally occurring peptides. Early observations that the SST-14 molecule was amenable to a wide range of chemical modifications allowed the synthesis of structural analogs with enhanced metabolic stability. One such analog developed in 1982 is the long-acting cyclic octapeptide, *octreotide acetate*[6,37] (Sandostatin, SMS201-995; see Fig. 169-1). Virtually 100% of this drug is absorbed after subcutaneous administration, and it is eliminated from plasma with a half-life of 70 to 113 min.[37] The bioresponse is maintained for 8 or more hours after a single injection. Octreotide thus has therapeutic efficacy with two to three daily subcutaneous (SC) injections and has emerged as the first SST analog suitable for long-term treatment.[38] Long-acting slow-release formulations of both octreotide (Sandostatin LAR [long-acting release]) and a second octapeptide analog *lanreotide* (BIM23014, Somatulin [AU: Q1a]) have become available.[37,39–42] *Sandostatin* incorporates octreotide into microspheres of a biodegradable polymer (polyDL-lactide-co-glycolide glucose), which allows slow release of the drug by cleavage of the polymer ester linkage through hydrolysis in tissues.[37,39] It is administered as a once-a-month intramuscular (IM) depot injection and, after a lag period of 7 to 10 days, produces stable blood octreotide concentrations comparable to that of continuous infusion.[39] Lanreotide is available only as the slow-release formulation, and because of its comparatively shorter duration of action (10–14 days), it must be injected two to three times per month.[40,41] Both analogs are at least as effective as SC octreotide in blocking the excessive production of hormones from neuroendocrine tumors of the gastrointestinal tract, pancreatic islets, and pituitary.[37–42] Furthermore, they have a safety profile similar to that of the SC injections, and, because of better patient compliance, are likely to become the drugs of choice for SST pharmacotherapy. Both the subcutaneous and LAR forms of octreotide are approved by the Food and Drug Administration for the treatment of carcinoid tumors, VIPomas, and acromegaly. Lanreotide should shortly be available in North America. Octreotide and lanreotide bind to only three of the five SSTRs (types 2, 3, and 5) (see Table 169-2), displaying high affinity for subtypes 2 and 5, moderate affinity for subtype 3, and no binding to types 1 and 4.[2,3,6,21] The binding affinity of these analogs for subtypes 2 and 5 is comparable to that of SST-14, which indicates that they are neither selective for these subtypes nor more potent than endogenous SST. A series of high-affinity *nonpeptide agonists* have been identified for several of the human SSTRs. These should facilitate the development of orally active subtype-selective therapeutic compounds.[34]

TREATMENT OF NEUROENDOCRINE AND NONNEUROENDOCRINE TUMORS

Octreotide provides potent palliative therapy for hormone-producing neuroendocrine tumors (Table 169-3). It acts in two ways to *combat the effects of hormone hypersecretion:* (a) directly on tumor cells to *inhibit secretion,* and (b) indirectly to *block the action* of the hypersecreted hormone at its target site. In addition, octreotide may cause *tumor shrinkage* or *stabilization of tumor growth* in some instances by shrinkage of tumor-cell volume through long-term inhibition of secretion (comparable to the shrinkage of prolactinomas induced by dopamine agonists) and inhibition of tumor growth via cytostatic and cytotoxic (apoptotic) effects (see Fig. 169-4).

Binding studies have shown that neuroendocrine as well as common solid nonneuroendocrine tumors are rich in SSTRs (Table 169-4).[3,38] Currently available binding analyses, however, cannot distinguish the individual SSTR subtypes because of the lack of subtype-selective radioligands. Accordingly, investiga-

TABLE 169-3.
Proven and Potential Clinical Applications of Somatostatin Analogs

Disorder	Indication
HORMONE-PRODUCING TUMORS	
Gastroenteropancreatic	
Carcinoid	Definite
VIPoma	Definite
Glucagonoma	Definite
Insulinoma	Probable
Gastrinoma	Possible
Somatostatinoma	Possible
GHRH-producing tumors	Possible
Pituitary	
Acromegaly	Definite
TSH-producing adenoma	Definite
Nelson syndrome	Probable
Others	
Paraneoplastic ACTH-producing tumors	Possible
Medullary carcinoma of thyroid	Possible
GASTROINTESTINAL APPLICATIONS	
Variceal bleeding	Probable
Pancreatic fistula	Probable
Secretory diarrhea	Probable
AIDS-related diarrhea	Probable
Postgastrectomy dumping	Possible
Scleroderma	Possible
ORTHOSTATIC HYPOTENSION	Possible
DIABETES	Possible

VIP, vasoactive intestinal peptide; *GHRH*, growth hormone-releasing hormone; *TSH*, thyroid-stimulating hormone; *ACTH*, adrenocorticotropic hormone; *AIDS*, acquired immunodeficiency syndrome.

tors have resorted to mRNA analysis and receptor immunocytochemical analysis with *subtype-selective antibodies* to characterize the pattern of expression of the five SSTR subtypes. Investigation of mRNA expression for the five SSTRs in more than 100 pituitary tumors, both secretory (producing GH, TSH, prolactin, or ACTH) and nonsecretory (i.e., chromophobe adenomas), and in 32 gastroenteropancreatic tumors (i.e., carcinoid, insulinoma, glucagonoma) has revealed multiple SSTR genes in most tumors.[3,43–45] SSTR1 and SSTR2 appear to be the predominant forms in all tumors. Pituitary adenomas are also rich in the expression of SSTR5. Many nonneuroendocrine tumors (e.g., breast and renal carcinomas) are also SSTR positive.[43,45] The extent of malignant disease as well as differential tumor expression of SSTRs may account for the variable clinical response observed with different tumor types. The presence of octreotide-sensitive subtypes, such as SSTR2 and SSTR5, in the majority of neuroendocrine tumors correlates with the responsiveness of these tumors to treatment with the analog.

Treatment is indicated in patients with severe symptoms and resultant metabolic derangements that require control before surgery or other therapy; in patients with residual tumor or metastatic end-stage disease who have had relapse after standard therapeutic modalities (e.g., surgery, chemotherapy, and hepatic artery embolization); and as prophylaxis against acute crises resulting from sudden discharge of tumor products, such as in carcinoid crisis. In these instances, octreotide administration has produced extended and useful symptomatic remissions. The initial dosage may be 50 to 100 μg of SC octreotide twice daily or 10 mg IM of octreotide LAR per month. The dosage may be increased gradually over 6 to 12 months (or as required) to 500 μg three times daily of SC octreotide and 30 mg per month of the LAR preparation. Generally, clinical improvement parallels a reduction in the plasma level of the hormone being hypersecreted by the tumor.

TABLE 169-4.
Expression of Somatostatin Receptors (SSTRs) in Tumors in Vitro and in Vivo

		INCIDENCE OF SOMATOSTATIN RECEPTORS					
		In Vitro					In Vivo
		% Positive for SSTR mRNA					
Tumor	*n*	*SSTR1*	*SSTR2*	*SSTR3*	*SSTR4*	*SSTR5*	Number Positive by Receptor Scan
GASTROENTEROPANCREATIC TUMORS							
Carcinoid	26	77	81	35	40	45	37/39 (95%)
Insulinomas	4	100	75	50	100	0	5/8 (63%)
Glucagonomas	2	100	100	100	100	0	
Gastrinomas							10/10 (100%)
PITUITARY ADENOMAS							
GH*	38–41	53	90	47	5	85	12/15 (80%)
TSH							2/2 (100%)
PRL*	17–19	84	63	35	6	71	
ACTH*	7–9	56	67	25	0	86	
Nonfunctioning*	35–36	31	61	46	13	49	6/8 (75%)
OTHER TUMORS							
Pheochromocytoma	11	100	100	73	73	73	2/3 (67%)
Medullary thyroid carcinoma	14	29	79	36	0	64	11/17 (65%)
Breast carcinoma	100	39	98	40	24	35	39/52 (75%)
Renal carcinoma	13	85	100	0	46	NT	
Meningioma	14	86	100	54	50	71	11/11 (100%)
Glioma	7	100	100	66	71	57	

mRNA, messenger RNA; *GH*, growth hormone; *TSH*, thyroid-stimulating hormone; *PRL*, [AU: Q8]; *ACTH*, adrenocorticotropic hormone; *NT*, not tested.
*The number of tumors analyzed for each of the different subtypes varied slightly in the pooled data shown.
(Data from Patel YC. Molecular pharmacology of somatostatin receptor subtypes. J Endocrinol Invest 1997; 20:348; Lamberts SWJ, Krenning EP, Reubi JC. The role of somatostatin and its analogs in the diagnosis and treatment of tumors. Endocr Rev 1991; 12:450; Vikic-Topic S, Raisch KP, Kvols LK, Vuk-Pavlovic S. Expression of somatostatin receptor subtypes in breast carcinoma, carcinoid tumor, and renal cell carcinoma. J Clin Endocrinol Metab 1995; 80:2974; Schaer J-C, Waser B, Mengod G, Reubi JC. Somatostatin receptor subtypes sst_1, sst_2, sst_3 and sst_5 expression in human pituitary, gastroentero-pancreatic and mammary tumors: comparison of mRNA analysis with receptor autoradiography. Int J Cancer 1997; 70:530; and Evans AA, Cook T, Laws SAM, et al. Analysis of somatostatin receptor subtype mRNA expression in human breast cancerBr J Cancer 1997; 75:798.)

GASTROENTEROPANCREATIC TUMORS

CARCINOID TUMORS

SST analogs play a central role in the management of symptoms of metastatic carcinoid disease. More than 200 cases of metastatic carcinoid tumors and carcinoid syndrome treated with octreotide have now been reported.[6,38,42,46–49] The drug is highly effective in this condition and produces a marked clinical and biochemical improvement. Flushing and diarrhea, the two most prominent symptoms, are rapidly relieved in >90% of patients. The clinical improvement is paralleled by a reduction in urinary 5-hydroxyindoleacetic acid (5-HIAA) levels, which drop by >50% in 70% of treated patients *without, however, being completely normalized in any patient.* A *small proportion* of patients (~14%) show *measurable regression of hepatic and lymph node metastases.*[46,49] In 80 patients treated with octreotide, median survival from the diagnosis of metastatic disease was 8.8 years compared with 1.8 years in historical controls. The average dose required for symptomatic and biochemical control ranges from 100 to 150 μg SC every 8 hours. Because of the dual actions of SST in blocking both the secretion and the action of hormones overproduced by tumors, the dose required to control symptoms such as diarrhea may be lower than that necessary for reducing urine 5-HIAA levels. *Resistance* to therapy eventually occurs with an increase in tumor bulk. Such resistance may be due to down-regulation of SST receptors or, more likely, to the emergence of receptor-negative or more virulent clones. Recurrence of disease on therapy may be controlled in some but not all patients by increasing the dose. Doses as high as 1 to 2 mg SC every 8 hours have been administered in this disease and appear to be well tolerated. A study comparing SC and long-acting formulations of octreotide found that monthly injections of octreotide LAR were as effective as SC octreotide in controlling the symptoms and in suppressing urinary 5-HIAA levels in 79 patients.[42] The recommended average dose is 20 mg octreotide LAR, increasing to 30 to 60 mg in some patients with resistant or advanced disease. Lanreotide 30 mg IM every 10 to 14 days is also effective.[41] In addition to its application in long-term treatment of metastatic carcinoid disease, octreotide is very useful in preventing carcinoid crisis when administered intravenously in susceptible patients immediately before and for 7 to 10 days after surgery, chemotherapy, or hepatic artery embolization.

VIPOMAS

Like carcinoid tumors, VIPomas tend to be malignant, with extensive metastatic disease from the outset. Octreotide has become the *first-line drug* for the symptomatic control of this disease. Of 25 patients with VIPoma treated with octreotide for 15 months, 85% showed improvement in or resolution of diarrhea, which was associated with a reduction in plasma levels of vasoactive intestinal peptide in 60%.[47–49] The effect of octreotide is usually rapid and occurs with relatively low doses, 50 to 100 μg every 8 to 12 hours. With time, efficacy is lost in some patients and high-dose regimens are required. Reduction in tumor size has been reported in as many as 40% of patients treated with octreotide for 2 months or longer.[49]

GLUCAGONOMAS

Approximately 10 patients with glucagonomas who have been treated with octreotide have been described.[47–49] Glucagonomas are slowly growing, malignant tumors associated with severe constitutional symptoms as well as a characteristic rash (see Chap. 220). Therapy with octreotide resolves the rash in a few days and improves other symptoms such as weight loss, anorexia, abdominal pain, and diarrhea. Because no other form of therapy exists for the systemic manifestations of glucagonoma, especially its dermatologic complication, octreotide has assumed a primary role in the medical treatment of this disorder. Usually little effect is seen on the size of the tumor.

INSULINOMAS

Unlike non–B cell tumors, 90% of insulinomas are benign and can be cured by surgical resection. Octreotide suppresses insulin levels by >50%, elevates blood glucose levels, and prevents hypoglycemic attacks in many patients.[47–49] Thus, it is effective in the *preoperative treatment of patients with benign insulinoma.* Diazoxide, however, also lowers insulin levels effectively in this setting. It remains to be determined whether octreotide offers any specific advantage. In most patients with *malignant insulinoma,* octreotide is effective in *preventing hypoglycemic attacks.* Loss of efficacy is common, however, and it may be overcome by increasing the dosage. Of greater concern is the *worsening* of hypoglycemia in some patients as a result of the greater suppression by octreotide of the counterregulatory hormones (GH and glucagon) than of insulin. In view of this possibility, plasma glucose levels should be monitored carefully at the initiation of octreotide therapy.

GASTRINOMAS

Gastrinomas are commonly malignant islet cell tumors that have metastasized at the time of diagnosis. In the >50 reported cases treated with octreotide, the response has been variable, with only modest reductions in gastrin levels.[47–49] Furthermore, tumor growth may progress during octreotide treatment. Because the clinical manifestations of gastrinoma result from the hypersecretion of gastric acid, which can be controlled effectively by oral medications such as H_2-receptor antagonists or the Na^+/H^+ adenosine triphosphatase inhibitor omeprazole, octreotide serves only an adjunctive role in treatment of this disorder.

TUMORS PRODUCING GROWTH HORMONE–RELEASING HORMONE

Several patients with GHRH-producing tumors (bronchial carcinoid tumors or metastatic islet cell tumors) who received treatment with octreotide showed good symptomatic and biochemical response.[49] Octreotide reduced plasma concentrations of GHRH and GH, probably through a dual effect on tumor cells and pituitary somatotropes.

TREATMENT OF PITUITARY TUMORS

ACROMEGALY

SST analogs significantly reduce GH secretion and IGF-I levels in patients with acromegaly and have become *effective agents in the treatment of this disorder.*[6,37–40,47,49–52] Their use is indicated in the treatment of patients with a macroadenoma who have persistent disease after transsphenoidal surgery, as interim treatment in patients awaiting the full effects of external irradiation, and as preoperative treatment for 2 to 3 months to improve the medical condition of patients with severe disease. They can also be offered as primary therapy to patients who refuse surgery or those with severe medical problems that preclude surgery. Octreotide has been proposed as primary therapy for patients with invasive macroadenomas not causing chiasmatic compression, who are unlikely to be cured surgically.[51] This is an attractive idea, especially with the availability of slow-release preparations; it needs to be further assessed in prospective studies comparing the relative efficacy and cost effectiveness of primary SST analog therapy versus surgery for treatment of acromegaly.[51] With SC injections of 100 μg octreotide three times daily (mean optimal efficacious dosage), a prompt reduction in plasma GH levels occurs, followed by a decline in circulating IGF-I levels during the first week.[50,52] This is accompanied by immediate relief of many of the clinical symptoms of acromegaly, including fatigue, headache, excessive perspiration, arthralgia, and soft-tissue swelling.[50,52] Relief of headache is often seen immediately after the injections are started and before serum GH levels have declined, probably as a result of a vascular or analgesic action of the drug. Improvement in facial

coarsening and acral enlargement occurs after longer periods of treatment. Sustained improvement with minimal side effects has been noted with treatment for 10 or more years. Drug resistance may develop during long-term treatment, necessitating increased dosages. In a double-blind, randomized, multicenter study of 115 patients with acromegaly,[52] administration of octreotide at a dosage of 100 μg three times a day for 6 months was effective in reducing GH levels in 71% of patients and IGF-I levels in 93%. Mean integrated GH levels were reduced 70% from 40 ± 13 μg/L to 12 ± 4 μg/L, and mean integrated IGF-I levels were suppressed 60% from 4800 ± 354 U/L to 1900 ± 200 U/L. Normalization of GH secretion, defined as a reduction of integrated mean GH levels to <5 μg/L, occurred in 53% of patients, whereas IGF-I levels normalized in 68%. A decrease in pituitary tumor size (25–50%) has been observed in 20% to 47% of patients with acromegaly receiving long-term octreotide therapy.[50–53] Tumor shrinkage may be dose dependent, as it is greater with larger doses of octreotide. Preoperative treatment for 8 to 12 weeks shrinks invasive somatotrope macroadenomas by ~40%, but whether such shrinkage affects the surgical outcome remains controversial.[53] Early results with the slow-release SST preparations suggest that administration of octreotide LAR (20–30 mg per month) and lanreotide (30–60 mg two to three times per month) is as effective as multiple daily SC injections of octreotide in controlling GH hypersecretion.[39,40] In most patients with acromegaly, SST analogs are more effective in lowering GH levels than the dopamine agonists bromocriptine or cabergoline.[51] Occasionally, however, patients (typically those with mixed GH/prolactin-producing tumors) exhibit greater sensitivity to dopamine receptor agonists. In addition, use of a combination of SST analogs and dopamine-receptor agonists is of value in some patients who do not respond to either drug alone.

Thyrotropin-Secreting Pituitary Adenomas. *Most TSH-secreting tumors are sensitive to octreotide treatment.*[6,47,49,54] In 73 such tumor cases, octreotide (50–750 μg SC two to three times daily) reduced TSH secretion in 92% of cases and α-subunit secretion and 93%, with normalization of TSH in 79% and restoration of the euthyroid state in the majority.[54] In 52% of patients, clear evidence of tumor shrinkage was found. Treatment is indicated for residual tumor after surgery and/or radiotherapy. The place of SST analogs as primary therapy for these tumors remains to be established.

ADRENOCORTICOTROPIC HORMONE–SECRETING PITUITARY ADENOMAS

Although SST receptors have been identified in corticotrope adenomas, these tumors generally show *poor* responsiveness to octreotide. A *few* patients with invasive corticotrope adenomas associated with Nelson syndrome have responded to octreotide therapy with a decrease in ACTH secretion as well as a possible reduction in tumor size.[6] Likewise, some cases of *paraneoplastic ACTH secretion from bronchial and thymic carcinoids* can be controlled by octreotide.

NONFUNCTIONING PITUITARY ADENOMAS

Many nonfunctioning pituitary adenomas express SST receptors, with a preponderance of the octreotide-sensitive SSTR2 and SSTR5 subtypes (see Table 169-4). These tumors secrete low levels of gonadotropins, but generally show *little* change in tumor size with octreotide therapy despite inhibition of glycoprotein hormone and subunit release in some instances.[6,49]

POSSIBLE ONCOLOGIC APPLICATIONS

Although for many years neuroendocrine tumors have been known to possess SSTRs and to be amenable to treatment with SST analogs, the more recent realization that common solid tumors such as breast, colon, and prostate cancers are also rich in SSTRs has led to mounting interest in the more general oncologic usefulness of SST analogs.[2,3,6,43,45] Any effect of SST on these tumors appears to be quite variable, however, probably due to patient selection (e.g., early vs. end-stage disease); the absence of appropriate SSTRs in the tumors being treated (e.g., tumors expressing SSTR1 and SSTR4 do not respond to octreotide; SSTR3 expression is required for inducing apoptosis); the presence of mutated p53 gene, which abrogates the apoptotic effect of SST; and the dose and duration of treatment. Most current interest is focused on breast cancer because (a) the incidence of SSTR expression is high,[43,45] (b) SST analogs inhibit the growth of breast cancer cells in vivo and in vitro by inducing cell growth arrest and apoptosis,[2,55] (c) octreotide potentiates the antineoplastic effects of tamoxifen in experimental mammary carcinoma in the rat,[56] and (d) SC octreotide treatment for 6 weeks to 6 years in combination with norprolac (a dopamine-receptor agonist to inhibit prolactin secretion) enhanced the effectiveness of tamoxifen therapy in 22 patients with advanced breast cancer.[57] These findings have generated interest in SST as *adjuvant therapy for breast cancer* and have led to several multicenter North American clinical trials involving >3,000 patients. These currently ongoing studies will look at the effect of high-dose octreotide given alone as a monthly injection for 2 years or in combination with tamoxifen to women with estrogen receptor–positive stage I and stage II breast cancer.

GASTROINTESTINAL APPLICATIONS

Short- or long-term octreotide administration is useful in treating numerous gastrointestinal disorders (see Table 169-3). These conditions are more common than neuroendocrine tumors and account for much of the hospital-based usage of octreotide. SST is a potent constrictor of the splanchnic circulation and is effective in controlling variceal bleeding. In a randomized, double-blind, placebo-controlled trial of 120 patients, infusion of SST-14 at a dosage of 250 μg per hour for 5 days controlled bleeding and reduced transfusion requirements.[58] In a study of 100 patients, octreotide given intravenously for 48 hours was as effective as emergency sclerotherapy in the treatment of acute variceal hemorrhage.[6] The antisecretory effects of SST on the pancreas have led to the successful use of octreotide in the treatment of pancreatic fistulas. More than 60 patients so treated have been described.[59] Most reports indicate a closure rate of pancreatic fistulas approximating 70% within a week. In addition to the diarrhea that occurs with hormone-secreting tumors, other forms of secretory diarrhea such as that associated with high-output ileostomy, diabetic diarrhea, AIDS diarrhea, chemotherapy-induced diarrhea, and diarrhea associated with amyloidosis all have been reported to be variably controlled with octreotide.[47] In these diarrheal states, octreotide acts by blocking the normal production of gastric and pancreatic exocrine secretion destined for reabsorption in the distal bowel, and by directly inhibiting intestinal fluid and electrolyte secretion. In a randomized double-blind trial involving 10 patients with severe postgastrectomy dumping syndrome, the administration of octreotide 100 μg 30 minutes before eating prevented the development of vasomotor symptoms (early dumping) as well as the hypoglycemia and diarrhea characteristic of late dumping.[60] Finally, in patients with scleroderma and intestinal dysmotility, the short-term administration of octreotide improved intestinal motility by stimulating the frequency of intestinal migrating motor complexes and reducing bacterial overgrowth, which led to an improvement in abdominal symptoms such as nausea, bloating, and pain.[61]

ORTHOSTATIC HYPOTENSION

Postprandial and orthostatic hypotension in patients with autonomic neuropathy is abolished by low dosages of octreotide (0.2–0.4 μg/kg). In these cases, the drug acts as a potent pressor

agent and has emerged as a new form of therapy for this condition as well as for other types of postprandial hypotension, such as that which occurs in the elderly.[62]

SIDE EFFECTS

Although the acute administration of SST produces a large number of inhibitory effects, continued exposure results in an *escape from the acute effects of the peptide.*[2,6] This may be due to up-regulation of some of the receptor subtypes, which compensates for the desensitized responses of others and thereby maintains normal overall SST responsiveness. Side effects associated with the long-term administration of octreotide for up to 2 years have been remarkably few.[6,37,39–42,49,50–52] Most patients complain of pain at the injection site, and abdominal cramps and mild steatorrhea to which they become tolerant after 10 to 14 days. No nutritional deficiency has been reported with long-term octreotide therapy. Patients also adapt rapidly to some of the other effects of SST (e.g., inhibition of insulin and TSH secretion). A mild impairment of glucose tolerance may occur, consisting of a mild increase in postprandial glucose levels only, with maintenance of normal fasting glucose levels. Normal thyroid function is maintained and hypothyroidism is rare. Some effects, however, do persist; for example, inhibition of gallbladder emptying causes a significant increase in the incidence of biliary sludge and cholesterol gallstones in 20% to 30% of patients after 1 to 2 years of treatment.[6] Those receiving long-term treatment warrant initial ultrasonographic evaluation, and subsequently evaluation as necessary, depending on symptoms. The incidence of adverse effects with the slow-release preparations of SST is comparable to that with the subcutaneous injections.[37,39,40–42] Interestingly, the persistent steatorrhea and mild diabetes mellitus that are associated with the chronic hypersomatostatinemia in patients with SST-producing tumors[36] are not observed in patients during long-term treatment with the slow-release forms of the SST analogs, despite the sustained high blood levels of the drugs. This no doubt reflects the narrower binding specificity of the synthetic SST analogs, which binds to only three of the SSTR subtypes, compared with SST-14 and SST-28, which are typically produced by somatostatinomas and bind to all five SSTRs (see Table 169-2). Although normal tissues adapt to the long-term effects of octreotide, hormone-producing tumors continue to respond to octreotide injections with persistent suppression of hormone secretion, frequently for several years. This suggests a *differential regulation of SSTRs in normal tissues and in tumors.* Tumors express a higher density of SSTRs than do surrounding normal tissues. Conceivably, SSTRs in tumors behave differently due to a loss of normal receptor regulatory function, due to an alteration in the pattern and composition of the various subtypes expressed, or due to abnormal receptor signaling.

SOMATOSTATIN-RECEPTOR SCANS

A method for the in vivo imaging of SSTR-positive tumors and their metastases has been developed using as radionuclides [^{123}I]Tyr^3 octreotide or an indium-labeled octreotide preparation that is now available commercially (^{111}In-diethylenetriamine pentaacetic acid[DTPA]-D-Phe-1-octreotide).[37,38,63,64] The rationale for the method lies in the demonstration that most endocrine tumors that respond to octreotide therapy do so because they are rich in SSTRs. Direct binding studies of surgically removed specimens have revealed a higher density of receptors in tumor tissue than in the surrounding healthy tissue.[38] After intravenous administration, the radioligand binds to SSTRs on primary and metastatic tumor cells, which then can be visualized by computerized γ-scintigraphy. Unbound radioactive material is rapidly degraded in the liver and excreted in the bile, or eliminated through the kidneys. The technique is relatively simple and effective. Among 59 patients with metastatic carcinoid disease or pancreatic endocrine tumors, primary tumors and their metastases were successfully localized in all but five cases (see Table 169-4). Particularly impressive is the ability of the receptor-scanning technique to visualize many unsuspected metastases that escape detection by clinical examination and conventional imaging techniques such as computed tomographic scanning and magnetic resonance imaging.[38,63] Overall, the specificity of the method is high as judged by the close correlation among the in vivo tumor receptor scans, the inhibitory effect of octreotide on the secretion of hormone by the tumor, and the presence of SSTRs as demonstrated by direct in vitro binding studies of surgically removed tumor samples.[38,63] SSTR scanning offers several distinct advantages over the currently used standard imaging methods. The first is its high power of resolution for tumors as small as 1 cm in diameter, which are difficult to visualize with conventional scanning techniques.[63] Second, because the whole body is imaged, abnormalities in areas not under clinical suspicion can be detected, and the full extent of metastatic disease accurately mapped. Third, this method provides a functional index of the SSTR status of tumor cells that could be useful in tumor management. For instance, positivity for receptors can predict tumor responsiveness to SST therapy and may serve as a prognostic index of a favorable outcome for some tumors. The technique has some limitations. The first is that secretory tumors that do not express SSTRs are not amenable to analysis with this method. Second, because octreotide does not bind to two of the SSTR subtypes (types 1 and 4), those tumors that uniquely express these receptor isoforms will escape detection. SST-receptor scans are now available at most major centers and are widely used in the *assessment of carcinoid and islet cell tumors, paragangliomas, pheochromocytomas,* and *medullary thyroid carcinoma.*[38] They are of *little value in the imaging of pituitary tumors,* which are better defined by conventional techniques. Because of the rich expression of the type 2 SSTR in immune and inflammatory cells, lesions of several *granulomatous, inflammatory, and immune disorders* have been successfully imaged by SSTR scintigraphy, for example, rheumatoid joints, sarcoid lesions, Hodgkin's and non-Hodgkin's lymphomas, and thyroid eye disease. The value of SST-receptor scan in the routine assessment of these disorders, however, remains to be determined.

SOMATOSTATIN RECEPTOR–TARGETED RADIOABLATION OF TUMORS

The property of rich SSTR expression by tumors which allows their visualization by the receptor-imaging approach can be further applied to achieve receptor-targeted ablation of the tumors. Binding of radioligand to SSTRs on the cell surface triggers their internalization.[2] Specifically, SSTR subtypes 2, 3, and 5, which bind octreotide, all undergo agonist-dependent internalization, which suggests that the use of octreotide-based ligands coupled to α- or β-emitting radioisotopes could provide a method for delivering targeted radiation to the interior of the cell. Preliminary results with [^{111}In-DTPA]-octreotide [AU: Q2] in several patients with inoperable metastatic islet and carcinoid tumors suggest partial tumor responses as determined by radiographic tumor shrinkage.[65] A second analog of octreotide labeled with yttrium-90 (^{90}Y-DOTA-D-Phe^1-Tyr^3 octreotide) [AU: Q3] which is a more potent β-emitting isotope that has been reported to be highly effective in inducing radionecrosis of human small cell lung tumor transplanted into nude mice, is undergoing clinical trials.[37] Because SSTRs are expressed in many normal cells that would undoubtedly take up the radioligands, the question of whether significant damage to organs

in which the DTPA-molecule is replaced by another chelator, DOTA, tetraazacyclo

(e.g., the pituitary, islets, and gut) occurs with this type of treatment remains to be determined. Nonetheless, this is a promising new approach that could be applied not just to neuroendocrine tumors but also to all SSTR-rich tumors, and it awaits further study.

REFERENCES

1. Reichlin S. Somatostatin. N Engl J Med 1983; 309:1495.
2. Patel YC: Somatostatin and its receptor family. Frontiers Neuroendocrinol 1999; 20:157.
3. Patel YC. Molecular pharmacology of somatostatin receptor subtypes. J Endocrinol Invest 1997; 20:348.
4. Patel YC, Liu JL, Galanopoulou AS, Papachristou DN. Production, action, and degradation of somatostatin. In: Jefferson LS, Cherrington AD, eds. The handbook of physiology, The endocrine pancreas and regulation of metabolism. [AU: Q3a] New York: Oxford University Press, ~~3999~~, in press.
5. Epelbaum J, Dournaud P, Fodor M, Viollet C. The neurobiology of somatostatin. Crit Rev Neurobiol 1994; 8:25.
6. Lamberts SWJ, Van Der Lely A-J, de Herder WW. Drug therapy: octreotide. N Engl J Med 1996; 334:246.
7. Patel YC, Tannenbaum GS, eds. Somatostatin: basic and clinical aspects. Metabolism 1990; 39(Suppl 2).
8. Patel YC. General aspects of the biology and function of somatostatin. In: Weil C, Muller EE, Thorner MO, eds. Somatostatin. Basic and clinical aspects of neuroscience series, vol 4. Berlin: Springer-Verlag, 1992:1.
9. De Lecea L, Criado JR, Prospero-Garcia O, et al. A cortical neuropeptide with neuronal depressant and sleep-modulating properties. Nature 1996; 381:242.
10. Hokfelt T, Efendic S, Hellerstrom C, et al. Cellular localization of somatostatin in endocrine-like cells and neurons of the rat with special reference to the A_1 cells of the pancreatic islets and to the hypothalamus. Acta Endocrinol (Copenh) 1975; 80 (Suppl 200):5.
11. Patel YC, Reichlin S. Somatostatin in hypothalamus, extrahypothalamic brain and peripheral tissues of the rat. Endocrinology 1978; 102:523.
12. Baetens D, Malaisse-Lagae F, Perrelet A, et al. Endocrine pancreas: three dimensional reconstruction shows two types of islets of Langerhans. Science 1979; 206:1323.
13. Larsson LI. Distribution and morphology of somatostatin cells. Adv Exp Biol Med 1985; 188:383.
14. Aguila MC, Dees WL, Haensly WE, McCann SM. Evidence that somatostatin is localized and synthesized in lymphoid organs. Proc Natl Acad Sci U S A 1991; 88:11485.
15. Elliott DE, Blum AM, Li J, et al. Preprosomatostatin messenger RNA is expressed by inflammatory cells and induced by inflammatory mediators and cytokines. J Immunol 1998; 160:3997.
16. Shoelson SE, Polonsky KS, Nakabayashi T, et al. Circulating forms of somatostatin-like immunoreactivity in human plasma. Am J Physiol 1986; 250:E428.
17. Taborsky GT Jr, Ensinck JW. Contribution of the pancreas to circulating somatostatin-like immunoreactivity in the normal dog. J Clin Invest 1984; 73:216.
18. Patel YC, Rao K, Reichlin S. Somatostatin in human cerebrospinal fluid. N Engl J Med 1977; 296:529.
19. Rubinow DR, Davis CL, Post RM. Somatostatin in neuropsychiatric disorders. In: Weil C, Muller EE, Thorner MO, eds. Somatostatin. Basic and clinical aspects of neuroscience series, vol 4. Berlin: Springer-Verlag, 1992:29.
20. Montminy M, Brindle P, Arias J, et al. Regulation of somatostatin gene transcription by cAMP. In: Somatostatin and its receptors. Ciba Foundation Symposium 190. West Sussex: John Wiley and Sons, 1995:7.
21. Reisine T, Bell GI. Molecular biology of somatostatin receptors. Endocr Rev 1995; 16:427.
22. Bruno JF, Yun XU, Song J, et al. Tissue distribution of somatostatin receptor subtype messenger ribonucleic acid in the rat. Endocrinology 1993; 133:2561.
23. Kumar U, Sasi R, Suresh S, et al. Subtype-selective expression of the five somatostatin receptors (hSSTR1-5) in human pancreatic islet cells: a quantitative double-label immunohistochemical analysis. Diabetes 1999; 48:77.
24. Pan MG, Florio T, Stork PJC. G protein activation of a hormone-stimulated phosphatase in human tumor cells. Science 1992; 256:1215.
25. Reardon DB, Dent P, Wood SL, et al. Activation in vitro of somatostatin receptor subtypes 2, 3, or 4 stimulates protein tyrosine phosphatase activity in membranes from transfected Ras-transformed NIH 3T3 cells: coexpression with catalytically inactive SHP-2 blocks responsiveness. Mol Endocrinol 1997; 11:1062.
26. Sharma K, Patel YC, Srikant CB. Subtype selective induction of p53-dependent apoptosis but not cell cycle arrest by human somatostatin receptor 3. Mol Endocrinol 1996; 10:1688.
27. Tannenbaum GS, Epelbaum J. Somatostatin. In: Costio JL, ed. Handbook of physiology, vol 5. Hormonal control of growth. Sect vii, The endocrine system. New York: Oxford, 1999:221.
28. D'Alessio DA, Sieber C, Beglinger C, et al. A physiologic role for somatostatin-28 as a regulator of insulin secretion. J Clin Invest 1989; 84:857.
29. Colturi TJ, Unger RH, Feldman M. Role of circulating somatostatin in regulation of gastric acid secretion, gastrin release and islet cell function. Studies in healthy subjects and duodenal ulcer patients. J Clin Invest 1984; 74:417.
30. Gyr K, Beglinger C, Kohler E, et al. Circulating somatostatin: physiological regulator of pancreatic function? J Clin Invest 1987; 79:1595.
31. Yamada T. Gut somatostatin. In: Reichlin S, ed. Somatostatin: basic and clinical status. New York: Plenum, 1987:221.
32. Juarez RA, Rubinstein M, Chan EC, et al. Increased growth following normal development in middle aged somatostatin deficient mice. In: Program of the Annual Meeting of the Society for Neuroscience; October 1997; New Orleans. Abstract 659.10:1684.
33. Shimon I, Taylor JE, Dong JZ, et al. Somatostatin receptor subtype specificity in human fetal pituitary culture. J Clin Invest 1997; 99:789.
34. Rohrer SP, Birzin ET, Mosley RT, et al. Rapid identification of subtype-selective agonists of the somatostatin receptor through combinatorial chemistry. Science 1998; 282:737.
35. Zheng H, Bailey A, Jiang MH, et al. Somatostatin receptor subtype 2 knockout mice are refractory to growth hormone, negative feedback on arcuate neurons. Mol Endocrinol 1997; 11:1709.
36. Krejs GJ, Orci L, Conlon JM, et al. Somatostatinoma syndrome: biochemical, morphological and clinical features. N Engl J Med 1979; 301:285.
37. Marbach P, Bauer W, Bodmer D, et al. Discovery and development of somatostatin agonists. Pharm Biotechnol 1998; 11:183.
38. Lamberts SWJ, Krenning EP, Reubi JC. The role of somatostatin and its analogs in the diagnosis and treatment of tumors. Endocr Rev 1991; 12:450.
39. Lancranjan L, Bruns C, Grass P, et al. Sandostatin LAR: pharmacokinetics, pharmacodynamics, efficacy, and tolerability in acromegalic patients. Metabolism 1995; 44:18.
40. Giusti M, Gussoni G, Cuttica CM, et al. Effectiveness and tolerability of slow release lanreotide treatment in active acromegaly: six-month report on an Italian multicenter study. J Clin Endocrinol Metab 1996; 81:2089.
41. Tomassetti P, Migliori M, Gullo L. Slow-release lanreotide treatment in endocrine gastrointestinal tumors. Am J Gastroenterol 1998; 93:1468.
42. Rubin J, Ajani J, Schirmer W, et al. Octreotide acetate long-acting formulation versus open-label subcutaneous octreotide acetate in malignant carcinoid syndrome. J Clin Oncol 1999; 17:600.
43. Vikic-Topic S, Raisch KP, Kvols LK, Vuk-Pavlovic S. Expression of somatostatin receptor subtypes in breast carcinoma, carcinoid tumor, and renal cell carcinoma. J Clin Endocrinol Metab 1995; 80:2974.
44. Schaer J-C, Waser B, Mengod G, Reubi JC. Somatostatin receptor subtypes sst_1, sst_2, sst_3 and sst_5 expression in human pituitary, gastroentero-pancreatic and mammary tumors: comparison of mRNA analysis with receptor autoradiography. Int J Cancer 1997; 70:530.
45. Evans AA, Cook T, Laws SAM, et al. Analysis of somatostatin receptor subtype mRNA expression in human breast cancer. Br J Cancer 1997; 75:798.
46. Kvols LK, Moertal OG, O'Connell MJ, et al. Treatment of the malignant carcinoid syndrome: evaluation of a long-acting somatostatin analogue. N Engl J Med 1986; 315:663.
47. Gorden P, Comi RJ, Maton PN, et al. Somatostatin and somatostatin analog (SMS 201-995) in treatment of hormone secreting tumors of the pituitary and gastrointestinal tract and nonneoplastic diseases of the gut. Ann Int Med 1989; 110:35.
48. Wynick D, Bloom SR. The use of the long-acting somatostatin analog octreotide in the treatment of gut neuroendocrine tumors. J Clin Endocrinol Metab 1991; 73:1.
49. Maton PN, Avaraki RF. Therapeutic use of somatostatin and octreotide acetate in neuroendocrine tumors. In: Weil C, Muller EE, Thorner MO, eds. Somatostatin. Basic and clinical aspects of neuroscience series, vol 4. Berlin: Springer-Verlag, 1992:55.
50. Sassolas G, Harris AG, James-Deidier A, et al. Long-term effect of incremental doses of the somatostatin analog SMS 201-995 in 58 acromegalic patients. J Clin Endocrinol Metab 1990; 71:391.
51. Melmed S, Jackson I, Kleinberg D, Klibanski A. Current treatment guidelines for acromegaly. J Clin Endocrinol Metab 1998; 83:2646.
52. Ezzat S, Snyder PJ, Young WF, et al. Octreotide treatment of acromegaly. Ann Intern Med 1992; 117:711.
53. Barkan AL, Lloyd RV, Chandler WF, et al. Preoperative treatment of acromegaly with long-acting somatostatin analog SMS 201-995: shrinkage of invasive pituitary macroadenomas and improved surgical remission rate. J Clin Endocrinol Metab 1988; 67:1040.
54. Beck-Peccoz P, Brucker-Davis F, Persani L, et al. Thyrotropin-secreting pituitary tumors. Endocr Rev 1996; 17:610.
55. Sharma K, Srikant CB. Induction of wild type p53, bax and acidic endonuclease during somatostatin signaled apoptosis in MCF-7 human breast cancer cells. Int J Cancer 1998; 76:259.
56. Weckbecker G, Tolcsvai L, Stolz B, et al. Somatostatin analogue octreotide enhances the antineoplastic effect of tamoxifen and ovariectomy on 7, 12-dimethylbenz(a)anthracene-induced rat mammary carcinomas. Cancer Res 1994; 54:6334.
57. Bontenbal M, Foekens JA, Lamberts SWJ, et al. Feasibility, endocrine and anti-tumor effects of a triple endocrine therapy with tamoxifen, a somatostatin analogue and an antiprolactin in post-menopausal breast cancer: a randomized study with long-term follow-up. Br J Cancer 1998; 77:115.
58. Burroughs AK, McCormick PA, Hughes MD, et al. Randomized double blind placebo controlled trial of somatostatin for variceal bleeding. Gastroenterology 1990; 99:1388.
59. Torres A, Landa J, Moreno-Azcoita M, et al. Somatostatin in the management of gastrointestinal fistulas. Arch Surg 1992; 127:97.

60. Geer RJ, Richards WO, O'Dorisio TM, et al. Efficacy of octreotide acetate in treatment of severe postgastrectomy dumping syndrome. Ann Surg 1990; 212:678.
61. Soudah HC, Hasler WL, Owyang C. Effect of octreotide on intestinal motility and bacterial overgrowth in scleroderma. N Engl J Med 1991; 325:1461.
62. Hoeldtke RD, Israel BC. Treatment of orthostatic hypotension with octreotide. J Clin Endocrinol Metab 1989; 68:1051.
63. Lamberts SWJ, Bakker WH, Reubi J-C, et al. Somatostatin receptor imaging in the localization of endocrine tumors. N Engl J Med 1990; 323:1246.
64. Hofland LJ, Breeman WAP, Krenning EP, et al. Internalization of [DOTA°, ^{125}I-Tyr^3] octreotide by somatostatin receptor-positive cells in vitro and in vivo: implications for somatostatin receptor-targeted radioguided surgery. Proc Assoc Am Phys 1999; 111:63.
65. McCarthy KE, Woltering EA, Espenan GD, et al. In situ radiotherapy with ^{111}In-pentetreotide: initial observations and future directions. Cancer J Sci Amer 1998; 4:94.

CHAPTER 170

KININS

DOMENICO C. REGOLI

THE KALLIKREIN–KININ SYSTEM

CHEMISTRY

The kinins are potent vasodilator peptides that are contained in large precursors (*kininogens*), from which they are released into the blood and biologic fluids through the action of proteolytic enzymes (*kallikreins*). In contrast to neuropeptides and many other endogenous hormonal agents that are synthesized and stored in nerve and endocrine cells, kinins are generated in the blood and tissues.[1] The kallikreins, which are responsible for the formation of kinins, originate from the liver (*plasma kallikreins*), from exocrine glands (*glandular kallikreins*),[2] from the kidney, and from other organs and tissues.[3] The kallikreins exist in blood and tissues as precursors (prekallikreins) that are activated by various chemical and physical factors. Among the endogenous activators are the Hageman factor, several enzymes (trypsin, plasmin, factor XI), and, in vitro, glass surfaces, kaolin, collagen, and other charged substances, such as cellulose sulfate.[4,5] Plasma prekallikrein (with a molecular mass of 130,000 daltons) is the precursor of kallikrein (95,000–100,000 daltons), which interacts with the high-molecular-mass kininogen (88,000–114,000 daltons) to release the nonapeptide *bradykinin*[5] (Fig. 170-1). Glandular kallikreins are acidic glycoproteins (27,000–43,000 daltons) that release the decapeptide kallidin (see Fig. 170-1) from kininogens of low molecular mass (48,000–70,000 daltons).[2,3,6] Kallikreins and kininogens have been cloned; sequence structures of the enzymes and the substrates are known (see comprehensive review[7,8]).

INACTIVATION

Kinins are rapidly inactivated by several proteolytic enzymes present in plasma and tissues that act either at the amino or at the carboxyl end of the kinins (see Fig. 170-1). The metabolic products of kinins are inactive except for the bradykinin that is released from kallidin by the aminopeptidase, and the desArg^9 bradykinin or desArg^{10} kallidin that is released from bradykinin and kallidin by *kininase I*.[9,10] The most efficient system for inactivating kinins and activating angiotensin I to angiotensin II is *kininase II*, a carboxydipeptidase that is widely distributed in plasma, endothelial cells, and various organs, such as the lung and the kidney.[9]

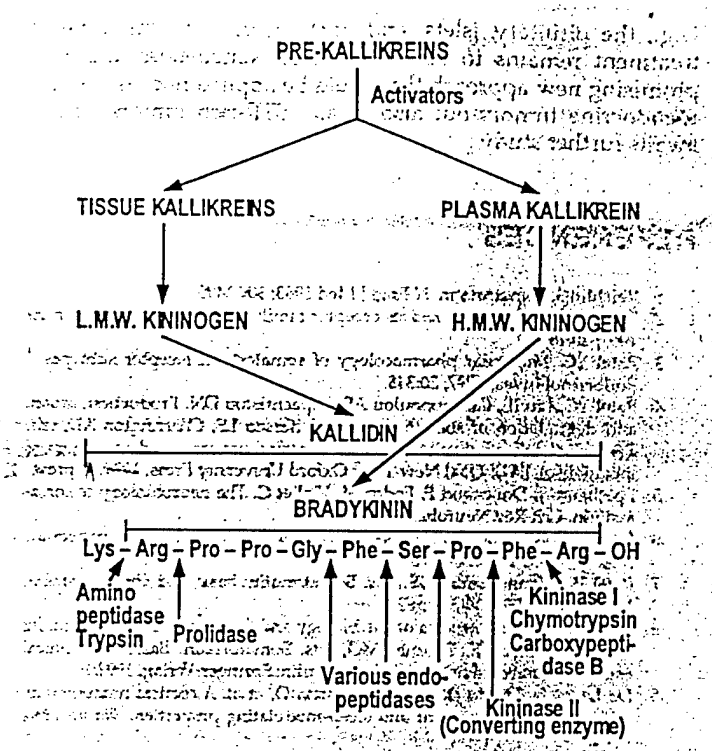

FIGURE 170-1. Formation and degradation of kinins. (*LMW*, low molecular weight; *HMW*, high molecular weight.) (From Regoli D. Polypeptides et antagonistes. In: Giroud J-P, Mathé G, Meyniel G, eds. Pharmacologie clinique: bases de la thérapeutique, 2nd ed. Paris: Expansion Scientifique Française, 1988:691.)

Kininase II is particularly active in the pulmonary vascular bed: 80% to 95% of kinins are eliminated during the few seconds in which the blood passes through the pulmonary circulation.[11] Because of their rapid inactivation in the lung and in other tissues, the biologic half-lives of bradykinin and kallidin in the dog are 0.27 and 0.32 minutes, respectively. Thus, as a result of the balance between the simultaneous processes of production and inactivation, kinins circulate at very low concentrations.

MEASUREMENT IN BLOOD

BLOOD LEVELS IN HEALTHY SUBJECTS

Various investigators have reported extreme variations (from 0.07–5.0 ng/mL) in circulating kinin concentrations in healthy volunteers, using either bioassays or radioimmunoassays.[10] One group has reported a concentration of 0.025 ng/mL, a value 100 to 200 times lower than any previously reported.[12] Such discrepancies are attributable largely to the fact that prekallikreins in blood are rapidly activated by contact with glass surfaces and by numerous other physical and chemical factors.[1] Therefore, most of the data on the blood concentration of kinins reported since the 1970s reflect figures that are much too high compared to more recent results obtained with sensitive radioimmunoassays.[4] When both types of assays have been used for the same plasmas, radioimmunoassay has yielded values two to six times higher than those derived from bioassay, probably because antibodies that are directed against the C-terminal part of the kinin molecules measure both the biologically active kinins and some inactive metabolites.[4,10]

BLOOD LEVELS IN DISEASE

An increase of bradykinin-like material (measured by bioassay or radioimmunoassay) has been reported in the blood of patients affected by the dumping syndrome, postgastrectomy

REVISED Msc. CE 9522

IMMUNOHISTOCHEMICAL DETECTION OF SOMATOSTATIN RECEPTOR TYPES 1-5 IN MEDULLARY CARCINOMA OF THE THYROID

Mauro Papotti[§], Ujendra Kumar[†], Marco Volante[§], Carla Pecchioni[§], and Yogesh C. Patel[†]

Department of Biomedical Sciences and Oncology, University of Turin, Italy[§], and Fraser Laboratories, Departments of Medicine and Neurology and Neurosurgery, McGill University and Royal Victoria Hospital, Montreal, Canada H3A 1A1[†].

Short Title: **Somatostatin Receptor Subtypes in Medullary Thyroid Carcinoma**

Correspondence: Dr. Y.C. Patel

Royal Victoria Hospital, Room M3-15

687 Pine Avenue West

Montreal, Quebec H3A 1A1

Canada

Tele: (514) 842-1231 ext. 5042

Fax: (514) 849-3681

E-mail: yogesh.patel@muhc.mcgill.ca

Summary

BACKGROUND We have analysed the distribution of the five somatostatin receptors (sst1-5) by immunohistochemistry in a large retrospective series of 51 medullary carcinoma of the thyroid (MCT) specimens and correlated the pattern of sst expression with expression of somatostatin (SRIF) peptide, tumor pathology and clinical outcome.

MEASUREMENTS Immunohistochemistry was performed with rabbit polyclonal antipeptide antibodies directed against the extracellular domains or cytoplasmic tail of human (h) sst1-5. SRIF immunoreactivity was investigated in parallel paraffin sections.

RESULTS 85% of the tumors were positive for one or more sst, localized to both tumor cells as well as surrounding peritumoral structures, especially blood vessels. 49% of the tumors were positive for sst1, 43% for sst2, 47% for sst3, 4% for sst4, and 57% for sst5. 51% of tumors expressed one or two sst subtypes; 33% were positive for three or more sst isoforms. All five sst receptors were detected in only two cases. Tumors expressing octreotide sensitive subtypes (sst2,3,5) accounted for 75% of the series. 50% of the tumors coexpressed SRIF suggesting tumor cell regulation by endogenous SRIF via paracrine/autocrine circuits. There was no correlation between sst1-5 expression and age, sex, tumor size or stage, histological type or clinical outcome. Simultaneous analysis of primary tumor and lymph node metastases revealed a similar pattern of sst immunoreactivity indicating that sst expression is not modified in the course of disease progression.

CONCLUSIONS With the exception of sst4, MCT display a rich but heterogeneous expression of

sst subtypes. Immunohistochemical typing of sst receptor expression using specific antireceptor antibodies represents an ideal approach for characterizing sst subtype expression in MCT for optimizing receptor targeted diagnosis and therapy with SRIF analogs.

Medullary carcinoma of the thyroid (MCT) accounts for approximately 5% of all primary thyroid malignancies (Saad *et al.*, 1984). The tumours arise from parafollicular calcitonin-producing cells (C-cells) and are related to carcinoid, pheochromocytoma and islet cell tumours whose progenitor cells form part of the diffuse neuroendocrine system. The peptide somatostatin (SRIF) is co-produced by a subset of normal human parafollicular cells whereas other C cells contain calcitonin alone (Van Noordan *et al.*, 1977; Yamada *et al.*, 1977). It is thus not surprising that many medullary thyroid carcinomas secrete SRIF which may be released directly into the circulation and which can serve as a circulating tumour marker. Furthermore, injections of SRIF inhibit calcitonin release suggesting that SRIF that is endogenously produced in the thyroid may act locally as a paracrine/autocrine regulator of C-cells (Linehan *etal.*, 1979). Somatostatin-positive MCT are associated with a favourable prognosis. Other markers have also been identified in MCT and include Carcinoembryonic antigen (CEA), Chromogranin A and various other hormonal peptides which are focally expressed by tumour cells (Schroder *et al.*, 1992; Papotti *et al.*, 1996).

Somatostatin blocks hormonal and exocrine secretion from many tissues and inhibits cell proliferation (Reichlin, 1983; Patel, 1999). These actions are mediated via a family of seven transmembrane domain G-protein coupled receptors with 5 molecular subtypes termed sst1-5 (Patel, 1999; Patel, 1997). These receptors are widely distributed in normal human tissues, typically as a multiple subtypes that coexist in the same cell (Patel, 1999; Patel, 1997; Kumar *et al.*, 1999; Patel *et al.*, 1994). The majority of human tumours, either benign or malignant are also generally positive for sst receptors featuring more than one isotype (Patel, 1997). These include functioning and non-functioning pituitary tumours, carcinoid tumours, islet cell tumours, thyroid carcinoma, pheochromocytoma, breast carcinoma, renal carcinoma, prostate carcinoma, meningioma, and

glioma (Patel, 1997). The general pattern of sst expression in these tumours suggests a very high frequency of sst 2mRNA in all tumours. mRNA for sst1 is also very abundant followed by sst 3 and 4. Expression of sst5 appears to be tumour specific.

Expression of sst receptors in MCT has been investigated by several different techniques (Reubi *et al.*, 1987; Reubi *et al.*, 1991; Lamberts *et al.*, 1991; Kwekkeboom *et al.*, 1993; Kurtaran *et al.*, 1996; Obyrne *et al.*, 1996; Behr *et al.*, 1997; Tisell *et al.*, 1997; Mato *et al.*, 1998). The earliest report was based on binding analysis and failed to identify sst receptors in the few cases tested (Reubi *et al.*, 1987). A subsequent larger series showed a heterogenous distribution of SRIF binding sites in 8/19 cases as revealed by autoradiography (Reubi *et al.*, 1991). A much higher proportion of primary and metastatic MCT have been shown to be positive for sst receptors by *in vivo* receptor scintigraphy with indium labelled octreotide. (Lamberts *et al.*, 1991; Kwekkeboom *et al.*, 1993; Kurtaran *et al.*, 1996; Obyrne *et al.*, 1996; Behr *et al.*, 1997; Tisell *et al.*, 1997). These types of *in vitro* and *in vivo* binding studies using labelled SRIF (which binds all five sst subtypes), or octreotide (which binds sst subtypes 2, 3, 5), however, cannot determine tumour expression of specific sst subtypes.In an attempt to characterize sst subtype expression, Mato et al analysed 14 cases of MCT for sst1-5 mRNA by Reverse Transcriptase Polymerase Chain Reaction (RT-PCR) and found sst mRNA expression in 12 of the 14 tumours (Mato *et al.*, 1998). Although RT-PCR is a sensitive technique, capable of elucidating sst subtype expression, it is based on mRNA analysis which may not necessarily correlate with receptor protein expression. Furthermore, this method cannot determine the cellular and subcellular pattern of sst expression. Since there are no subtype-specific radio ligands currently available for quantifying individual receptor populations, we have resorted to immunohistochemistry using a panel of polyclonal antipeptide antibodies against human (h) sst1-5 that we have developed. (Kumar *et al.*, 1999; Kumar *et al.*, 1997). Here we have characterized the distribution of all 5 sst receptors by immunohistochemistry in 51 MCT tumours and correlated their pattern of expression with the expression of SRIF peptide, clinical pathological parameters, and clinical outcome.

Materials and Methods

Tumors

51 cases of MCT encountered between 1974-1997 in which residual paraffin blocks were available for further sectioning, were retrieved from the pathology files of the University of Turin. All cases where reviewed and the final diagnosis was confirmed either on morphological grounds or on immunohistochemical findings (Calcitonin and chromogranin A positive; thyroglobulin negative). A representative block of each tumor was selected for immunohistochemical analysis .

Clinical Pathological Data

The 51 cases comprised 20 males and 31 females with a mean age of 49 years (median age 50) (Table 1). Eight cases were hereditary in the setting of MEN2A- or MEN2B-affected families, and the remaining 43 were apparently sporadic tumours. In five cases, cervical lymph node metastases were studied in parallel. Clinico-pathological data were available in 46 cases (5 cases were lost to follow-up) and included tumor size, tumor stage, disease progression, current status and outcome. Mean tumor size was 3.3cm. Three cases had extrathyroidal involvement at surgery (Stage pT4). Cervical lymph node metastases were found at operation in 25/45 (55.5%) of patients in whom node dissection was performed. 12 patients developed local recurrences or lymph node metastases or distant spread 1 to 12 years after diagnosis. Excluding the 2 cases of postoperative death, and the 5 patients lost to follow up, 23 are currently alive and free of disease 1-17 years after operation and the remaining 21 /44 are either alive with disease progression or have died from their disease 1- 27 years after surgery.

Antibodies to sst1-5

Antipeptide rabbit polyclonal antibodies specific for sst1-5 were produced and characterized as described elsewhere (Kumar *et al.*, 1999; Kumar *et al.*, 1997). Synthetic oligopeptides corresponding to deduced sequences in the amino terminal segment or extracellular loop 3 or cytoplasmic tail of human (h) sst1-5 were conjugated to keyhole limpet haemocyanin with glutaraldehyde. Rabbits were immunized and the resulting antisera characterized by the ability to inhibit [^{125}I LTT] SRIF-28 binding to membrane sst receptors, by immunocytochemistry of stable

CHO-K1 cell individually transfected with hsst1-5, and by western blot analysis.

Immunohistochemistry

5μM thick sections were collected onto poly-L-lysine-coated slides and processed for immunohistochemistry. Sections were incubated with hsst1-5 primary antibodies (diluted 1/200 overnight at room temperature). Somatostatin was detected using a commercially available antibody (Oxford Biomarketing, Oxford UK) incubated at 1:3000 dilution for 2h at room temperature after antigen retrieval using 3-minute passages in microwave oven in citrate buffer pH 6.0. After successive washes in Tris-buffered saline, sections were incubated with goat anti-rabbit secondary antibody at room temperature followed by exposure to peroxidase-labelled streptavidin (LSAB2, Dako, Glostrup, Denmark). Diaminobenzidine served as substrate for the peroxidase reaction. Nuclei were either unstained or lightly counterstained with hemalum. Controls used to validate the specificity of the sst immunoreactivity included pre-immune serum in place of primary antibody and antibody absorbed with excess antigen. (Kumar *et al.*, 1999; Kumar *et al.*, 1997).

Data Analysis

Statistical analysis was performed using the chi-square test.

Results

Immunohistochemistry

The results of the immunohistochemical analysis of SRIF and sst1-5 are summarized in Table 1. Immunoreactivity for sst1-5 was identified in 27, 22, 24, 2, and 29 of the 51 MCT tumors respectively corresponding to a positivity rate of 49% for sst1, 43% for sst2, 47% for sst3, 4% for sst4, and 57% for sst5. Overall 43 out of 51 (84%) of MCT tumors were positive for at least one sst subtype, 51% of tumors expressed one or two sst subtypes and a third (33.3%) were positive for three or more sst isoforms. All five sst receptors were detected in 2 cases only. Tumors expressing octreotide sensitive subtypes (sst2, 3, 5) accounted for 38/51 (75%) of the series.

In positive cases, sst1-5 immunostaining was present in 20-80% of the neoplastic cell

population and was localized predominantly to the plasma membrane and variably within the cytoplasm (Fig. 1a,b,d,e,g,i). One third of the cases had limited tumor clusters or single cells reactive only (approximately 5-10% of the tumor) and were labelled as "focal positive". The immunoreactivity observed in each case was specific and was not seen in control sections stained with pre-immune sera or with antigen absorbed antibody. (Fig.1f,h). In cases expressing more than one sst subtype, the spatial distribution of the individual types in the tumor cells overlapped partially only (Fig. 2a-d). While some areas of the same tumor nests were positive for all of the sst subtypes expressed by the given tumor, this was not the case in the majority of MCT which displayed a heterogenous pattern of distribution of the various sst subtypes. Peritumoral thyroid tissue was generally negative for sst expression. In capsular or stromal tissues, blood vessel walls, especially smooth muscle cells were immunostained by antibodies to sst1 and sst2 and there was focal expression of sst3 and sst5 (Fig. 1d,e). The pattern of expression of sst subtypes in the five cases of lymph node metastases that were studied, revealed a similar receptor profile to that of the corresponding primary tumors.

Expression of SRIF

Serial tumor sections were immunostained for SRIF and showed 50% of cases (25/51) to be positive (Table 2). Immunoreactive SRIF was usually confined to a small subset (5-10%) of tumor cells (Fig. 2e-h). A comparison of the expression of sst1-5 with that of SRIF showed that of the 25 cases positive for SRIF, 21 also expressed at least 1 sst type and 10 were reactive for 3 or more ssts (Table 2). SRIF expression however was positive in 4 of the 6 tumors that lacked any sst receptors. No significant association of SRIF expression with any particular sst type was observed. Likewise a comparison of sst expression with clinical or pathological parameters revealed no significant correlation with sex, age, family history, tumor size or stage, clinical evolution, or outcome. In addition SRIF expression was not significantly associated with a favourable prognosis.

Discussion

The present study represents the first immunohistochemical localization of all 5 sst receptors in human MCT. We show that 85% of tumors express sst receptors, which are localized to both

tumor cells as well as surrounding peritumoral structures especially blood vessels. Two thirds of the tumors express more than one sst subtype and half the tumors are also positive for SRIF. sst5, sst1, sst3 and sst2 are frequently expressed subtypes occurring in 40-60% of tumors whereas sst4 is virtually undetectable.

To date, sst expression in MCT has been evaluated by binding assays using non-selective radioligands such as [^{125}I]LTT SRIF-28 (which binds all 5 sst subtypes) and [^{125}I] Tyr^{3}-octreotide (which binds sst2, 3, 5 but not sst1 and sst4) or by RT-PCR and *in situ* hybridization which detects sst mRNA but not sst-protein (Reubi *et al.*, 1987; Reubi *et al.*, 1991; Mato *et al.*, 1998; Reubi *et al.*, 1994). Furthermore with the possible exception of *in situ* hybridization, none of these procedures can map the cellular distribution of the various sst subtypes. Immunohistochemistry thus is clearly the method of choice for characterizing sst subtype expression in MCT and other tumors, but is dependent on the availability of specific antireceptor antibodies. Several groups have now produced polyclonal antibodies to one or more sst subtypes and used them successfully in immunocytochemistry (Kumar *et al.*, 1999; Patel *et al.*, 1994; Hunyady *et al.*, 1997; Helboe *et al.*, 1997; Schindler *et al.*, 1997; Janson *et al.*, 1998; Khare *et al.*, 1999). Our panel of antibodies against all 5 sst subtypes has been validated by western blots and used successfully to localize sst1-5 antigens at cellular and subcellular levels by fluorescence or peroxidase immunocytochemistry in human ilets, rat pituitary and aorta, in tumor cell lines, and in cells transfected with sst genes (Kumar *et al.*, 1999; Patel *et al.*, 1994; Kumar *et al.*, 1997; Khare *et al.*, 1999).

Because our study was carried retrospectively on fixed paraffin embedded tissue which is not optimal for mRNA analysis, and because of the limited availability of matching frozen specimens of MCT tumors, it was not possible to analyse sst expression at both protein and mRNA levels in this series. However a recent report by Mato et al described the pattern of expression of sst1-5 mRNA by RT-PCR in 14 MCT tumors and found expression of sst1, 2, 3 and 5 in 28%, 79%, 36% and 64% of cases respectively, whereas sst4 was absent (Mato *et al.*, 1998). Except for a slightly higher incidence of sst1 and a lower incidence of sst2, our results generally show good agreement suggesting that sst mRNA in these tumors can serve as an index of sst protein expression. 65% of

the tumors in our series were positive for one or more of the sst subtypes 2, 3, 5 which binds to octreotide. This is in close agreement with the results of somatostatin receptor scanning in patients with MCT using Indium-octreotide which has shown positive tumor uptake in 58-72% of cases (Lamberts *et al.*, 1991; Kwekkeboom *et al.*, 1993; Kurtaran *et al.*, 1996; Obyrne *et al.*, 1996; Behr *et al.*, 1997;Tisell *et al.*, 1997). Four of the tumors in our series expressed solely the sst1 subtype which would not be detected by receptor scans using octreotide-based radionuclides. Furthermore sst1 was an abundant subtype in half the tumors where it was expressed with additional subtypes. This means that the sensitivity of current somatostatin receptor scans could be improved with radio-ligands with a broader specificity to include sst1 in addition to sst2, 3, 5. Besides MCT, cell lines derived from papillary, follicular and anaplastic thyroid carcinoma have been reported to show sst mRNA expression as analysed by RT-PCR (Ain *et al.*, 1997). However the pattern of sst subtype expression is different from that in MCT with preferential expression of subtypes 3 and 5, weak expression of sst1 and sst2 and virtual absence sst4.

Although SRIF is a normal constituent of a subset of calcitonin producing cells, the peptide has been variably localized in MCT tumors. For instance Pacini et al detected SRIF by immunohistochemistry in 63% of tumors and correlated its expression with a favourable prognosis (Pacini *et al.*, 1991). Mato et al localized SRIF immunoreactivity in all of the 14 MCT cases, whereas Kwekkeboom *et al* localized the peptide by immunohistochemistry in only 1 of 8 tumors (Kwekkeboom *et al.*, 1993; Mato *et al.*, 1998). In our series 50% of cases displayed SRIF immunoreactivity in a small percentage of the neoplastic cell population. The majority of these cases were also positive for at least one sst subtype suggesting that endogenous sst interacts with its own receptors through paracrine/autocrine circuits. Contrary to the results of Pacini *et al* (1991) we found no correlation between SRIF immunoreactivity and the clinical outcome of MCT and were unable to confirm the reported beneficial prognostic influence of SRIF expression.

Comparison of sst expression with clinical and pathological parameters revealed no correlation with age, sex, tumor size or stage. Likewise the histological type or the clinical outcome showed no relationship to any given sst subtype in agreement with the findings of Reubi *et al* (Reubi

et al., 1991). Simultaneous analysis of primary tumor and lymph node metastases in a small number of cases revealed a similar pattern of sst immunoreactivity indicating that sst expression is not modified in the course of disease progression. With respect to tumor grade, an earlier report (Reubi *et al.*, 1991) found the presence of SRIF binding sites to be associated with well differentiated MCT. We could not confirm that sst expression was more common in differentiated tumors as opposed to diffusely growing solid and necrotic tumors. This could be because grading of MCT tumors is difficult and not as reliable as for other types of cancers.

Within the normal thyroid gland, C-cells are presumed targets of SRIF action and are likely to be sst positive since administration of SRIF has been shown to inhibit calcitonin secretion (Linehan *et al.*, 1979). We could not identify sst immunostaining of any normal C-cells in those sections in which there was sufficient peritumoral tissue for analysis. Although normal thyroid cells were reported by Ain *et al* (1997) to express sst3 and sst5 mRNA by RT-PCR, normal thyroid follicles were unreactive by immunohistochemistry in the present study. The peritumoral structures that were positively labelled by sst antisera were smooth muscle cells in the media of blood vessels which stained diffusely with anti-sst1 and sst2 antibodies and focally by anti-sst3 and sst5.

In conclusion, we have shown that like other neuroendocrine tumors, MCT is rich in sst receptors which were demonstrated by immunohistochemistry in 85% of tumor samples studied. Receptor types 1, 2, 3, and 5 are the predominant isoforms expressed, whereas sst4 is virtually absent. 70% of the tumors express more than one sst subtype and 50% coexpress SRIF suggesting tumor cell regulation by endogenous SRIF via paracrine/autocrine circuits. Immunohistochemical typing of sst receptor expression using specific antireceptor antibodies represents an ideal approach for characterizing sst subtype expression in MCT for optimising receptor targeted diagnosis and therapy with SRIF analogues.

Acknowledgements

We are grateful to Professor G. Bussolati (University of Turin) for his suggestions and to Mr. A. Grua for the photomicrographs. This work was supported by grants from the Italian Ministry of

University and Research, Rome ("60%" to M.P.), from the Regione Piemonte, Turin (grant no. 165 of Health Research Project DGR 34-23230 to M.P.) and by grants from the Medical Research Council of Canada (MT-10411), and the NIH (NS32160-05) to Y.C.P.

References

Ain, K.B., Taylor, K.D., Tofiq, S., Venkataraman, G. (1997) Somatostatin receptor subtype expression in human thyroid and thyroid carcinoma cell lines. *Journal of Clinical Endocrinology and Metabolism,* **82**, 1857-1862.

Behr, T.M., Gratz, S., Markus, P.M., Dunn, R.M., Hufner, M., Schauer, A., Fischer, M., Munz, D.L., Becker, H., Becker, W. (1997) Anti-carcinoembryonic antigen antibodies versus somatostatin analogs in the detection of metastatic medullary thyroid carcinoma. *Cancer*, **80**, 2436-2457.

Helboe, L., Moller, M., Norregaard, L., Schiodt, M., Stidsen, C.E. (1997) Development of selective antibodies against the human somatostatin receptor subtypes sst1-sst5. *Molecular Brain Research,* **49,** 82-88.

Hunyady, B., Hipkin, R.W., Schonbrunn, A., Mezey, E. (1997) Immunohistochemical localization of somatostatin receptor SSTR2A in the rat pancreas. *Endocrinology,* **138**, 2632-2635.

Janson, E.T., Stridsberg, M., Gobl, A., Westlin, J.E., Oberg, K. (1998) Determination of somatostatin receptor subtype 2 in carcinoid tumors by immunohistochemical investigation with somatostatin receptor subtype 2 antibodies. *Cancer Research,* **58**, 2375-2378.

Khare, S., Kumar, U., Sasi, R., Puebla, L., Calderon, L., Lemstrom, K., Hayry, P., and Patel, Y.C. (1999) Differential regulation of somatostatin receptor types 1-5 in rat aorta after angioplasty. *FASEB Journal*, **13**, 387-394.

Kumar, U., Laird, D., Srikant, C.B., Escher, E., Patel, Y.C. (1997) Expression of the five somatostatin receptor (SSTR1-5) subtypes in rat pituitary somatotrophes: quantitative analysis by double-label immunofluorescence confocal microscopy. *Endocrinology*, **138,** 4473-4476.

Kumar, U., Sasi, R., Suresh, S., Patel, A., Thangaraju, M., Metrakos, P., Patel, S.C., and Patel, Y.C. (1999) Subtype-selective expression of the five somatostatin receptors (hSSTR1-5) in human pancreatic islet cells. *Diabetes*, **48**, 77-85.

Kurtaran, A., Leimer, M., Kaserer, K., Yang, Q., Angelberger, P., Niederle, B., Virgolini, I. (1996) Combined Use of ^{111}In-DTPA-D-Phe-1-Octreotide (OCT) and ^{123}I-Vasoactive intestinal peptide (VIP) in the localization diagnosis of medullary thyroid carcinoma (MTC). *Nuclear*

Medicine & Biology, **23**, 503-507.

Kwekkeboom, D.J., Reubi, J.C., Lamberts, S.W.J., Bruining, H.A., Mulder, A.H., Oei, H.Y., Krenning, E.P. (1993) *In Vivo* somatostatin receptor immaging in medullary thyroid carcinoma. *Journal of Clinical Endocrinology & Metabolism*, **76**, 1413-1417.

Lamberts, S.W.J., Krenning, E.P., Reubi, J.C. (1991) The role of somatostatin and its analogs on the diagnosis and treatment of tumors. *Endocrine Reviews*, **12,** 450-482.

Linehan, W.M., Cooper, C.W., Bolman, R.M. III, Wells, S.A. Jr. (1979) Inhibiton of *in vivo* secretion of calcitonin in the pig by somatostatin. *Endocrinology,* **104**, 1602-1607.

Mato, E., Matias-Guiu, X., Chico, A., Webb, S.M., Cabezas, R., Berna, L., De Leiva, A. (1998) Somatostatin and somatostatin receptor subtype gene expression in medullary thyroid carcinoma. *Journal of Clinical Endocrinology and Metabolism,* **83**, 2417-2420.

Obyrne, K.J., Ohare, N., Sweeney, E., Freyne, P.J., Cullen, M.J. (1996) Somatostatin and somatostatin analogues in medullary thyroid carcinoma. *Nuclear Medicine Communications,* **17,** 810-816.

Pacini, F., Basolo, F., Elisei, R., Fugazzola, L., Cola, A., Pinchera, A. (1991) Medullary thyroid cancer. An immunohistochemical and humoral study using six separate antigens. *American Journal of Clinical Pathology,* **95**, 300-308.

Papotti, M., Sambataro, D., Pecchioni, C., Bussolati, G. (1996) The pathology of medullary carcinoma of the thyroid: review of the literature and personal experience on 62 cases. *Endocrine Pathology,* **7,** 1-20.

Patel, Y.C. (1997) Molecular pharmacology of somatostatin receptor subtypes. *Journal of Endocrinological Investigation,* **20**, 348-367.

Patel, Y.C. (1999) Somatostatin and its receptor family. *Frontiers in Neuroendocrinology,* **20**, 157-198.

Patel, Y.C., Panetta, R., Escher, E., Greenwood, M., Srikant, C.B. (1994) Expression of multiple somatostatin receptor genes in AtT-20 cells. *Journal of Biological Chemistry*, **269**, 1506-1509.

Reichlin, S. (1983) Somatostatin. *New England Journal of Medicine,* **309,** 1495-1501, 1556-1563.

Reubi, J.C., Chayvialle, J.A., Franc, B., Cohen, R., Calmettes, C., Modigliani, E. (1991) Somatostatin receptors and somatostatin content in medullary thyroid carcinomas. *Laboratory*

Investigation, **64**, 567-573.

Reubi, J.C., Maurer, R., von Verder, K., Torhorst, J., Klijn, J.C.M., Lamberts, S.W.J. (1987) Somatostatin receptors in human endocrine tumors. *Cancer Research*, **47**, 551-558.

Reubi, J.C., Schaer, J.C., Waser, B., Mengod, G. (1994) Expression and localization of somatostatin receptor SSTR1, SSTR2, and SSTR3 messenger RNAs in primary human tumors using *in situ* hybridization. *Cancer Research,* **54**, 3455-3459.

Saad, M.F., Ordonez, N.G., Rashid, R.K., Guido, J.J., Hill, C.S. Jr., Hickey, R.C., Samaan, N.A. (1984) Medullary carcinoma of the thyroid. *Medicine,* **63**, 319-342.

Schindler, M., Sellers, L.A., Humphrey, P.P., Emson, P.C. (1997) Immunohistochemical localization of the somatostatin SST2(A) receptor in the rat brain and spinal cord. *Neuroscience,* **76**, 225-240.

Schroder, S., Holl, K., Padberg, B.C. (1992) Pathology of sporadic and hereditary medullary thyroid carcinoma. *Recent Results Cancer Research*, **125**, 19-45.

Tisell, L.E., Ahlman, B., Wangberg, B., Hansson, G., Molne, J., Nilsson, O., Lindstedt, G., Fjalling, M., Forsell-Aronsson, E. (1997) Somatostatin receptor scintigraphy in medullary thyroid carcinoma. *British Journal of Surgery*, **84**, 543-547.

Van Noorden, S., Polak, J.M., Pearse, A.G.E. (1977) Single cellular origin of somatostatin and celcitonin in the rat thyroid gland. *Histochemistry*, **53**, 243-7.

Yamada, Y., Ito, S., Matsubara, Y., Kobayashi, S. (1977) Immunohistochemical demonstration of somatostatin-containing cells in the human, dog and rat thyroid. *Tohoku Journal of Experimental Medicine*, **122**, 87-92.

FIGURE LEGENDS

FIGURE 1. Representative sections of medullary thyroid carcinoma illustrating pattern of expression of sst protein. sst immunostaining was predominantly localized to the plasma membrane but was also variably observed in the cytoplasm. **(a)** case 7 - Nests of polygonal tumor cells positive for sst1 at both membrane (arrowheads) and cytoplasmic levels. **(b)** case 19 - sst2 immunostaining appears mainly membranous in several tumor cells (arrow heads), while normal thyroid follicles are negative (arrow). **(c)** case 19 - the specificity of anti-sst2 antibody is demonstrated by negative staining of the same tumor region as in b immunostained with the antiserum preadsorbed with the immunizing peptide. **(d,e)** case 40 - cytoplasmic staining with occasional membrane reinforcement is characteristic of sst3 (arrow heads); capillary endothelial cells are also reactive (arrows) **(f)**; The same tumor area as in d,e shows no reaction using preimmune rabbit serum. **(g-j)** case 40 - sst5 expression in this case shows preferential membrane localization (g,i) (arrowheads); control sections reacted with preimmune serum show no staining **(h)**; neural thyroid thyroid follicles appear to be unreactive **(j)**. Sections were processed for peroxidase immunocytochemistry and lightly counterstained with haemalum **(a-d, f-h)**; 400 x **e, i, j**.

FIGURE 2: Sections of medullary thyroid carcinoma (case 38, 42) analysed for simultaneous expression of sst receptors and somatostatin (SRIF). **a-d.** Polygonal tumor cells in the same tumor showing variable cytoplasmic and/or membranes (arrows) staining for sst1 **(a)**, sst2 **(b)**, sst3 **(c)**, and sst5 **(d)**. sst4 was negative in both tumors (not shown). **e,f** In the same tumor area, a weak positivity for sst2 **(e)** is associated with the presence of SRIF (arrows) **(f)**. **g,h** Case 42 illustrating diffuse localization of sst3 **(g)** in a tumor area also displaying intense focal expression of SRIF (arrows) **(h)**. Sections were processed for peroxidase immunocytochemistry and lightly counterstained with haemalum. **(a-d, 1000 x); (e & f, 200 x); (g & h, 400 x)**.

Table 1

N°	Sex/age	Size (cm)	pTNM	H/S	Rec/mts	Status	SRIF	sst status				
								1	*2*	*3*	*4*	*5*
1	F/60	5	$pT_4N_1M_0$	H		NED 10	-	-	-	+f	-	+f
2	F/36	3	$pT_2N_0M_0$	S		NED 17	-	-	-	+f	-	+f
3	F/71	1.5	$pT_2N_0M_0$	S		DOC 12	-	-	+f	-	-	-
4	F/64	5	$pT_3N_0M_0$	S		NED 12	-	+f	-	+f	-	+f
5	F/51	3.5	$pT_2N_0M_0$	S		NED 5	-	-	-	-	-	-
6	M/20	3.5	$pT_2N_0M_0$	S		lost	-	-	-	-	-	+d
7	M/68	2.5	$pT_2N_1M_0$	S	med, ln, bone	DOD 8	-	+d	+d	-	-	-
8	F/46	3.5	$pT_2N_0M_0$	S		NED 7	+	+d	+f	-	-	+f
9	F/28	2	$pT_{2b}N_0M_0$	H		NED 6	-	+d	+f	-	-	+f
10	M/27	3	$pT_{2b}N_0M_0$	H		NED 15	-	+d	-	-	-	-
11	F/20	4.5	$pT_{3b}N_1M_0$	S	trachea, lung	AWD 5	-	+f	-	-	-	-
12	M/47	0.5	$pT_{1b}N_1M_0$	S	local	AWD 5	-	+d	-	-	-	-
13	F/64	3	$pT_2N_1M_0$	S	trachea, lung	AWD 4	+	+d	+d	+f	+d	+d
14	F/33	2	$pT_2N_0M_0$	S		NED 4	+	-	-	-	-	-
15	F/55	1.5	$pT_{2b}N_1M_0$	S	med, ln	DOD 2	+	-	-	+f	-	+f
16	M/74	2	$pT_2N_0M_0$	S		DOD 1	+	-	-	+d	-	+d
17	F/50	3.5	$pT_2N_0M_0$	S		NED 3	+	-	+d	-	-	+d
18	F/60	1.5	$pT_3N_0M_0$	S		lost	-	-	-	+d	-	+d
19	M/58	5	$pT_3N_1M_0$	S		DOD 11	-	+d	+d	+d	-	+d
20	M/28	0.7	$pT_1N_1M_0$	S		AWD 1	-	-	-	-	-	+f
21	M/32	0.7	$pT_{1b}N_1M_0$	H	local	AWD 1	-	+f	-	-	-	-
22	F/51	5	$pT_4N_1M_1$	S	lung	AWD 2.3	+	+d	+f	-	-	-
23	M/16	2.5	$pT_{4b}N_1M_0$	H		AWD 2	+	+f	-	+d	-	-
24	M/29	4	$pT_2N_0M_0$	S		AWD 12	-	+d	+f	+d	-	-
25	M/27	4	$pT_2N_1M_0$	S		lost	+	-	-	+d	-	+d
26	F/68	6	$pT_3N_0M_0$	S		POD	+	-	-	-	-	-
27	F/70	2	$pT_3N_1M_0$	S		NED 4	+	+d	+d	-	-	+f
28	M/75	4	$pT_2N_xM_1$	S	bone	DOD 4	+	+d	+d	+f	+d	+d
29	F/68	20	$pT_3N_0M_0$	S		POD	-	-	-	-	-	-
30	M/68	4	$pT_2N_1M_0$	S		NED 1	+	+d	-	-	-	+d
31	F/62	2	$pT_2N_0M_0$	S		NED 8	-	-	-	+d	-	+d
32	M/55	n.a.	n.a.	S		NED 5	+	+f	+f	-	-	+d
33	F/53	5	$pT_3N_1M_0$	S		DOD 8	+	+d	+f	-	-	+f
34	F/47	2.5	$pT_2N_0M_0$	S		NED 2	+	+d	+f	-	-	-
35	F/55	2.1	$pT_2N_xM_0$	S		NED 4	-	+d	-	+d	-	+f
36	M/31	2.5	$pT_2N_1M_1$	S	ln, bone, liver	DOD 2	+	+d	-	+f	-	-
37	F/68	1.7	$pT_2N_1M_0$	H		NED 1.5	-	+f	+d	-	-	-
38	F/47	1.8	$pT_2N_0M_0$	S		NED 2.5	+	-	+d	-	-	-
39	F/36	3.3	$pT_2N_0M_0$	H	liver	AWD 27	+	-	-	+d	-	+d
40	M/62	5	$pT_3N_1M_0$	S		DOD 7	+	-	+f	+d	-	+d
41	F/34	4	$pT_2N_xM_0$	S		lost	-	+f	+d	+d	-	+d
42	F/44	3	$pT_2N_1M_0$	S		AWD 5	+	+d	+d	+d	-	+d
43	M/77	8	$pT_{3b}N_0M_0$	S		NED 1.5	-	-	-	-	-	-
44	M/23	3.3	$PT_2N_1M_0$	S	ln, local	NED 1	+	+d	+d	+d	-	+d
45	M/83	0.3	$pT_1N_1M_0$	S		NED 1	-	-	-	-	-	-
46	M/59	4	$pT_2N_0M_0$	S		NED 1	+	-	-	-	-	-
47	F/46	2	$pT_2N_1M_0$	S		NED 1	+	+d	-	+d	-	+d
48	F/48	0.8	$pT_1N_xM_0$	S		lost	-	+d	+f	+d	-	+d
49	F/48	1.7	$pT_2N_1M_0$	S		NED 2	-	-	-	+d	-	+d
50	F/28	2	$pT_2N_1M_0$	H		AWD 1.2	+	-	-	-	-	-
51	F/32	2.5	$pT_2N_1M_0$	S	med, bone, liver, ln	AWD 2	-	-	+f	+d	-	-

Abbreviations. pTNM: pathological staging; H: hereditary; S: sporadic; Rec: recurrences; mts: metastases; SRIF: somatostatin; sst: somatostatin receptors; n.a.: not available; med: mediastinum; ln: lymph node; NED: no evidence of disease; DOD: died of disease; DOC: died of other causes; AWD: alive with disease; POD: post-operatve death; d: diffuse (20-80%); f: focal (5-20%).

TABLE 2

Immunohistochemical Detection of SRIF and sst1-5 in 51 Medullary Carcinomas of the Thyroid

Antigen	No. Positive	% Positive
SRIF	25/51	49%
sst1	25/51	49%
sst2	22/51	43%
sst3	24/51	47%
sst4	2/51	4%
sst5	29/51	57%
SRIF + sst*	21/51	41%

Abbreviations: SRIF, somatostatin; sst, somatostatin receptor; *, at least one sst subtype coexpressed with somatostatin.

would yield proteins of 13, 11, or 6 kD. Proteins of 11 and 6 kD size are seen by Western blot; Bax N-terminal antibodies detected no protein, consistent with an alternate translation start. BAXζwas TA-cloned into a vector containing Lac promoter; 100% of colonies contained insert in antisense orientation, suggesting BAXζmay select against E.coli growth. Evidence that BAXζpromotes cell death includes (1) stable transfectants could not be established and (2) increased cell death followed transient transfection of A2780 and Cos-7 cell lines. Confocal microscopy data on co-localization of a BAXζ-GFP (Green Fluorescent Protein) fusion construct with MitoTracker Red dye and with BAXα-fusion protein are pending. Thus, BAXζpromotes cell death despite absence of the BH3 domain; its cellular localization and potential interactions with Baxαremain to be defined (Support:ACS RPG9806101-CCE).

#982 PORE-FORMING ABILITY OF CLEAVED BCL-2 RELEASES HEMOGLOBIN FROM SHEEP RED BLOOD CELLS. Catheryne Chen, and B. Chen, *Wayne State Sch of Medicine, Detroit, MI*

Bcl-2 family proteins are thought to control the opening of the permeability pore on mitochondria and facilitate the release of cytochrome c. We showed recently that Z-LLL-CHO, a reversible proteasome inhibitor, is a potent inducer of apoptosis in human THP-1 leukemia cells. Apoptosis induced by Z-LLL-CHO is mediated through a cytochrome c-dependent pathway, which results in the activation of caspase-9 and -3 and the cleavage of mitochondrial Bcl-2 into a shortened fragment, Bcl-2/Δ34. The role of Bcl-2/Δ34 fragment in regulating cytochrome c release was investigated. Results from cell fractionation and immunoblot analyses showed that Bcl-2 and Bcl-2/Δ34 are located on the mitochondria of THP-1 cells. Treatment of isolated mitochondria with recombinant caspase-3 induced the same cleavage of Bcl-2 *in vitro* and caused the release of cytochrome c from mitochondria. The pore-forming ability of Bcl-2/Δ34 was examined using sheep red blood cells (RBC) with *in vitro* translated Bcl-2/Δ34. Bcl-2/Δ34 fragment protein, generated from *in vitro* translation, was relocated rapidly to sheep RBC and, in the presence of anti-Bcl-2 antibodies, triggered a rapid release of hemoglobin from RBC. Treatment of sheep RBC with anti-Bcl-2 antibodies alone did not trigger hemoglobin release. Our results suggest that, upon "enforced dimerization," Bcl-2/Δ34 fragment can form pores in membranes and contribute to the release of cytochrome c in apoptosis.

#983 PROTEASOME-MEDIATED DOWNREGULATION OF PHOSPHORYLATED BCL2 -A KEY REGULATOR FOR ANTI-APOPTOTIC FUNCTION OF NATIVE BCL2? Aruna Basu, Sun Ah You, and Subrata Haldar, *Ireland Cancer Ctr, Metro Health/ Case Western Reserve Univ, Cleveland, OH, and Rammelkamp Ctr For Edu & Res*

The oncogene derived protein Bcl2 and its family members such as Bcl-xL, Mcl-1 can confer negative control in the pathway of cellular suicide machinery. The reversible phosphorylation of the components in the apoptotic-signaling pathway is likely to be an important regulatory mechanism to control the fate of a cell. Phosphorylation of anti -apoptotic proteins such as Bcl2, Bcl-xL or Mcl-1 can regulate their function depending on the apoptotic trigger or cell type. Studies reported here document the ability of cantharidin, a highly potent Group 2A phosphatase (PP2A) inhibitor to trigger phosphorylation of Bcl2 in a panel of cancer cells. Due to cantharidin exposure, phosphorylated Bcl2 is either cleaved to a 22 kDa fragment or completely down regulated depending on cell type. Interestingly, by site directed mutagenesis, we confirm that Bcl2 phosphorylation precedes its cleavage. Further studies reveal that degradation of phospho Bcl2 is mediated by proteasomes. Proteasome -mediated phospho Bcl2 cleavage predominantly occurs at G0-G1-S phase of cell cycle. Interestingly, while accumulation of phosphoforms of Bcl2 promotes death advantage to cancer cells, its downregulation by proteasome might render native Bcl2 (non phospho forms) to exert anti-apoptotic function.

#984 GENOMIC ORGANIZATION AND EVOLUTIONARY CONSERVATION OF MCL-1, AN ANTIAPOPTOTIC BCL-2 FAMILY GENE. Chandra P Leo, S. Y Hsu, and A. J W Hsueh, *Stanford Univ Med Ctr, Stanford, CA, and Univ of Leipzig, Leipzig, Germany*

Mcl-1 (Myeloid cell leukemia-1) is an antiapoptotic member of the Bcl-2 family and has been implicated in the pathobiology of different human neoplasms. In the present study, we determined the genomic organization of the human Mcl-1 locus and identified two previously unknown Mcl-1 orthologs. The human Mcl-1 protein is encoded by three exons, separated by two introns of 0.35 kbp and >1.0 kbp size, respectively. We compared the genomic structure of Mcl-1 with that of other mammalian Bcl-2-related genes. This analysis revealed that the localization of introns with respect to nucleotide sequences encoding the functionally critical BH (Bcl-2 homology),) domains is partially conserved between Mcl-1 and other antiapoptotic Bcl-2 family members. These findings suggest their possible derivation from a common evolutionary ancestor. In order to further explore the evolution of the Mcl-1 gene, we searched for novel Mcl-1 orthologs in other species. By performing yeast-two hybrid screenings and homology searches in public databases, we identified two previously unknown Mcl-1-homologous cDNA sequences in rat and zebrafish. The deduced rat Mcl-1 amino acid sequence is 78% identical with the human Mcl-1 protein, including a complete conservation of the Bcl-2 homology domains BH1, BH2 and BH3 as well as the transmembrane region. The zebrafish sequence represents the first Bcl-2 family gene described in teleosts, its closest homolog among mammalian Bcl-2 family members being Mcl-1. A comprehensive analysis of the new Mcl-1 homolog those in other species showed a number of universally conserved residue may therefore lead to the identification of new structural features important fo function of Mcl-1.

#985 A ROLE FOR PROTEIN KINASE C IN PHOSPHORYLATION INACTIVATION OF THE DEATH AGONIST BAD. Xianjun Fang, Shuangxin and Gordon B Mills, *MD Anderson Cancer Ctr, Houston, TX*

BAD, a distant member of the Bcl-2 family, exerts its proapoptotic e through forming heterodimer with Bcl-2 and Bcl-X_L. The function of BA regulated, in part, by phosphorylation of Serine-112 (S-112) and Serine (S-136). Phosphorylation at either site induces dissociation of BAD from Bcl-2 Bcl-X_L and translocation to the cytosol where it binds to 14-3-3. A numb signaling molecules including Akt/PKB, PKA and MAPK have been implicate BAD phosphorylation. Here we describe an essential role for protein kina (PKC) activity in the regulation of BAD phosphorylation. In HEK 293 and 3T3 c phosphorylation of BAD at S-112 and S-136 is differentially stimulated by gr or survival factors, suggesting that multiple signaling pathways are involved ir regulation of BAD phosphorylation. Growth/survival factor-induced phospho tion of BAD, particularly at the S-112 site, is highly sensitive to PKC inhibi Bisindolymaleimide I and Ro-31-8220. Activation of PKC by treatment of cult cells with TPA is sufficient to induce BAD phosphorylation at both sites, pa ularly at S-112. A mutant platelet-derived growth factor receptor that retains ability to activate the PLC-PKC signaling pathway, with all other known signa functions inactivated, retains the ability to stimulate BAD phosphorylatio S-112. Furthermore, PKC inhibitors enhance BAD-induced apoptosis in tr fected cells. These results collectively indicate a role for PKC in phosphoryla and function of the death molecule BAD.

#986 BCL-XS INDUCES CYTOCHROME C RELEASE, REDISTRIBUTI OF AIF, AND UNIQUE CHANGES IN CHROMATIN STRUCTURE WITHO CASPASE ACTIVATION IN 3T3 CELLS. Jordan S Fridman, Santos A Su Guido Kroemer, and Jonathan Maybaum, *Ctr National de la Research Scien Villejuif, France, and Univ of Michigan, Ann Arbor, MI*

Expression of bcl-XS in 3T3 cells (using a tetracycline-regulated retro expression system) induces cell death without requiring or activating caspas Upon expression of bcl-XS the mitochondria lose their membrane potential (ΔΨ and the cristae swell, becoming unfolded and disorganized. Furthermore, c chrome c is released into the cytosol (without detectable caspase activation) a the mitochondrial intra-membrane protein AIF (apoptosis inducing factor) rel tributes in the cell, but not into the nucleus. Even in the absence of AIF entry i the nucleus, the nuclear chromatin (upon expression of bcl-XS) condenses in large clumps but does not form organized crescents about the nuclear periphe as is the case upon induction of caspases and apoptosis by addition of anti-F antibody and actinomycin D. These changes in chromatin structure also oc without detectable cleavage of DFF45/ICAD. This cell death pathway is unique that a pro-death bcl-2 family member kills without induction of caspases (up release of cytochrome c) and with morphological changes to the nucleus that a unique from caspase-mediated changes in Fas/Act D treated cells. These alt ations are not accounted for by activation of DFF40/CAD (by cleavage of DFF-ICAD) or by translocation of AIF to the nucleus and may represent a no pathway of programmed cell death.

#987 SHP-1-DEPENDENT, CASPASE-8-MEDIATED, ACIDIFICATION AN APOPTOSIS ARE NOT DEPENDENT ON MITOCHONDRIAL DYSFUNCTIO Danni Liu, Giovanni Martino, Muthusamy Thangaraju, Monika Sharma, Faw Halwani, Shi-Hsiang Shen, Yogesh C Patel, and Coimbatore B Srikant, *Mayo C & Fdn, Rochester, MN, McGill Univ, Montreal, PQ, Canada, McGill Univ and Rc Victoria Hosp, Montreal, PQ, Canada, and NRC Biotech Res Institute, Montre PQ, Canada*

Activation of initiator and effector caspases, and mitochondrial changes th involve a reduction in its membrane potential and release of cytochrome c (cyt into the cytosol, are characteristic features of apoptosis. These changes a associated with cell acidification in some models of apoptosis. The hierarchic relationship between the activation of the initiator and effector caspases, mit chondrial dysfunction and acidification has, however, not been deciphered. W have shown that somatostatin (SST), acting via the src homology 2 bear tyrosine phosphatase SHP-1, induces acidification and apoptosis in HTB- clone of MCF-7 cells (Thangaraju et al., J. Biol. Chem.274: 29549-29555, 199 We have now invetigated the temporal sequence of apoptotic events link caspase activation, acidification and mitochondrial dysfunction and the effects the proton ionophore nigericin-induced pH clamping and cell permeable ta rapeptide aldehyde inhibitors of specific caspases in this system. We report ha that (i) SHP-1-mediated caspase-8 activation is required for intracellular acid cation.(ii) decrease in pH is necessary for the activation of the effector caspase (iii) the reduction in mitochondrial membrane potential, cyt c release a caspase-9 activation occur distal to SST-induced acidification, and (iv) depleti of ATP ablates SST-induced cyt c release and caspase-9 activation, but not ability to induce effector caspases and apoptosis. These data reveal that SH 1-/caspase-8-mediated acidification occurs at a site other than the mitocho drion and that SST-induced apoptosis is not dependent on the disruption mitochondrial function and caspase-9 activation.

DEPARTMENT OF DEFENSE BREAST CANCER RESEARCH PROGRAM MEETING:
ERA OF HOPE, Atlanta, Georgia, June 8-12, 2000

APOPTOTIC SIGNALLING BY SOMATOSTATIN RECEPTOR TYPE 3 (SSTR3) REQUIRES MOLECULAR SIGNALS IN THE RECEPTOR C-TAIL

Y.C. Patel, M. Rocheville, L. Seeman, R. Sasi, C.B. Srikant, S. Khare, M. Chan, and U. Kumar

Fraser Laboratories, Departments of Medicine and Neurology and Neurosurgery, Royal Victoria Hospital and Montreal Neurological Institute, Montreal, Quebec H3A 1A1

yogesh.patel@muhc.mcgill.ca

Somatostatin (SST) acts through five G protein coupled receptors (SSTR1-5) to inhibit proliferation of normal and tumor cells. Breast cancers are rich in SSTRs and may be amenable to treatment with selective SST compounds. In 98 primary ductal NOS tumors, we found expression of mRNA for SSTR1,2,3,4,5 by RT-PCR in 91%, 96%, 98%, 76%, and 54% respectively. In CHO cells individually transfected with SSTR1-5, we have previously reported that activation of SSTR1,2,4,5 induces cell cycle arrest (SSTR5 > 2 > 4 > 1) whereas SSTR3 uniquely triggers apoptosis. Complementary experiments to test the effect of antisense blockade of individual endogenous SSTRs on cell proliferation of MCF7 cells (which express SSTR1,2,3,5) confirmed the relatively high potency of SSTR3 and SSTR5 in inducing antiproliferation. Treatment with selective nonpeptide agonists for SSTR1-5 (provided by Merck) documented the potent effect of the SSTR3 selective agonist L-796778 in inducing apoptosis. To characterize the structural determinants of SSTR3-dependent apoptosis, we conducted mutational analysis of the role of the cytoplasmic C-tail of hSSTR3 in inducing apoptosis with the following mutants: (i) deletion of the hSSTR3 C-tail (ΔC-tail); (ii) introduction of a palmitoylation motif in hSSTR3 C-tail (P6). SSTR3 is the only SSTR whose C-tail does not possess a palmitoylation anchor shown in other receptors to be important in receptor function; (iii) chimeric hSSTR3/hSSTR5 receptor substituting the C-tail domain of hSSTR3 with that of hSSTR5 (C4). Wild type (wt) and mutant SSTR3 were stably expressed in HEK cells cultured with or without SST-14 (1 μM). Cell numbers and apoptosis were monitored by MTT and TUNEL assays respectively. Compared to nontransfected HEK cells, wt hSSTR3 cells treated with SST-14 showed 56 ± 8% inhibition of cell growth at day 4. The ΔC-tail and P6 mutants displayed marked attenuation of the ability to inhibit SST-14-induced cell growth (39 ± 12% and 27 ± 8% respectively of the maximum response of wt hSSTR3). Deletion of the C-tail of hSSTR3 (Δ C-tail) or substitution of hSSTR3 C-tail with that of hSSTR5 (C4) abrogated the cytotoxic property of hSSTR3. Conclusions: SST inhibits proliferation of breast tumor cells via multiple SSTRs. SSTR3 and SSTR5 are the principal antiproliferative subtypes and differentially induce apoptosis (SSTR3) or cytostasis (SSTR5). Apoptotic signalling by SSTR3 requires molecular signals in the receptor C-tail.

The U.S. Army Medical Research and Material Command under DAMD17-96-1-6189 supported this work.

DEPARTMENT OF DEFENSE BREAST CANCER RESEARCH PROGRAM MEETING:
ERA OF HOPE, Atlanta, Georgia, June 8-12, 2000

hSSTR SUBTYPE-SELECTIVITY FOR CYTOTOXIC AND CYTOSTATIC ANTIPROLIFERATIVE SIGNALING

C.B. Srikant, K. Sharma, M. Thangaraju, D. Liu, Y.C. Patel and S-H. Shen

Fraser Laboratories, Department of Medicine, McGill University and
Royal Victoria Hospital, Montreal, Quebec, Canada H3A 1A1

* mdcs@musica.mcgill.ca

Somatostatin (SST) is a pluripotent hormone that regulates cell proliferation not only by suppressing the secretion of mitogenic hormones but also by inhibiting their actions. SST analogs exert cytotoxic action and induce apoptosis in estrogen-sensitive, but not estrogen-insensitive, breast cancer cells. In tumors arising in other sites such as the pituitary, its growth inhibitory action is cytostatic and elicits cell cycle arrest, but not apoptosis. Such diverse effects may be due to the heterogeneity of expression of the five SST receptors (SSTR) and signaling pathways in tumor cells. Cytostasis, which predominantly triggers G_1 cell cycle arrest, can be caused by the retinoblastoma gene product Rb, the tumor suppressor protein p53 or the proto-oncogene product c-Myc. p53 and c-Myc inhibit cell cycle progression in presence of growth factors, but promote apoptosis in their absence. p53 induced G_1 arrest requires induction of cyclin-dependent kinase inhibitor $p21^{Waf1/Cip1}$ whereas apoptosis requires induction of Bax. In order to define the molecular mediators that regulate cytotoxic and cytostatic actions of SST, we investigated the involvement of these cell cycle modulators in SSTR subtype-selective antiproliferative signaling in CHO-K1 cells stably expressing individual hSSTRs 1-5. Our findings have demonstrated that apoptosis is signaled uniquely through hSSTR3 and is associated with the induction of *wt* p53 and Bax. Induction of *wt* p53 by SST occurs rapidly and precedes the onset of apoptosis, is not associated with induction of $p21^{Waf1/Cip1}$ or c-Myc and does not invoke G_1 arrest. Moreover, hSSTR3-signaled apoptosis was associated with caspase-8-mediated intracellular acidification since prevention of acidification by pH clamping blocked SST-induced apoptosis, but not caspase-8 activation. By contrast, acting via the other four hSSTRs, SST induced Rb in its hypophosphorylated form and triggered G_1 arrest. The relative efficacy of these receptors to initiate cytostatic signaling was hSSTR5>hSSTR2>hSSTR4~hSSTR1. A marginal increase in $p21^{Waf1/Cip1}$ was also observed in hSSTR5 expressing cells. hSSTR3-mediated cytotoxic and hSSTR5-medited cytostatic actions of SST are tyrosine phosphatase SHP-1-mediated suggesting that diversification of subtype-selective signaling occurs distal to SHP-1. C-tail truncation mutants of hSSTR5 displayed progressive loss of antiproliferative signaling proportional to the length of deletion. These novel findings provide a rational basis for exploiting the cytotoxic and cytostatic actions of SSTR subtype-selective agonists in cancer therapy.

The U.S. Army Medical Research and Materiel Command under DAMD17-96-1-6189 supported this work.

Please select Print from the file menu to print your Abstract.

Category: Basic Science; 9. Hormones & Cancer

ENDO 2000 The Endocrine Society 82nd Annual Meeting

Filename: 851226
Abstract Format Type: Regular Abstract Session , Consider for Oral Presentation
Category: Basic Science; 9. Hormones & Cancer
Corresponding Author: Yogesh C. Patel, M.D., Ph.D.
Department/Institution: Fraser Laboratories, Royal Victoria Hospital, Room M3-15
Address: 687 Pine Avenue West, Montreal, Quebec, Canada, H3A 1A1
Phone: (514) 842-1231 ext. 5042 **Fax:** (514) 849-3681 **E-Mail:** yogesh.patel@muhc.mcgill.ca
Award: Travel Grant Award
Keywords: somatostatin, receptors, apoptosis

APOPTOTIC SIGNALLING BY SOMATOSTATIN RECEPTOR TYPE 3 (SSTR3) REQUIRES MOLECULAR SIGNALS IN THE RECEPTOR C-TAIL.

M Rocheville [1]*, U Kumar [1], L Semaan [1], R Sasi [1], C B Srikant [1], S Khare [1], M Chan [1] and Y C Patel [1]. (Sponsored by Yogesh C. Patel) [1]Fraser Laboratories, Dept. of Medicine & Pharmacology and Therapeutics, McGill University & Royal Victoria Hospital, Montreal, Quebec, Canada.

Somatostatin (SST) acts through a family of five G protein coupled receptors (SSTR1-5) to inhibit the proliferation of normal and tumour cells. In CHO-K1 cells individually transfected with SSTR1-5, we have previously reported that activation of SSTR1,2,4,5 induces cell cycle arrest (SSTR5 > 2 > 4 > 1) whereas SSTR3 uniquely triggers apoptosis. Complementary experiments to test the effect of antisense blockade of individual endogenous SSTRs on cell proliferation of MCF7 breast cancer cells (which express SSTR1,2,3,5) confirmed the relatively high potency of SSTR3 and SSTR5 in inducing antiproliferation. Treatment with selective nonpeptide agonists for SSTR1-5 (provided by Merck) documented the potent effect of the SSTR3-selective agonist L-796778 in inducing apoptosis. To characterize the structural determinants of SSTR3-dependent apoptosis, we conducted mutational analysis of the role of the cytoplasmic C-tail of hSSTR3 in inducing apoptosis with the following mutants: (i) deletion of the hSSTR3 C-tail (R3Δ C-tail); (ii) introduction of a palmitoylation motif in hSSTR3 C-tail (Palm R3) . SSTR3 is the only SSTR whose C-tail does not possess a palmitoylation anchor shown in other receptors to be important in receptor function. (iii) Chimeric hSSTR3/hSSTR5 receptor substituting the C-tail domain of hSSTR3 with that of hSSTR5 (R3/R5-C-tail chimera). Wild type (wt) and mutant SSTR3 were stably expressed in HEK cells cultured with or without SST-14 (1 uM). Cell numbers were monitored by MTT assay and apoptosis by TUNEL and HOECHST assays. Like wt hSSTR3, the mutant receptors were functionally coupled to inhibition of adenylyl cyclase measured as dose-dependent inhibition of forskolin-stimulated cAMP by SST-14. Maximum cAMP inhibition at 1 uM SST-14 was 45 $\pm$ 2% for wt hSSTR3, 50 $\pm$ 3% for R3-Δ-C-tail, 23 $\pm$ 4% for Palm R3, 63 $\pm$ 4% for R3/R5-C-tail chimera. Compared to nontransfected HEK cells, wt hSSTR3 cells treated with SST-14 showed 56 $\pm$ 8% inhibition of cell growth at day 4. TUNEL and HOECHST assays at day 2 revealed 20-30% apoptotic cells. The R3Δ-C-tail and Palm R3 mutants displayed marked attenuation of the ability to inhibit SST-14 induced cell growth

(39 ± 12% and 27 ± 8% respectively of the maximum response of wt hSSTR3). Deletion of the C-tail of hSSTR3 (R3Δ C-tail) or substitution of hSSTR3 C-tail with that of hSSR5 (R3/R5-C-tail chimera) abrogated the cytotoxic property of hSSTR3. **Conclusions**: SSTR3 and SSTR5 are the principal antiproliferative subtypes and differentially induce apoptosis (SSTR3) or cytostasis (SSTR5). Apoptotic signalling by SSTR3 requires molecular signals in the receptor C-tail.

Disclosure: There is no disclosure information to present

Yc Patel 2/2/00.

Sponsor Signature: (Yogesh C. Patel) **Date:**

Return To Thank You

Note: Use the buttons on the left to move between screens or the "Reload" button if you encounter an error message.

MULTIPLE SOMATOSTATIN RECEPTOR SUBTYPES (SSTRs) CAN INDUCE APOPTOSIS THROUGH FORMATION OF HETERO-OLIGOMERS WITH SSTR3

Rocheville M*[1] , Kumar U[1], Patel RC[2], Patel YC[1]

[1]Fraser Labs, Departments of Medicine and Pharmacology and Therapeutics, Royal Victoria Hospital and McGill University, Montreal, Canada and [2] Department of Physics and Chemistry, Clarkson University, Potsdam, New York, USA

Somatostatin (SST) induces variable apoptosis in tumor cells. When hSSTR1-5 are studied as monotransfectants in CHO-K1 cells, hSSTR3 is the only subtype that induces apoptosis. Since tumor cells endogenously express multiple SSTRs and often all five isoforms in the same cell, and since SSTRs are capable of forming functional hetero-oligomers with other family members, we wondered whether SSTRs other than SSTR3 could induce apoptosis through hetero-oligomerization with SSTR3. We selected for study MCF-7 human breast cancer cells which we showed by immunocytochemistry and RT-PCR to express SSTR1, 2, 3, 5 but not SSTR4. Cells were treated for 24-48 h with 10^{-9}-10^{-7} M subtype-selective nonpeptide agonists (obtained from Merck). Apoptosis was assessed by TUNEL and Hoechst 33258 staining, as well as DNA fragmentation analysis by gel electrophoresis. Agonists for SSTR1, 2, 3, 5 each produced time- and dose-dependent apoptosis with the following rank order SSTR1 (25 ± 3%), SSTR2 (23 ± 4%), SSTR3 (18 ± 5%), SSTR5 (18 ± 4%) whereas the SSTR4 selective agonist was without effect. Treatment of MCF-7 cells with antisense oligonucleotides to hSSTR3 (10 µg/ml) for 2 days prior to treatment with SST analogs abrogated apoptotic cell death induced by SSTR1,2,3, and 5. This effect was not seen with sense SSTR3 oligonucleotide. In light of our recent finding that SSTRs can signal directly on the membrane through hetero-oligomerization, the differential ability of SSTR1,2, and 5 to induce apoptosis when coexpressed with SSTR3, but not when expressed as a monotransfectant, suggests that SSTR3 is an obligatory receptor for SST-induced apoptosis, and that other SSTR subtypes can also induce apoptosis through hetero-oligomerization with SSTR3.

Office Use Only

*Abstract must fit into above text box

Once you have completed your Abstract, rename your file, save the file onto your drive, CLICK HERE and proceed to STEP 3 on the website to submit your Abstract to ICE2000.

Program 11th International Congress of Endocrinology, Sydney, Australia, October 29-November 2, 2000.

sydneyabstract

Original Abstract Form

Office Use Only

CYTOTOXIC AND CYTOSTATIC ANTIPROLIFERATIVE ACTIONS OF SOMATOSTATIN

Srikant, C B[1*], Sharma, K[1], Thangaraju M[1], Liu D[1], Martino G[1], Patel Y C [1] Shen S-H[2]

[1]Fraser Laboratories, Department of Medicine, McGill University and Royal Victoria Hospital, Montreal, Quebec, Canada H3A 1A1; [2]Pharmaceutical Sector, NRC Biotechnology Research Institute, Montreal, PQ, Canada H4P 2R2.

Somatostatin (SST) is a pluripotent hormone that regulates cell proliferation by suppressing the secretion of mitogenic hormones and by directly inhibiting cell growth. The direct antiproliferative action of SST analogs in cancer cells can trigger apoptosis (cytotoxic effect) or cell cycle arrest (cytostatic effect). The retinoblastoma gene product Rb or the tumor suppressor protein p53 can promote growth arrest. The latter inhibits cell cycle progression when growth factors are present but facilitates apoptosis in their absence. G_1 cell cycle arrest requires inhibition of cyclin-dependent kinases (cdk) whereas apoptosis requires induction of Bax. In order to define the molecular mediators that regulate cytotoxic and cytostatic actions of SST, we investigated the involvement of these cell cycle modulators in SSTR subtype-selective antiproliferative signaling in CHO-K1 cells stably expressing individual hSSTRs 1-5. Our findings have established that SST induces apoptosis uniquely through hSSTR3 while it triggers G_1 arrest via other subtypes (hSSTR5>hSSTR2>hSSTR4~hSSTR1). hSSTR3 signaled apoptosis is associated with the induction of *wt* p53 and Bax as well as caspase-8-mediated intracellular acidification. These events precede mitochondrial changes associated with apoptosis. By contrast, its inhibition of cell cycle progression via the other hSSTRs was shown to be due to the induction of Rb in its hypophosphorylated form as well as cdk inhibitors of the p21 family. Both cytotoxic and cytostatic actions of SST are mediated via the tyrosine phosphatase SHP-1 suggesting that diversification of SSTR subtype-selective antiproliferative signaling occurs distal to SHP-1. These data provide a rational basis for exploiting the cytotoxic and cytostatic actions of SSTR subtype-selective agonists in cancer therapy.

Abstract must fit into above text box

Once you have completed your Abstract, rename your file, save the file onto your drive, CLICK HERE and proceed to STEP 3 on the website to submit your Abstract to ICE2000.

Program 11th International Congress of Endocrinology, Sydney, Australia, October 29-November 2, 2000.

Created on 5/9/00 4:04 PM